Hawke's Bay 3D Aquifer Mapping Project:

Heretaunga Plains SkyTEM data processing and resistivity models

October 2021
Hawkes Bay Regional Council Publication No. 5566

HAWKES BAY
REGIONAL COUNCIL
TE KAUNIHERA Ā-ROHE O TE MATAU-A-MĀUI

ISSN 2703-2051 (Online)
ISSN 2703-2043 (Print)

HAWKES BAY REGIONAL COUNCIL
TE KAUNIHERA Ā-ROHE O TE MATAU-A-MĀUI

(06) 835 9200
0800 108 838
Private Bag 6006 Napier 4142
159 Dalton Street . Napier 4110

Environmental Science

Hawke's Bay 3D Aquifer Mapping Project:

Heretaunga Plains SkyTEM data processing and resistivity models

October 2021
Hawkes Bay Regional Council Publication No. 5566

Prepared By:

GNS Science

ZJ Rawlinson RS Westerhoff RL Kellett

Aarhus University HydroGeophysics Group

N Foged

For: Hawke's Bay Regional Council

Reviewed by:
S Harper, Hawke's Bay Regional Council
S Cameron, GNS Science
J Pedersen, Aarhus University HydroGeophysics Group

.

ISSN 2703-2051 (Online)
ISSN 2703-2043 (Print)

Hawke's Bay 3D Aquifer Mapping Project: Heretaunga Plains SkyTEM data processing and resistivity models

ZJ Rawlinson
RS Westerhoff
N Foged
RL Kellett

GNS Science Consultancy Report 2021/93
October 2021

GNS SCIENCE
TE PŪ AO

DISCLAIMER

This report has been prepared by the Institute of Geological and Nuclear Sciences Limited (GNS Science) exclusively for and under contract to Hawke's Bay Regional Council. Unless otherwise agreed in writing by GNS Science, GNS Science accepts no responsibility for any use of or reliance on any contents of this report by any person other than Hawke's Bay Regional Council and shall not be liable to any person other than Hawke's Bay Regional Council, on any ground, for any loss, damage or expense arising from such use or reliance.

Use of Data:

Date that GNS Science can use associated data: October 2021

BIBLIOGRAPHIC REFERENCE

Rawlinson ZJ, Foged N, Westerhoff RS, Kellett RL. 2021. Hawke's Bay 3D Aquifer Mapping Project: Heretaunga Plains SkyTEM data processing and resistivity models. Wairakei (NZ): GNS Science. 90 p. Consultancy Report 2021/93.

CONTENTS

TABLES

FIGURES

APPENDICES

APPENDIX TABLES

EXECUTIVE SUMMARY

The Hawke's Bay 3D Aquifer Mapping Project (3DAMP) is a three-year initiative (2019–2022) jointly funded by the Provincial Growth Fund (now the Kānoa Regional Economic Development & Investment Unit), Hawke's Bay Regional Council (HBRC) and GNS Science (GNS). The project applies SkyTEM technology to improve mapping and modelling of groundwater resources within the Heretaunga Plains, Ruataniwha Plains and Poukawa and Otane Basins. 3DAMP involves collaboration between HBRC, GNS and the Aarhus University HydroGeophysics Group (HGG).

In January/February 2020, 2610.1 km of SkyTEM data were collected over the Heretaunga Plains by SkyTEM Australia, including four offshore lines. This report details the steps taken to develop resistivity models for the Heretaunga Plains survey area from the collected SkyTEM datasets, as well as the resultant resistivity models.

Both automatic and manual data processing were carried out by GNS to remove electromagnetic noise from the SkyTEM low-moment and high-moment data. This processing was quality-checked by HGG, post-processing was undertaken by GNS to check for any remaining artefacts and then a final quality check was undertaken by HGG.

Using the retained data, spatially constrained inversions were performed, creating both smooth and sharp resistivity models. Different inversion parameters were utilised for the four offshore flight lines, and so separate resistivity models are provided for the onshore and offshore data. For the onshore data, the system response modelling approach was used in the inversion of the data, enabling modelling of an additional five time gates within the ramp down time and thus providing higher-resolution information in the near-surface.

The SkyTEM survey reveals a detailed 3D resistivity picture of the subsurface. The onshore resistivity models have layer thicknesses of 1 m in the near-surface, increasing to 59 m at depth. For the smooth onshore model, the standard depth of investigation varies from 12 m (where only low-moment data was kept due to noise) to 650 m, with a mean of 276 m. The offshore resistivity models have layer thicknesses of 0.1 m in the near-surface, increasing to 10.6 m at depth. For the smooth offshore model, the standard depth of investigation varies from 20 m to 72 m, with a mean of 30 m.

Images of the resistivity model are made available in this report, and digital datasets have also been provided to HBRC.

Hydrogeological interpretation of the 3D resistivity results is needed to make full use of the SkyTEM survey results. This additional work will be described within a separate report.

This page left intentionally blank.

1.0 INTRODUCTION

The Hawke's Bay 3D Aquifer Mapping Project (3DAMP) is a three-year initiative (2019–2022) jointly funded by the Provincial Growth Fund (now the Kānoa Regional Economic Development & Investment Unit), Hawke's Bay Regional Council (HBRC) and GNS Science (GNS). The project applies SkyTEM technology to improve mapping and modelling of groundwater resources within the Heretaunga Plains, Ruataniwha Plains and Poukawa and Otane Basins. 3DAMP involves collaboration between HBRC, GNS and the Aarhus University HydroGeophysics Group (HGG).

SkyTEM is a specific airborne geophysical technique that uses transient (time-domain) electromagnetics (TEM) to investigate the shallow (up to ~500 m deep) electrical resistivity structure of the earth. The resistivity structure can then be interpreted in terms of geology (e.g. groundwater aquifers) and used to inform and improve geological/hydrological models. Data are collected using specialist equipment that is slung beneath a helicopter and flown at low elevations along closely spaced lines. A key advantage of this technique is that it enables a large amount of high-resolution data to be collected quickly and cost-effectively.

SkyTEM data were collected in the Hawke's Bay region during January/February 2020 by SkyTEM Australia. This data collection is described by SkyTEM Australia Pty Ltd (2020), as well as the collected magnetometer data (not addressed in this report).

This report details the steps taken to develop resistivity models for the Heretaunga Plains survey area (Figure 1.1) from the collected SkyTEM datasets (Table 1.1), as well as the resultant resistivity models. The report is structured as follows:

- A brief description of the SkyTEM system is provided in Section 2.
- Processing and noise removal are described in Section 3.
- Inversion procedures to develop the resistivity models are described in Section 4.
- Geophysical maps and cross-sections are provided in Appendices 1–3 and described in Section 5.
- Digital deliverables provided to HBRC are described in Section 5.4 and Appendix 4.

A standard reporting template has been used as the basis for this report (e.g. HGG 2017; Rawlinson et al. 2021).

Table 1.1 Survey details.

SkyTEM Survey, Heretaunga Plains	
Client	Hawke's Bay Regional Council
Key Persons	**GNS Science, New Zealand** Project lead/management: *Zara Rawlinson* Data processing, modelling and reporting: *Zara Rawlinson, Rogier Westerhoff, Richard Kellett* **HGG, Aarhus University, Denmark** Quality assurance: *Nikolaj Foged* **Hawke's Bay Regional Council** Project lead: *Jeff Smith, Simon Harper* **Project Haus** Project management: *Amanda Langley*
Locality	Heretaunga Plains, Hawke's Bay, New Zealand
Survey Period	28 January – 5 February 2020
SkyTEM System	SkyTEM312
Line km acquired	2610.1 km
Line spacing	170 m; 400 m offshore; 4–5 lines upper Ngaruroro River Valley
Mean flight speed	86 km/h
Mean flight altitude of the TEM loop	48 m

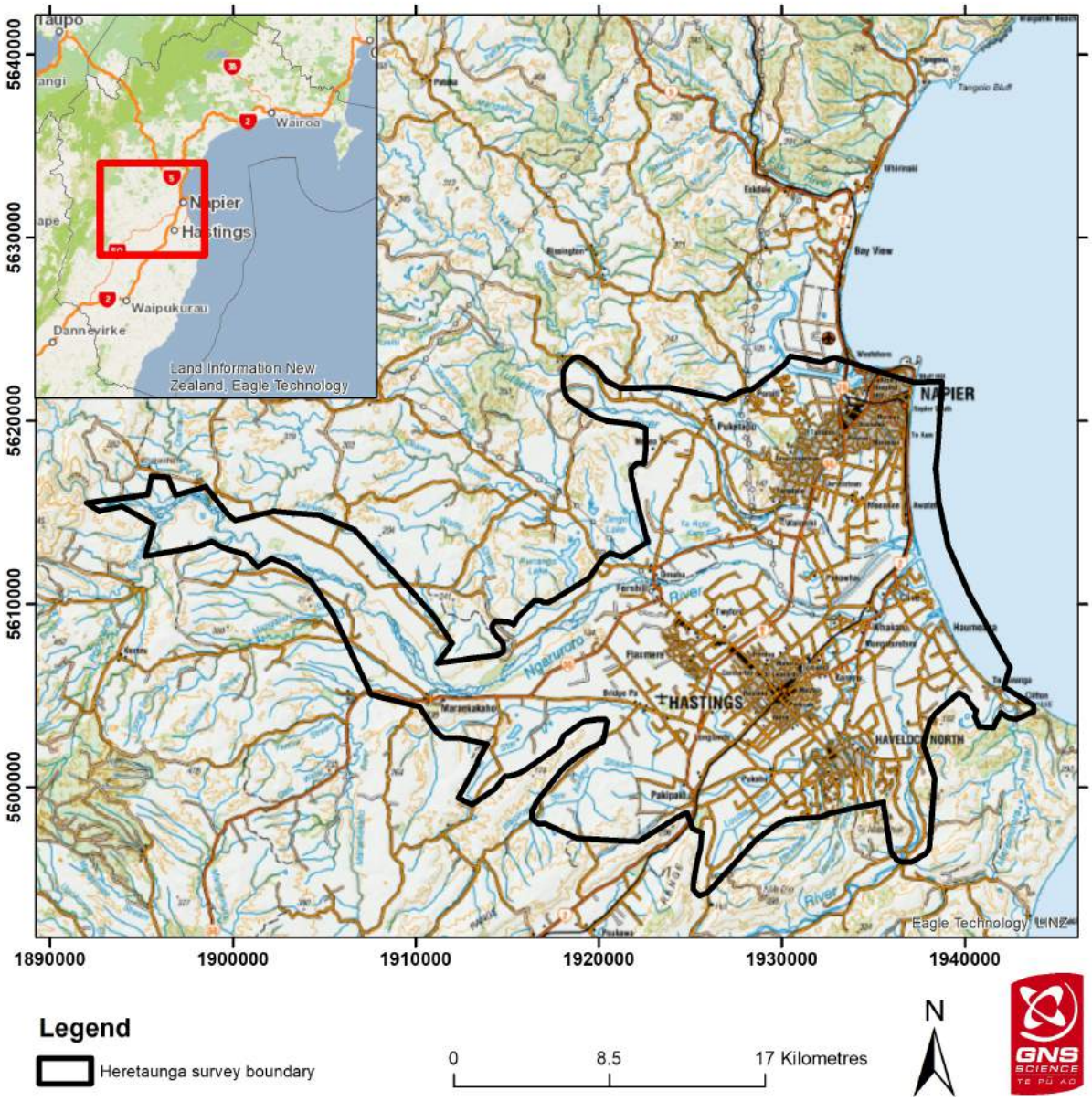

Figure 1.1 Location map of the Heretaunga Plains SkyTEM survey area.

2.0 THE SKYTEM SYSTEM

2.1 Overview

SkyTEM is a time-domain (transient) helicopter electromagnetic system designed for hydrogeophysical and environmental investigations. The following contains a general introduction to the SkyTEM system. A more thorough description of the SkyTEM method can be found in Sørensen and Auken (2004). A description of the TEM method in general can be found in Nabighian and Macnae (1991) and Jørgensen et al. (2003).

2.1.1 Instrument

Figure 2.1 shows the SkyTEM system with the hexagonal frame slung beneath the helicopter. The lengths of the frame sides are approximately 12 m. The transmitter loop is mounted on the frame in an octagonal polygon configuration. To obtain a close to zero coupling to the primary magnetic field, the z-receiver coil is placed at the back of the loop, approximately 2 m above the frame. Two lasers are placed on the frame, continuously measuring the distance to the ground surface below the loop, and two inclinometers measure the roll and pitch of the frame. Power is supplied by a generator placed on the sling cable between the helicopter and the loop, sufficiently away from the receiver to reduce noise. The positions of the various devices on the frame are shown in Figure 2.2.

2.1.2 Measurement Procedure

The configuration of the system is customised for each survey. Measurements are carried out with one or two transmitter moments, depending on the target geology. The standard configuration uses a low (LM) and high transmitter moment (HM), applied sequentially. For this survey, all data were acquired using interleaved low- and high-moment transmitter modes, consisting of 110 low-moment positive and negative pulse pairs at 275 Hz and 30 high-moment pulse pairs at 25 Hz, which repeats every 1.6 seconds (SkyTEM Australia Pty Ltd 2020). Data are recorded within ‘gates’, which are equivalent to specified time intervals. Lower numbered gates (earlier times) correspond to information related to shallower depths than higher numbered gates (later times). Standard processing utilises LM gates 9–26 and HM gates 16–38 (SkyTEM Australia Pty Ltd 2020).

The flight altitude depends on the flight speed, the roughness of the terrain and the presence of obstacles such as towers, tall trees and buildings. The nominal flight altitude for this survey was 45–55 m (frame height). Over forested areas, the altitude is increased to maintain safe clearance over the treetops. The flight speed can be adjusted to a maximum of 120 km/hr to balance survey time, data density on the ground, smearing of data recovered at depth and a more stable levelling of the transmitter loop. For the present survey, a mean speed of 84 km/hr was used.

Apart from GPS, altitude and TEM data, a number of instrument parameters are monitored and stored in order to be used for quality control when the data are processed.

2.1.3 Penetration Depth

The penetration depth for the SkyTEM system depends on the transmitter moment, geological settings, background noise level, flight speed and altitude. Normally, a penetration depth of 150–500 m can be achieved, but it strongly depends on the SkyTEM system set-up, the geological setting and the flight altitude (as air is highly resistive). During the inversion, a depth of investigation is estimated for each resistivity model (see Section 4.5).

2.2 Technical Specification

The system instrument set-up is shown in Figure 2.2. The positioning of the instruments and the corners of the octagon described by the transmitter coil are listed in Table 2.1. The origin is defined as the centre of the transmitter coil.

The SkyTEM system was configured in a standard two-moment set-up: low moment and high moment. The specifications of these are summarised in Tables 2.2–2.4. See SkyTEM Australia Pty Ltd (2020) for further details.

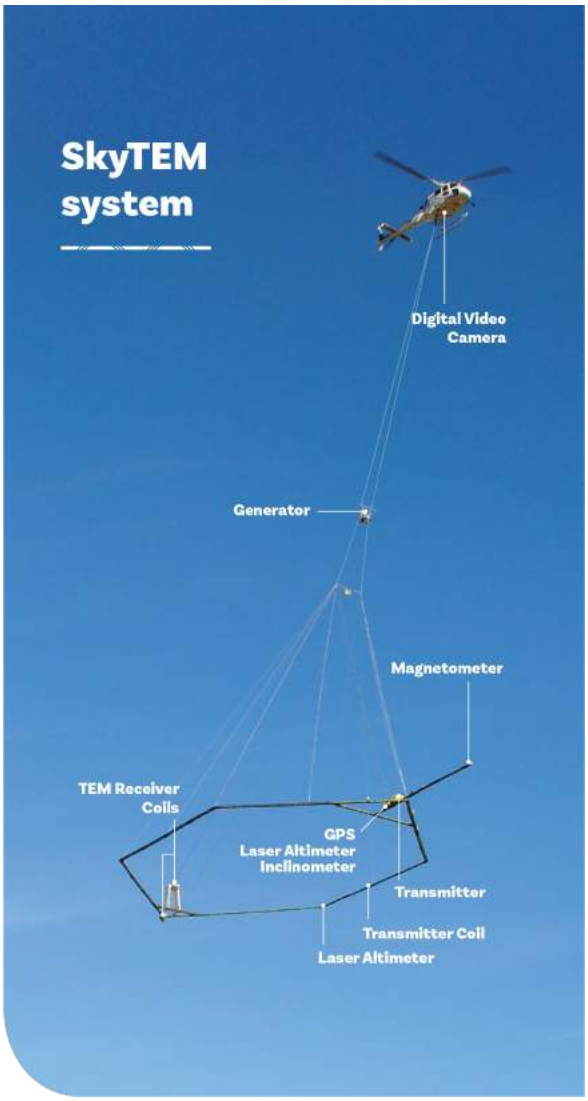

Figure 2.1 The SkyTEM312 system. The transmitter frame holds the inclinometers, laser-altimeters, receiver coils and instrumentation. For a detailed instrument set-up, see Figure 2.2. Figure from SkyTEM Australia Pty Ltd.

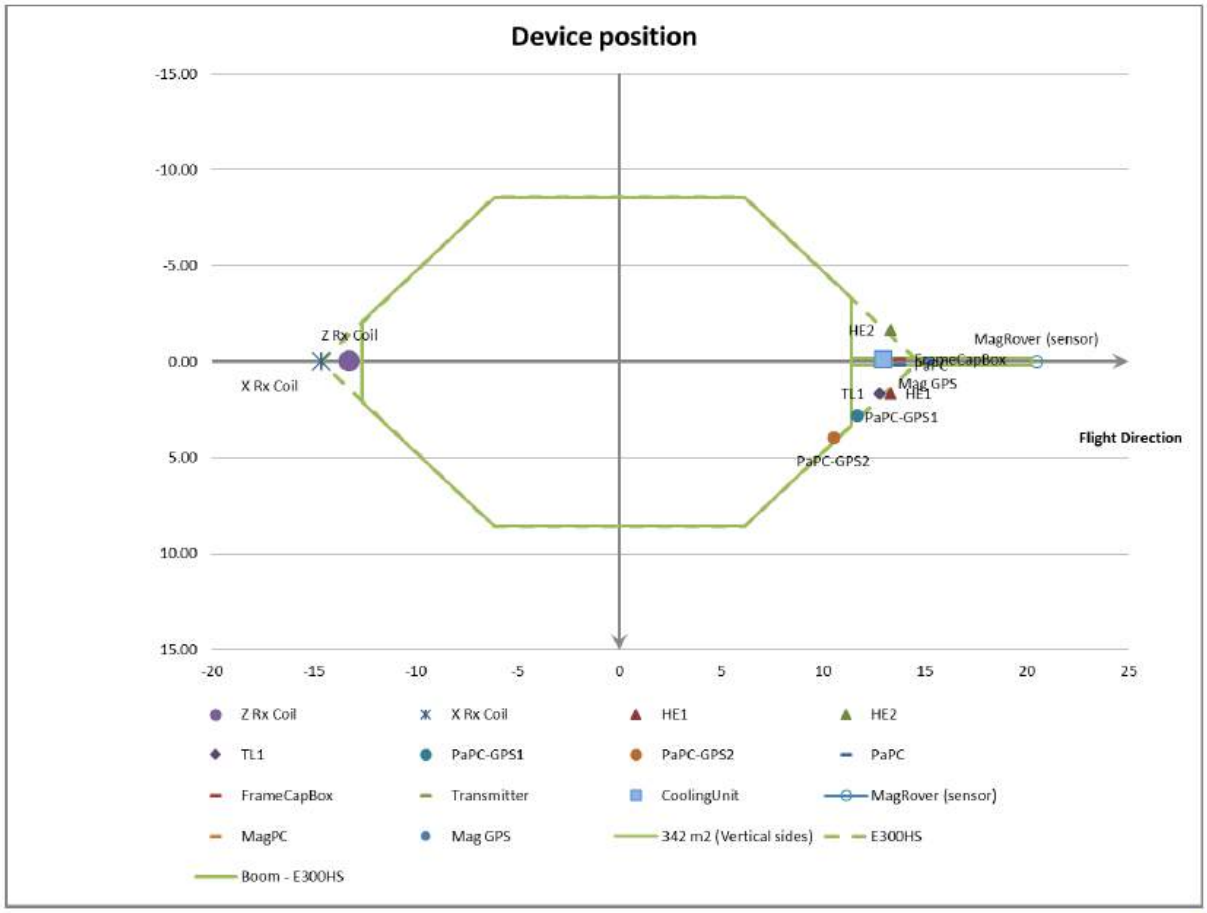

Figure 2.2 Instrument set-up for the SkyTEM312 system used. Figure from SkyTEM Australia Pty Ltd (2020).

Table 2.1 Summary of equipment and transmitter coil corner positioning. The origin is defined as the centre of the transmitter coil. Z is positive towards the ground.

Unit	X (m)	Y (m)	Z (m)
PaPC-GPS1 (GPS standard)	11.68	2.79	-0.16
PaPC-GPS2 (RTK DGPS)	10.51	3.95	-0.16
HE1 (Laser Altimeter 1)	13.31	1.62	-0.12
HE2 (Laser Altimeter 2)	13.31	-1.62	-0.12
TL1 (inclinometer)	13.12	1.45	-0.12
TL2 (inclinometer)	13.12	1.45	-0.12
Z Rx coil (EM Z-receiver coil)	-13.35	0.00	-2.00
X Rx coil (EM X-receiver coil)	-14.65	0.00	0.00
Loop corner 1	-12.64	-2.10	0.00
Loop corner 2	-6.14	-8.58	0.00
Loop corner 3	6.14	-8.58	0.00
Loop corner 4	11.41	-3.31	0.00
Loop corner 5	11.41	3.31	0.00
Loop corner 6	6.14	8.58	0.00
Loop corner 7	-6.14	8.58	0.00
Loop corner 8	-12.64	2.10	0.00

Table 2.2 Summary of low-moment and high-moment transmitter (Tx) and receiver (Rx) specifications.

Parameter	Low Moment	High Moment
Number of turns	2	12
Transmitter area	342.8 m^2	342.8 m^2
Tx current	~ 6 A	~ 110 A
Tx peak moment	~ 4,100 Am^2	~ 451,400 Am^2
Repetition frequency	275 Hz	25 Hz
Tx-on-time	0.8 ms	5.0 ms
Tx-off-time	1.018 ms	15.0 ms
Duty cycle	44%	25%
Gate time interval	*16.415 µs – 0.877 ms	436.415 µs – 13.156 ms
Parameter	**X**	**Z**
Rx coil effective area	115 m^2	175 m^2
Rx coil low pass cut-off frequency	250 KHz	160 KHz

* This earliest gate time corresponds to gate 9; however, in this report, gates 3–8 are also utilised (see Sections 3.1 and 4.1).

Table 2.3 SkyTEM312 low-moment channel times. All gate times are relative to the start of the transmitter current ramp down. Gates 3–8 are within the ramp down time (see Section 4.1).

LM Gate Number	Gate Width (µs)	Gate Open (µs)	Gate Centre (µs)	Gate Close (µs)
3	1.57	1.63	2.415	3.20
4	1.57	3.63	4.415	5.20
5	1.57	5.63	6.415	7.20
6	1.57	7.63	8.420	9.20
7	1.57	9.63	10.410	11.20
8	2.57	11.63	12.920	14.20
9	3.57	14.63	16.415	18.20
10	4.57	18.63	20.915	23.20
11	5.57	23.63	26.415	29.20
12	7.57	29.63	33.415	37.20
13	9.57	37.63	42.415	47.20
14	12.57	47.63	53.915	60.20
15	15.57	60.63	68.415	76.20
16	19.57	76.63	86.415	96.20
17	24.57	96.63	108.915	121.20
18	30.57	121.63	136.915	152.20
19	50.57	152.63	177.915	203.20
20	50.57	203.63	228.915	254.20
21	50.57	254.63	279.915	305.20

LM Gate Number	Gate Width (μs)	Gate Open (μs)	Gate Centre (μs)	Gate Close (μs)
22	100.57	305.63	355.915	406.20
23	100.57	406.63	456.915	507.20
24	100.57	507.63	557.915	608.20
25	151.57	608.63	684.415	760.20
26	201.57	760.63	861.415	962.20

Table 2.4 SkyTEM312 high-moment channel times. All gate times are relative to the start of the transmitter current ramp down.

HM Gate Number	Gate Width (μs)	Gate Open (μs)	Gate Centre (μs)	Gate Close (μs)
16	19.57	426.63	436.415	446.20
17	24.57	446.63	458.915	471.20
18	30.57	471.63	486.915	502.20
19	50.57	502.63	527.915	553.20
20	50.57	553.63	578.915	604.20
21	50.57	604.63	629.915	655.20
22	100.57	655.63	705.915	756.20
23	100.57	756.63	806.915	857.20
24	100.57	857.63	907.915	958.20
25	151.57	958.63	1034.415	1110.20
26	201.57	1110.63	1211.415	1312.20
27	252.57	1312.63	1438.915	1565.20
28	353.57	1565.63	1742.415	1919.20
29	403.57	1919.63	2121.415	2323.20
30	504.57	2323.63	2575.915	2828.20
31	707.57	2828.63	3182.415	3536.20
32	807.57	3536.63	3940.415	4344.20
33	1009.57	4344.63	4849.415	5354.20
34	1211.57	5354.63	5960.415	6566.20
35	1415.57	6566.63	7274.415	7982.20
36	1819.57	7982.63	8892.415	9802.20
37	2019.57	9802.63	10812.415	11822.20
38	2729.57	11822.63	13187.415	14552.20

3.0 PROCESSING

3.1 Pre-Processing – Primary Field Compensation

The magnetic field coupling between the receiver coils and transmitter loops is continuously hardware-monitored, providing a separate value for the magnetic field coupling during each transient sounding. High-altitude data are collected at an elevation of greater than 400 m altitude to identify the response of the system in the absence of electrical conductors. These data are used to remove the primary field during raw data correction in a process known as Primary Field Compensation (PFC). The PFC enables accurate modelling of the very early time gates and modelling of on-time gates in the LM by system response inversion in the Aarhus Workbench software to yield shallow geological information (Auken et al. 2020).

The PFC-corrected data and the LM system response were derived by SkyTEM Australia Pty Ltd (2020).

3.2 Workflow

The software package Aarhus Workbench was used for processing the SkyTEM data. Table 3.1 shows key processing settings in the Aarhus Workbench used for this survey.

The aim of this processing was to prepare data for the geophysical interpretation (inversion modelling). The processing primarily includes filtering and averaging of data, as well as culling and discarding distorted or noisy data.

The data processing can be divided into four steps:

1. Import of raw data into a fixed database structure. The raw data appear in the form of *.skb*, *.sps* and *.geo* files. *.skb* files contain the actual transient data from the receiver; *.sps* files contain GPS positions, tilts, altitudes, transmitter currents, etc; and the *.geo* file contains system geometry, low-pass filters, calibration parameters, turn-on and turn-off ramps, calibration parameters, etc. For a description of the SkyTEM file formats, see HGG (2011). Raw SkyTEM datasets were provided by SkyTEM Australia Pty Ltd (2020).
2. Automatic processing: automatic processing was applied to the GPS, altitude, tilt and TEM voltage data. This automatic processing includes numerous parameters that were adjusted to this specific survey.
3. Manual processing: inspection and correction of the results of the automatic processing for the data types in question.
4. Post-processing and quality checking of the data processing, including utilising preliminary inversion results.

All data are recorded with a common time stamp. This time stamp is used to link position, geometry and electromagnetic voltage data. The time stamp is given as the GMT time.

In the following section, a short description of the processing of the different data types is shown. A more thorough description of the SkyTEM data processing can be found in Auken et al. (2009).

Table 3.1 Processing settings.

Item	Parameter	Value
Software	Aarhus Workbench version	6.5.1
Noise processing	Data uncertainty: uniform data STD	Calculated from raw data stack (see Section 3.6). Additional 20% added to LM gates 3–8.
Stacking	Sounding distance along flight lines	1.6 s (~37 m lateral spacing at the average flight speed of 84 km/h)

3.3 GPS Positioning

The OMNISTAR HP (high precision) real-time differential correction service was used to provide real-time input to the channel GP2 (SkyTEM Australia Pty Ltd 2020).

The GP2 GPS data were shifted to the optimal measurement point of the SkyTEM system, which is approximately two-thirds of the distance from the centre of the frame towards the receiver coil. In this survey, the GPS data are shifted 8.8 m from the centre of the loop towards the rear of the system.

3.4 Roll and Pitch Data

The roll and pitch of the frame were measured and used to correct the altitude and voltage data. It is presumed that the frame is rigid so that the roll and pitch of the transmitter and receiver coils are identical. Pitch and roll will affect the orientation of the electromagnetic field relative to the ground surface. It will also affect the distance measured by the laser altimeters.

3.5 Altitude Data

The distance between the transmitter coil and the ground is measured with two independent lasers. Figure 3.1 shows an altitude data example over open country with a minor forest area. The aim of the altitude data processing is to remove laser reflections that do not come from the ground but typically bounce off the tree canopy and other above-ground features. The processing is based on the fact that reflections from treetops result in an apparently lower altitude than reflections from the surface. Automatic filtering of the altitude data was followed by a manual inspection and correction.

During automatic filtering, a Digital Elevation Model (DEM) was also applied. This DEM is used by Aarhus Workbench, along with the GPS elevation values, to calculate a GPS-based altitude. Here, ‘altitude’ means height above the ground, while ‘elevation’ means height above sea level. This GPS altitude was not used directly but was utilised as a guideline during manual altitude user edits. The DEM utilised was a 10 m resolution DEM derived from a 5 m resolution DEM that was created by HBRC using a combination of LiDAR and SRTM V2 data (Farrier 2020).

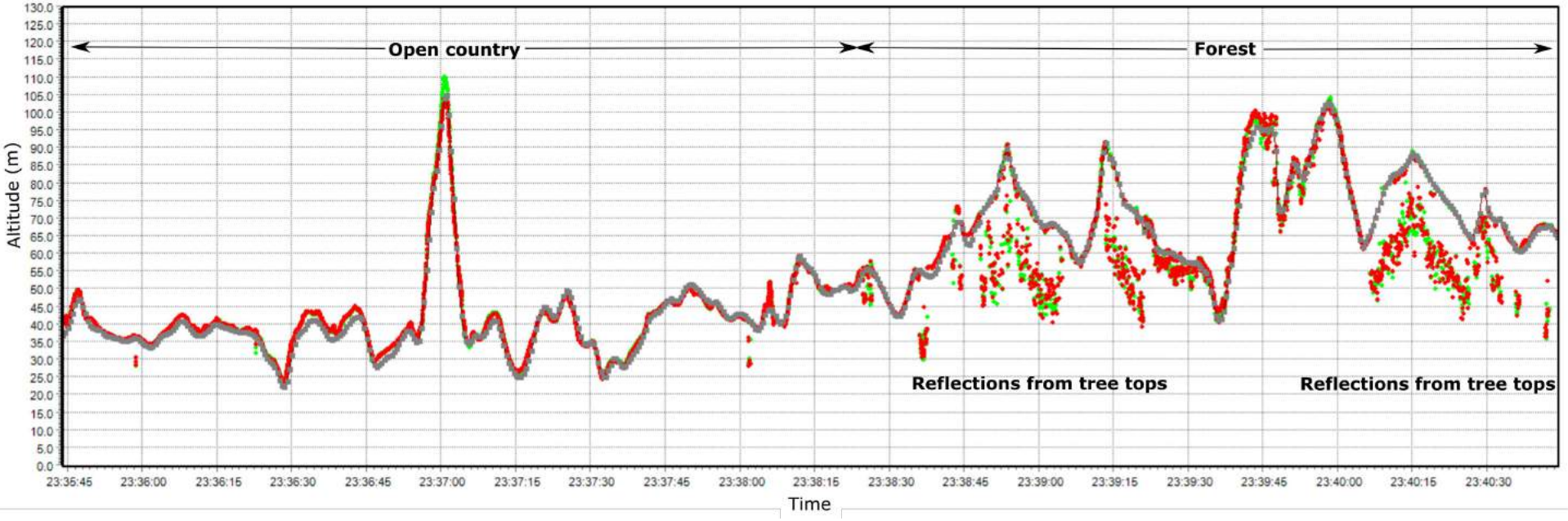

Figure 3.1 Green and red dots are raw data from the two laser altimeters. Grey dots are the resulting altitude after correcting the data. The time window holds approximate 7 km of data.

3.6 Voltage Data

The voltage data were gathered continuously along flight lines and alternately with LM and HM. Voltage data were collected by dB/dt probes, whose output voltage is proportional to the time derivative of the transverse flux passing through the area of the probe. The magnetic flux density time function is then determined as the integral of the induced voltage (also a time function) measured at the terminals of the probes. Voltage data is in units of V/(A*turns*m^4). The processing of voltage data was carried out in a two-step system: an automatic and a manual part. In the former, data were corrected for the transmitter/receiver tilt, stacking applied to create average data and automatic filters applied that were designed to cull coupled or noise-influenced data.

Stacking to create the average data was performed using a trapezoid-shaped filter (Figure 3.2). Average data is used to produce the resistivity models, so this stacking impacts the lateral resolution achieved. In this instance, time intervals of 2 s (stacking of one sample), 6 s (stacking of three samples) and 8 s (stacking of five samples) were used. This results in a sounding for each 1.6 s (~37 m based on average flight speed). Each sounding location will produce a resistivity model when data is inverted. The data uncertainty is calculated from the raw data stack.

Electromagnetic noise can be from capacitive couplings (e.g. buried cables), galvanic couplings (e.g. grounded power lines or fences), noise at specific frequencies, spikes and white noise. The size/extent of such a coupling will differ depending on the resistive quality of the underlying geology. If not removed, such noise will appear as artefacts within resistivity models developed from the data, such as the appearance of non-geological low-resistivity areas. Automatic processing procedures are not able to effectively remove electromagnetic noise. The manual inspection and removal of coupled data is therefore essential to obtain high-quality end results. GIS datasets of roads, powerlines, houses, railways and vineyards (LINZ Data Service 2021), as well as topographic (LINZ 2021) and geological base maps (Heron 2018), were used to help guide the processor's expectations of noise source locations. The sources of couplings evident in the data were not always possible to identify from these maps and datasets, but they corresponded to the bulk of the couplings evident.

Both raw data and average (stacked) data were assessed together to undertake manual removal of noise. Coupling, frequency and spike noise was removed from the raw data. White noise can be supressed by stacking raw data to create average samples, although, at a certain threshold, the signal level will not be distinguishable above the noise level. For example, data tends to be noisier where the geology is more resistive due to a lower signal. Average data was therefore culled below this noise threshold. Figure 3.3 shows an example of strongly coupled data. First, the coupled data were removed. Then, data were stacked into soundings. Finally, the late-time part of the sounding curves, below the background noise level, was excluded. Data was typically inspected within a three-minute window to facilitate close attention to detail.

The raw and average HM voltage data were processed first, and these manual HM edits were then transferred to the LM data. The LM data was then manually inspected. Additional couplings were commonly present in the LM data that were not present in the HM data and in fewer locations; there was no coupling in the LM data where there was a coupling in the HM data. The data were adjusted accordingly in these situations. As such, some areas may have only HM or only LM data retained. To provide the option of utilising on-time gates in the inversion modelling (providing higher near-surface resolution, see Section 4), LM gates 3–8 were enabled within the dataset prior to manual processing.

Rapid changes in helicopter altitude or orientation can also impact data quality due to the pitch/roll of the equipment not being able to be completely corrected for. This is particularly relevant towards the ends of lines where the helicopter performed a turning manoeuvre, as sufficient data may not have been trimmed to compensate for this. Data considered to be impacted too heavily by such changes were also removed.

Figure 3.2 Trapezium shaped moving average filter. Corner points are at different time gates and different lateral distances. In this instance, time intervals of 2 s (stacking of one sample), 6 s (stacking of three samples) and 8 s (stacking of five samples) were used.

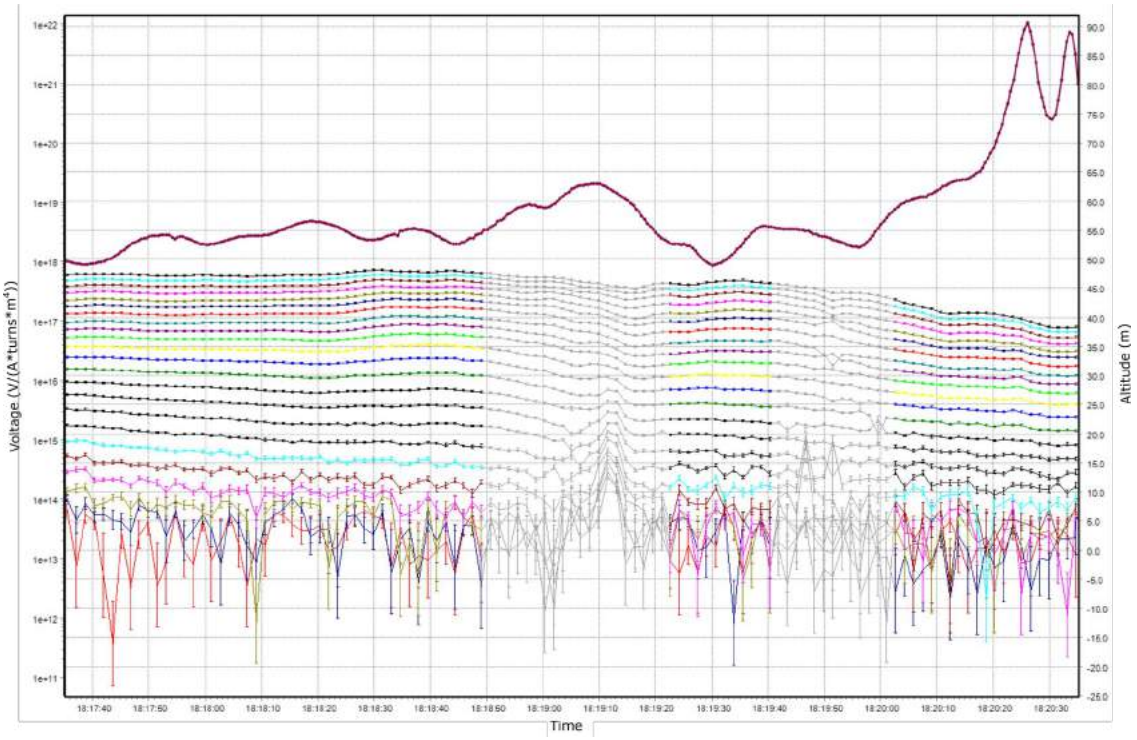

Figure 3.3 Data section example with coupled data. The section displays three minutes (~2.2 km) of data. The upper brown curve shows the flight altitude. Each of the lower curves shows raw high-moment data for a given gate time. The uppermost line represents gate 16 of the high moment, the line below that gate 17, etc. (gates 1–15 are not used). The grey lines represent data that have been removed due to couplings. Two couplings can clearly be identified. In this case, the couplings are associated with installations along roads. To the right of the image, it can be seen how the HM signal amplitude decreases as the helicopter altitude increases; this impact is further enhanced for LM data.

3.7 Quality Checking and Post-Processing

Following completion of manual voltage processing, the manual voltage processing was quality-checked by a different person. In this instance, quality checking was performed by HGG staff. Larger time windows of approximately 10 minutes were used for quality checking and to assist with an alternate view of the data trends and behaviour. The quality checker worked through all datasets manually and made manual edits where needed (adding or deleting data points).

Following the manual inspection of the voltage data, post-processing was undertaken. This involved calculating preliminary Laterally Constrained Inversions (LCI) for all data (see Section 4.2 for further details). These preliminary resistivity models were inspected alongside their data residuals[1] and other quality assurance maps to guide data inspection (see Section 5 for further details). For example, checking that, if a coupling was detected over a road, voltage data over this road were removed from all flight lines and that sufficient data was removed from either side of the road. Further manual edits to remove or add voltage data were performed, with the aim of reducing all residuals below approximately 1.2. This largely involved removing data that were below the noise floor. This procedure was performed iteratively: adjust data, re-run LCIs, re-inspect and then repeat if needed. Typically, this procedure was performed approximately five times. When this process was considered complete, a final quality check was provided by HGG.

1 The data residual describes how well the obtained resistivity models explain the recorded data (how well the data is fitted). The data residual values are normalised with the data standard deviation, so a data residual below 1 corresponds to a fit within one standard deviation.

4.0 INVERSION

Mathematical inversion is the calculation of the cause (m) of a set of observations (d_{obs}). It is called an inverse problem because it starts with the effects (observations) and then calculates the causes. In this work, a resistivity model of the earth (upper ~500 m of the subsurface geology) is calculated (m) based on the recorded SkyTEM data (d_{obs}) using established electromagnetic equations ($F(\,)$).

$$d_{obs} = F(m)$$

For such a complex and non-unique (multiple solutions can fit the observed data) mathematical problem, a direct solution is not able to be calculated. Therefore, an iterative procedure is used to reach a minimum mis-fit (difference) between modelled [$d_{est} = F(m_{est})$] and observed data (d_{obs}). This is a minimisation problem (a mathematical problem that searches for the smallest value, or global minimum), for which there are different algorithms available to improve computational efficiencies, with the objective being to find a global minimum. In this case, the inversion uses a 1D full non-linear damped least-squares solution (or Levenberg–Marquardt algorithm). The algorithm starting point is set by initial parameter estimates (prior values). If there are multiple minima present, then inappropriate prior values may bias the result to only find a local minimum; thus, prior values close to the true global minimum may be required to achieve the true global minimum. However, the algorithm is generally robust in terms of typically finding a solution, even if it starts very far from the final minimum.

Inversion of the dataset and evaluation of the inversion results were carried out using the Aarhus Workbench software package. The underlying inversion code (AarhusInv) was developed by the HydroGeophysics Group, Aarhus University, Denmark (Auken et al. 2015).

Model development using mathematical inversion is a non-unique process and follows an iterative process:

1. A starting (initial) resistivity model is created.
2. Using this resistivity model, an electromagnetic forward model is utilised to calculate the resultant voltage data.
3. The residual between the measured voltage data and the estimated voltage data from the forward model is calculated.
4. The resistivity model is adjusted, using rules imposed by the regularisation scheme applied (e.g. imposed prior knowledge, constraints between soundings, smooth/sharp requirements).
5. Steps 2–4 are repeated until the residual reaches a defined threshold value of less than one.

The inversion is a 1D full non-linear damped least-squares solution in which the transfer function of the instrumentation is modelled. The transfer function includes turn-on and turn-off ramps, front gate, low-pass filters and transmitter and receiver positions. The flight altitude contributes to the inversion scheme as a model parameter, with the laser altimeter readings as a constrained prior value.

The inversion settings for the sharp and smooth onshore inversions in Aarhus Workbench are listed in Table 4.1, and the layer structure is shown in Table 4.2. Due to known heterogeneity in the near-surface, within the smooth model, loose lateral constraints were utilised in the top 50 m, with tighter constraints at depths below this. Lithological logs from boreholes were

utilised to manually assess against inversion results to assess the value of this approach. The use of prior constraints for the inversion from both seismic data and boreholes were assessed and determined to be unsuitable due to small coverage areas and the potential for bias over such a large survey area.

Sea water is highly conductive and limits the depth of investigation. Therefore, such data requires a shallower model discretisation and a lower start model resistivity compared to the onshore set-up. The offshore inversion set-up is shown in Tables 4.3 and 4.4. Offshore monitoring in the area (HBRC 2021) at the time of the data collection (5 February 2020) identified resistivity of the seawater with an average of 0.2 ohm.m. As such, this value was used as an initial value for the upper ~10 m (equivalent to approximate bathymetry), with a subsequent gradual increase of the initial values up to 10 ohm.m. Additionally, early time gates were not used, and gates 8–10 LM and 15–19 HM were disabled following initial inversion testing that demonstrated an inability to match these data points.

Table 4.1 Inversion settings, smooth/sharp spatially constrained inversion set-up for the onshore models.

Item		**Value**
Software	Aarhus Workbench version	6.5.1
Model set-up	Number of layers Starting resistivities (Ωm) Thickness of first layer (m) Depth to last layer (m) Thickness distribution of layers	35 Auto 1.0 500.0 Log increasing with depth
Smooth model onshore: constraints / prior constraints	Horizontal constraints on resistivities (factor) Reference distance (m) Power law Vertical constraints on resistivities (factor) Prior, thickness Prior, resistivities Prior on flight altitude (m) Lateral constraints on flight altitude (factor) Minimum number of gates per moment	1.6 (layers 1–17); 1.3 (layers 18–35) 37 0.75 2.5 Fixed None +/- 0.2 1.5 7
Sharp model onshore: constraints / prior constraints	Horizontal constraints on resistivities (factor) Horizontal sharp Reference distance (m) Power law Vertical constraints on resistivities (factor) Vertical sharp Prior, thickness Prior, resistivities Prior on flight altitude (m) Lateral constraints on flight altitude (factor) Minimum number of gates per moment	1.04 400 37 0.75 1.12 200 Fixed None +/- 0.2 1.5 7

Table 4.2 Layer structure used for onshore resistivity models.

Layer	Thickness (m)	Depth to Bottom of Layer (m)
1	1	1
2	1.1	2.1
3	1.3	3.4
4	1.4	4.9
5	1.6	6.5
6	1.9	8.4
7	2.1	10.5
8	2.4	12.8
9	2.7	15.5
10	3	18.6
11	3.4	22
12	3.9	25.9
13	4.4	30.3
14	5	35.3
15	5.6	40.9
16	6.4	47.3
17	7.2	54.5
18	8.2	62.7
19	9.2	71.9
20	10.5	82.4
21	11.8	94.2
22	13.4	107.6
23	15.2	122.8
24	17.1	139.9
25	19.4	159.3
26	22	181.3
27	24.8	206.1
28	28.1	234.2
29	31.8	266.1
30	36	302
31	40.7	342.8
32	46.1	388.9
33	52.1	441
34	59	500
35	Inf*	-

* The last layer is modelled as an infinite half-space.

Table 4.3 Inversion settings, smooth/sharp spatially constrained inversion set-up for the offshore models.

Item		Value
Software	Aarhus Workbench version	6.5.1
Model set-up	Number of layers	35
	Starting resistivities (Ωm)	Auto
	Thickness of first layer	0.1 m
	Depth to last layer	80.0 m
	Thickness distribution of layers	Log increasing with depth
Smooth model offshore: constraints / prior constraints	Initial values	0.2 (layers 1–19); 0.5 (layer 20); 1.0 (layer 21); 2.0 (layer 22); 5.0 (layer 23); 10.0 (layers 24–35)
	Horizontal constraints on resistivities (factor)	1.3
	Reference distance	37 m
	Power law	0.75
	Vertical constraints on resistivities (factor)	2.0
	Prior, thickness	Fixed
	Prior, resistivities	None
	Prior on flight altitude	+/- 0.2 m
	Lateral constraints on flight altitude (factor)	1.5
	Minimum number of gates per moment	7
Sharp model offshore: constraints / prior constraints	Initial values	0.2 (layers 1–19); 0.5 (layer 20); 1.0 (layer 21); 2.0 (layer 22); 5.0 (layer 23); 10.0 (layers 24–35)
	Horizontal constraints on resistivities (factor)	1.04
	Horizontal sharp	400
	Reference distance	37 m
	Power law	0.75
	Vertical constraints on resistivities (factor)	1.12
	Vertical sharp	200
	Prior, thickness	Fixed
	Prior, resistivities	None
	Prior on flight altitude	+/- 0.2 m
	Lateral constraints on flight altitude (factor)	1.5
	Minimum number of gates per moment	7

Table 4.4 Layer structure used for offshore resistivity models.

Layer	Thickness (m)	Depth to Bottom of Layer (m)
1	0.1	0.1
2	0.1	0.2
3	0.1	0.3
4	0.2	0.5
5	0.2	0.7
6	0.2	0.9
7	0.2	1.1
8	0.3	1.4
9	0.3	1.7
10	0.4	2.0
11	0.4	2.5
12	0.5	2.9
13	0.5	3.5
14	0.6	4.1
15	0.7	4.8
16	0.8	5.7
17	1.0	6.6
18	1.1	7.7
19	1.3	9.0
20	1.5	10.5
21	1.7	12.2
22	1.9	14.1
23	2.2	16.4
24	2.6	19.0
25	3.0	21.9
26	3.4	25.4
27	4.0	29.3
28	4.6	33.9
29	5.2	39.1
30	6.0	45.2
31	7.0	52.1
32	8.0	60.1
33	9.2	69.4
34	10.6	80.0
35	Inf*	-

* The last layer is modelled as an infinite half-space.

4.1 System Response Modelling

System response modelling enables early time data (early gates) to be used when they would normally be excluded, thus improving near-surface resolution of the resistivity models. With the system response modelling scheme (Auken et al. 2020), the waveform, low-pass filters, etc. are not modelled separately but instead as a system response measured for the specific SkyTEM set-up. This approach enables accurate modelling of gates in the ramp down time.

For this survey, five extra gates (3–8) located during ramp down were included in the onshore inversion (Figure 4.1). The uncertainty of these data points was increased to 1.2 standard deviations (STD), which adds an additional 20% uncertainty compared to the 1.0 STD uncertainty utilised by the majority of the data points.

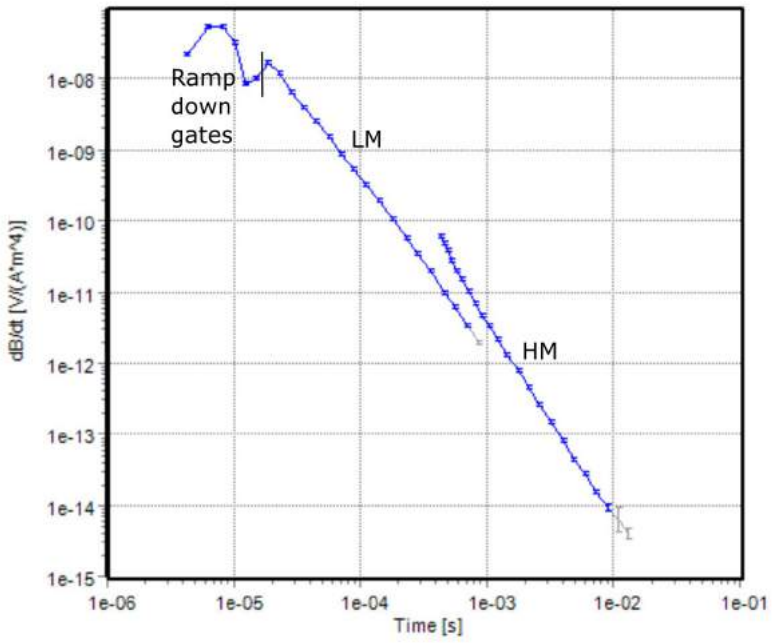

Figure 4.1 High-moment (right curve – HM) and low-moment (left curve – LM) dB/dt sounding curves. The gates left of the black line are located within the ramp down time.

4.2 Laterally Constrained Inversion

The LCI scheme is used for preliminary inversions of the SkyTEM data as part of the processing workflow. The LCI scheme uses constraints between the 1D models along flight lines. Ramp down gates 3–8 were not utilised for LCI inversions because they were used to generate smooth 1D models as a first pass to review data quality over the entire study area during post-processing and quality checks.

4.3 Spatially Constrained Inversion

The SCI scheme was used for the final inversions of the SkyTEM data. The SCI scheme uses constraints between the 1D models both along and across the flight lines, as shown in Figure 4.2. The constraints are scaled according to the distance between soundings.

The connections pattern of the constraints is designed using a Delaunay triangulation, which connects natural neighbour models. For line-oriented data, the Delaunay triangulation results in a model being connected to the two neighbour models at the flight line and typically 2–3 models at the adjacent flight lines (Figure 4.3).

Constraining the parameters enhances the resolution of resistivities and layer interfaces, which are not well resolved in independent inversion of the soundings.

SCI set-up parameters for this survey are listed in Table 4.1.

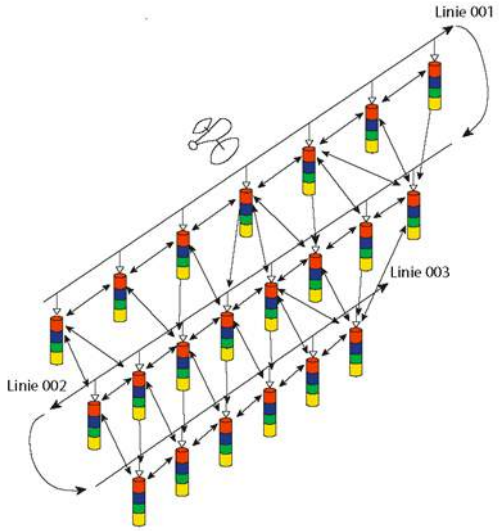

Figure 4.2 Schematic presentation of the spatially constrained inversion set-up. Constraints connect not only soundings located along the flight line but also those across them. Figure from HGG (2017).

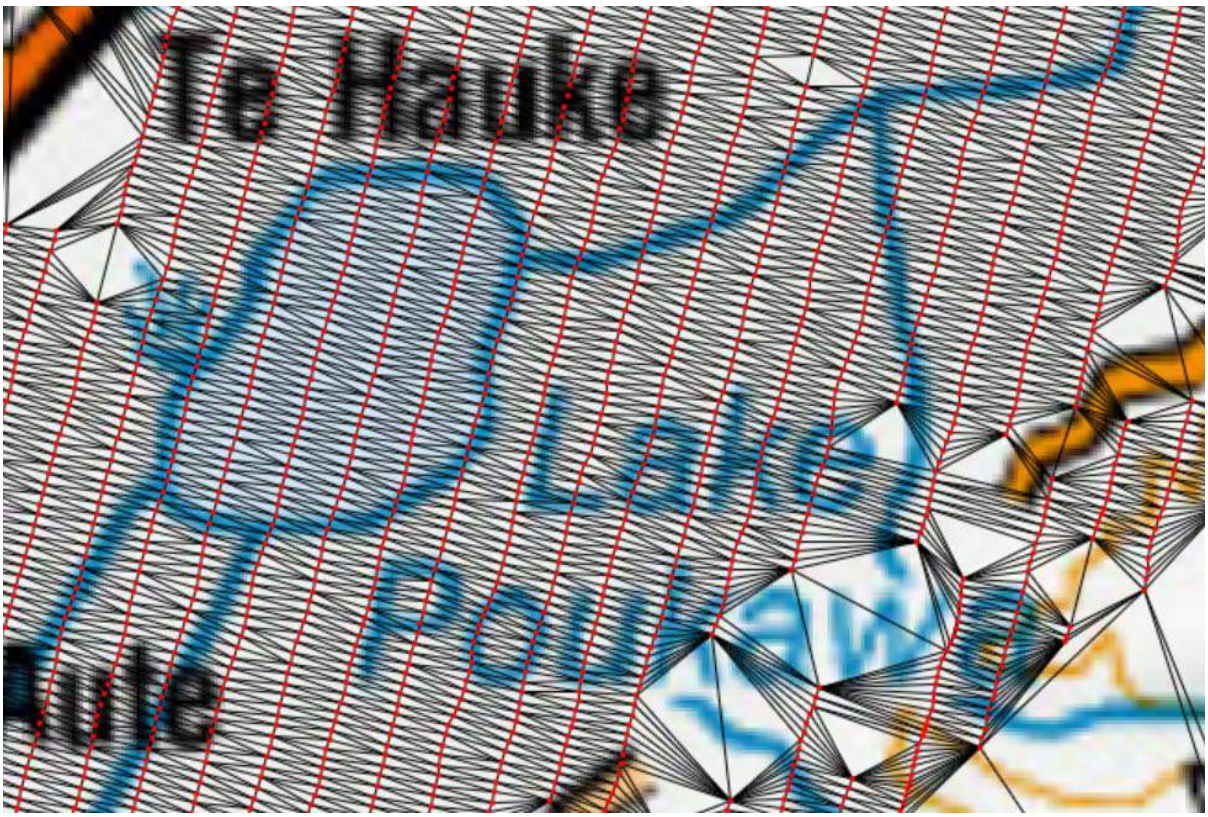

Figure 4.3 Example set-up of spatially constrained inversion constraints. The red points are the model positions. The black lines show the constraints created with the Delaunay triangles. The line distance in this example is 200 m.

4.4 Smooth, Sharp Inversion

Both a smooth and sharp model inversion were carried out. Both inversion types used the SCI set-up and the same model layers (Tables 4.2 and 4.4), but the regularisation scheme was different.

A smooth model is a many-layered model that uses a fixed layer structure (logarithmically increasing layer thicknesses), and the resistivity of each layer is solved for. The smooth regularisation scheme penalises the resistivity changes, resulting in the smoothest resistivity transitions both vertically and horizontally, as seen in Figure 4.4. As such, sharp geological layer boundaries may appear diffuse and picking geological layer boundaries is subjective. However, inclined layer sequences are more readily detected.

A sharp model uses the same model discretisation as the smooth model, but the model regularisation scheme is different. The sharp model regularisation scheme penalises the number of resistivity changes above a certain size, instead of the absolute resistivity changes (as in the smooth model regularisation scheme). The sharp model regularisation scheme therefore results in a model with few, but relatively sharp resistivity transitions. This allows for relative abrupt changes in resistivities while using the fixed layer thicknesses of the smooth model. An example is shown in Figure 4.4. Normally the SkyTEM are data explained equally well with the model types.

Assuming a geological layered environment, picking geological layer boundaries will be less subjective in a sharp model result compared to a smooth model.

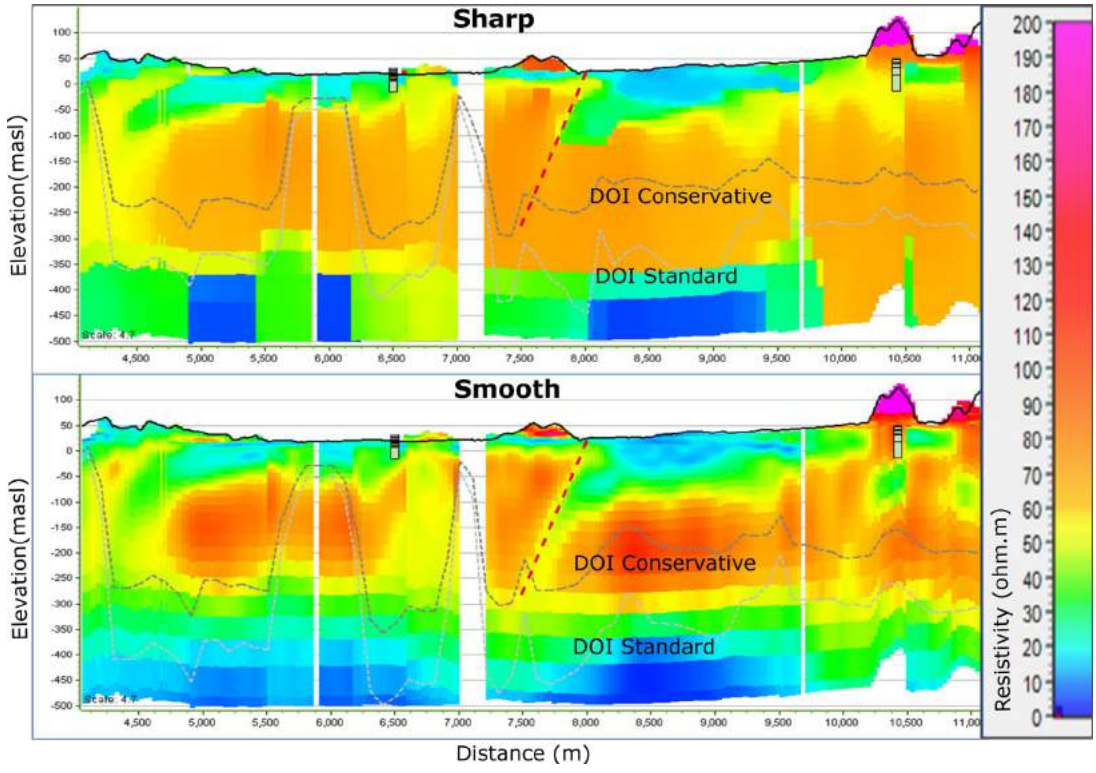

Figure 4.4 Profile examples of a sharp and smooth inversion of the same SkyTEM dataset showing resistivity in ohm.m. The grey lines show the depth of investigation (DOI; see Section 4.5). Dipping faults (approximate locations, consistent with surface fault maps [Heron 2018] and shown by the red dashed lines) are highlighted by the smooth model, while vertical layer boundaries are made more precise by the sharp model.

4.5 Depth of Investigation

For each resistivity model, a depth of investigation (DOI) is estimated, as described in Christiansen and Auken (2012). The DOI calculation takes into account the SkyTEM system transfer function, the number of data points, the data uncertainty and the resistivity model.

Electromagnetic fields are diffusive, and there is no discrete depth where information on the resistivity structure stops. Therefore, we provide both a conservative and standard DOI estimate. As a guideline, the resistivity structures above the DOI conservative value are well determined by the SkyTEM data; resistivity structures below the DOI standard value are very weakly determined by the data and should normally be disregarded.

The DOI conservative and standard estimates are included as point theme maps in Appendix 1. The cross-sections in Appendix 2 are blanked in depth at the DOI standard values. The resistivity models are blanked below the DOI standard value when compiling the mean resistivity maps.

5.0 MAPS AND CROSS-SECTIONS

To visualise the resistivity structures in the mapping area, a number of geophysical maps and cross-sections were created. Furthermore, a location map and a number of maps made for quality control are displayed in the appendices.

5.1 Location Map, Quality Control Maps

The location map and quality control maps described below are included in Appendix 1.

5.1.1 Model Location and Flight Lines

This map shows the actual flight lines. Black dots mark where data were disregarded due to line turns or noise. Blue dots mark where data were kept and inverted to a resistivity model.

Noisy data were primarily associated with powerlines, roads and the railway.

5.1.2 Moment Indication

This map shows whether both LM and HM data are present. In general, both moments were present for the whole survey. In some cases, noise was only observed in one of the moments, resulting in only data from the other moment being present.

5.1.3 Flight Altitude

This map shows the processed flight altitudes from the laser altimeters (distance from the frame to the ground). The flight altitude reflects the necessary safe distance to the ground, treetops, etc.

5.1.4 Data Residual

The data residual describes how well the obtained resistivity models explain the recorded data (how well the data is fitted). The data residual values are normalised with the data standard deviation, so a data residual below 1 corresponds to a fit within one standard deviation.

The data residual map in Appendix 1 is for the smooth inversion result. The data residuals for the sharp inversion are similar. There are some isolated areas that have relatively high data residual values (>2); this is primarily due to noisy data, which again is associated with low signal ground responses (resistive ground) and/or a high flight altitude. In general, the data residuals are very good (<0.6), which is expected for this type of environment and geological setting.

5.1.5 Number of Data Points

This map shows the number of data points (time gates from both HM and LM) in use for each resistivity model. Few data points correlate to areas with a low signal level (very resistive areas) and/or a relatively high flight altitude. The maximum number of data points available is 47 (24 LM and 23 HM gates).

5.1.6 Depth of Investigation

This map shows the DOI estimates for the smooth model inversion result (see Section 4.4 for a description of the DOI calculation). DOI maps in elevation and depths are included in Appendix 1.

5.2 Cross-Sections

Cross-sections of selected flight lines are included in Appendix 2. Each section shows the 1D models, which are blanked at the DOI standard value. Cross-sections of all flight lines are available in the delivered Aarhus Workbench workspace.

5.3 Mean Resistivity Maps

To make depth or horizontal slices, the mean resistivity in the depth or elevation intervals is calculated for each resistivity model and then interpolated to a regular grid.

Figure 5.1 shows how the resistivities of the layers in a model influence the calculation of the mean resistivity in a depth interval [A, B]. d_0 is the surface; d_1, d_2 and d_3 are the depths to the layer boundaries in the model. ρ_1, ρ_2, ρ_3 and ρ_4 are the resistivities of the layers.

The model is subdivided into sub-thicknesses $\Delta t_{1–3}$. The mean resistivity (ρ_{vertical}) is calculated as:

$$\rho_{vertical} = \frac{\rho_1 \cdot \Delta t_1 + \rho_2 \cdot \Delta t_2 + \rho_3 \cdot \Delta t_3}{\Delta t_1 + \Delta t_2 + \Delta t_3}$$

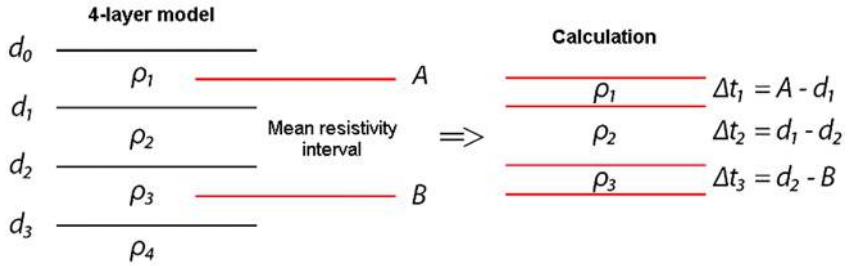

Figure 5.1 Illustration of how the resistivities of layers influence the mean resistivities in a depth interval [A, B]. Figure from HGG (2017).

In general terms, the mean resistivities in a depth interval are calculated using the equation below:

$$\bar{\rho} = \frac{\sum_{i=1}^{n} \rho_i \cdot \Delta t_i}{\sum_{i=1}^{n} \Delta t_i}$$

where *i* runs through the interval from 1 to the number of sub-thicknesses. The mean resistivity calculated by the above formula (ρ_{vertical}) is named the vertical mean resistivity, which is equal to the total resistance if a current flows vertically through the interval.

Resistivity mapping with a horizontal transmitter coil, only generates horizontal current flows in the ground. It is therefore most correct to perform the mean resistivity calculation with respect to a horizontal current flow in the mean resistivity interval. The horizontal mean resistivity ($\rho_{\text{horizontal}}$) is equal to the reciprocal of the mean conductivity (σ_{mean}) and is calculated as:

$$\rho_{horizontal} = \frac{1}{\sigma_{mean}} = \left[\frac{\sum_{1=1}^{n} \left(\frac{1}{\rho_i}\right) \cdot \Delta t_i}{\sum_{i=1}^{n} \Delta t_i} \right]^{-1}$$

For this survey, horizontal mean resistivity themes have been generated from the smooth model inversion. The resistivity models have been blanked at the DOI standard value prior to interpolating to the regular mean resistivity grids.

The interpolation of the mean resistivity values to regular grids was performed by Kriging interpolation, with a node spacing of 40 m, a search radius of 400 m and additional pixel smoothing in the presented bitmap images. The mean resistivity maps are placed in Appendix 3.

5.4 Deliverables

All digital maps and data are geo-referenced to coordinate system New Zealand Transverse Mercator (NZTM 2000) and New Zealand Vertical Datum 2020 (NZVD2016). Further details on the dataset formats are provided in Appendix 4.

It is possible that resistivity models could be regenerated in the future: for example, if a different DEM or inversion parameters were to be utilised (e.g. due to the collection of new information). Therefore, models are labelled as version 1, developed in the year 2021 (V1_2021).

5.4.1 Primary Datasets

The primary datasets delivered are the full resistivity models, which are delivered in readily accessible fixed format text files:

- *\xyz_ascii\Heretaunga_smooth_resistivitymodel_V1_2021_inv.xyz*
- *\xyz_ascii\Heretaunga _sharp_resistivitymodel_V1_2021_inv.xyz*
- *\xyz_ascii\Heretaunga_offshore_smooth_resistivitymodel_V1_2021_inv.xyz*
- *\xyz_ascii\Heretaunga _offshore_sharp_resistivitymodel_V1_2021_inv.xyz*

For example, the data can be read into Python via the following three lines of code:

```
import pandas as pd

headers=pd.read_csv(r'xyz_ascii\Heretaunga_smooth_resistivitymodel
_V1_2021_inv.xyz', delimiter='\s+', skiprows=26).columns[1:]

res=pd.read_csv(r'xyz_ascii\Heretaunga_smooth_resistivitymodel_V1_
2021_inv.xyz', delimiter='\s+', skiprows=27, names=headers)
```

Additionally, the Aarhus Workbench workspace is delivered, which contains the raw data, processed data, inversion results, theme maps and profiles. The workspace holds both the smooth and sharp inversion results. Proprietary Aarhus Workbench software from Aarhus GeoSoftware is required to open the files. This workspace could be utilised in the future for any changes, such as new DEM models and re-inversions.

- *AarhusWorkbenchWS_Heretaunga_V1_2021.zip*

Resistivity model *.gdb* files (Firebird database format used by, for example, proprietary Aarhus Workbench Software and Geoscene3D software) are also provided for both the sharp and smooth model:

- *\gdb\Heretaunga_smooth_resistivitymodel_V1_2021.gdb*
- *\gdb\Heretaunga_sharp_resistivitymodel_V1_2021.gdb*
- *\gdb\Heretaunga_offshore_smooth_resistivitymodel_V1_2021.gdb*
- *\gdb\Heretaunga _offshore_sharp_resistivitymodel_V1_2021.gdb*

5.4.2 Supplementary Datasets

Additional datasets are provided that can be derived from the primary datasets to provide immediate visualisation of select aspects of the primary datasets or provide additional information, such as quality control maps.

- Resistivity models in *.xyz* files (e.g. for importing into Leapfrog Software) for both the sharp and smooth model:
  - *\xyz\Heretaunga_smooth_resistivitymodel_V1_2021.xyz*
  - *\xyz\Heretaunga_sharp_resistivitymodel_V1_2021.xyz*
  - *\xyz\Heretaunga_offshore_smooth_resistivitymodel_V1_2021.xyz*
  - *\xyz\Heretaunga_offshore_sharp_resistivitymodel_V1_2021.xyz*
- Resistivity models in xyz-ascii files for both the sharp and smooth model. These include a *_dat.xyz* file with the data, as it was used in the inversion, and a *_syn.xyz* file with the synthetic forward calculation of the final model:
  - *\xyz_ascii\Heretaunga_smooth_resistivitymodel_V1_2021_dat.xyz*
  - *\xyz_ascii\Heretaunga_sharp_resistivitymodel_V1_2021_dat.xyz*
  - *\xyz_ascii\Heretaunga_offshore_smooth_resistivitymodel_V1_2021_dat.xyz*
  - *\xyz_ascii\Heretaunga_offshore_sharp_resistivitymodel_V1_2021_dat.xyz*
  - *\xyz_ascii\Heretaunga_smooth_resistivitymodel_V1_2021_syn.xyz*
  - *\xyz_ascii\Heretaunga_sharp_resistivitymodel_V1_2021_syn.xyz*
  - *\xyz_ascii\Heretaunga_offshore_smooth_resistivitymodel_V1_2021_syn.xyz*
  - *\xyz_ascii\Heretaunga_offshore_sharp_resistivitymodel_V1_2021_syn.xyz*
- Mean resistivity maps in depth (m) intervals (*XXXm_YYYm* corresponds to the interval from XXX m to YYY m) as image GeoTIFF files, ArcGIS ascii grid files and ArcGIS point shapefile format:
  - *\MRESD_smooth\XXXm_YYYm.tif*
  - *\MRESD_smooth\XXXm_YYYm.asc*
  - *\MRESD_smooth\XXXm_YYYm.shp*
  - *\MRESD_smooth\offshore_XXXm_YYYm.tif*
  - *\MRESD_smooth\offshore_XXXm_YYYm.asc*
  - *\MRESD_smooth\offshore_XXXm_YYYm.shp*
  - *\MRESD_sharp\XXXm_YYYm.tif*
  - *\MRESD_sharp\XXXm_YYYm.asc*
  - *\MRESD_sharp\XXXm_YYYm.shp*
  - *\MRESD_sharp\offshore_XXXm_YYYm.tif*
  - *\MRESD_sharp\offshore_XXXm_YYYm.asc*
  - *\MRESD_sharp\offshore_XXXm_YYYm.shp*
- Resistivity of each layer in ArcGIS point shapefile format, where X is in the range 1–35:
  - *\layers\smooth_ResInv_LayerX.shp*
  - *\layers\sharp_ResInv_LayerX.shp*

- *\layers\smooth_offshore_ResInv_LayerX.shp*
- *\layers\sharp_offshore_ResInv_LayerX.shp*

- Quality control maps in ArcGIS point shapefile format:
  - *\QC_maps\Heretaunga_AltInp.shp*
  - *\QC_maps\Heretaunga_ChaNum.shp*
  - *\QC_maps\Heretaunga_NoData_ChAll.shp*
  - *\QC_maps\Heretaunga_sharp_DOICon.shp*
  - *\QC_maps\Heretaunga_sharp_DOIConE.shp*
  - *\QC_maps\Heretaunga_sharp_DOISta.shp*
  - *\QC_maps\Heretaunga_sharp_DOIStaE.shp*
  - *\QC_maps\Heretaunga_sharp_DataRes_ChAll.shp*
  - *\QC_maps\Heretaunga_smooth_DOICon.shp*
  - *\QC_maps\Heretaunga_smooth_DOIConE.shp*
  - *\QC_maps\Heretaunga_smooth_DOISta.shp*
  - *\QC_maps\Heretaunga_smooth_DOIStaE.shp*
  - *\QC_maps\Heretaunga_smooth_DataRes_ChAll.shp*
  - *\QC_maps\Heretaunga_offshore_AltInp.shp*
  - *\QC_maps\Heretaunga_offshore_ChaNum.shp*
  - *\QC_maps\Heretaunga_offshore_NoData_ChAll.shp*
  - *\QC_maps\Heretaunga_offshore_sharp_DOICon.shp*
  - *\QC_maps\Heretaunga_offshore_sharp_DOIConE.shp*
  - *\QC_maps\Heretaunga_offshore_sharp_DOISta.shp*
  - *\QC_maps\Heretaunga_offshore_sharp_DOIStaE.shp*
  - *\QC_maps\Heretaunga_offshore_sharp_DataRes_ChAll.shp*
  - *\QC_maps\Heretaunga_offshore_smooth_DOICon.shp*
  - *\QC_maps\Heretaunga_offshore_smooth_DOIConE.shp*
  - *\QC_maps\Heretaunga_offshore_smooth_DOISta.shp*
  - *\QC_maps\Heretaunga_offshore_smooth_DOIStaE.shp*
  - *\QC_maps\Heretaunga_offshore_smooth_DataRes_ChAll.shp*

5.4.3 Input Datasets

The primary input datasets utilised were provided to HBRC as part of the SkyTEM Australia Pty Ltd (2020) report (see Section 1). An additional dataset utilised in this report was a 10 m resolution DEM in NZVD2016, which was derived from a 5 m resolution DEM that was created by HBRC using a combination of LiDAR and SRTM V2 data (Farrier 2020; see Section 3.5).

- *\DEM\HBRCSkyTEM_DEM_10m.asc*

6.0 CONCLUSION

In January/February 2020, 2610.1 km of SkyTEM data were collected over the Heretaunga Plains, including four offshore lines. Both automatic and manual data processing was carried out to remove electromagnetic noise from the low-moment and high-moment data. This processing was quality checked, post-processing was undertaken to check for any remaining artefacts and then a final quality check was undertaken.

Using the retained data, spatially constrained inversions were performed, creating both smooth and sharp resistivity models. Different inversion parameters were utilised for the four offshore flight lines, so separate resistivity models are provided for the onshore and offshore data. For the onshore data, the system response modelling approach was used in the inversion of the data, enabling modelling of five additional time gates in the ramp down time and thus providing higher resolution in the near-surface.

The SkyTEM survey reveals a detailed 3D resistivity picture of the subsurface. The onshore resistivity models have layer thicknesses of 1 m in the near-surface, increasing to 59 m at depth. For the smooth onshore model, the standard depth of investigation varies from 12 m (where only low-moment data was kept due to noise) to 650 m, with a mean of 276 m. The offshore resistivity models have layer thicknesses of 0.1 m in the near-surface, increasing to 10.6 m at depth. For the smooth offshore model, the standard depth of investigation varies from 20 m to 72 m, with a mean of 30 m.

Images of the resistivity model are made available in this report, and digital datasets have also been provided to HBRC.

Hydrogeological interpretation of the 3D resistivity results is needed to make full use of the SkyTEM survey results. This additional work will be described within a separate report.

7.0 ACKNOWLEDGEMENTS

This work has been jointly funded by the New Zealand Government's Provincial Growth Fund, Hawke's Bay Regional Council and GNS Science's Strategic Science Investment Fund (Ministry of Business, Innovation & Employment).

Thank you to Jeff Smith, Simon Harper, Tim Farrier (DEM) and Michelle McGuinness (Communications) of Hawke's Bay Regional Council for their contributions to this project. Thank you to Amanda Langley and Libby Tosswill of Project Haus for project management support.

Thank you to Chris Worts for Business Partnerships support and to Tusar Sahoo for contributions to Figure 4.4.

8.0 REFERENCES

Auken E, Christiansen AV, Kirkegaard C, Fiandaca G, Schamper C, Behroozmand AA, Binley A, Nielsen E, Effersø F, Christensen NB, et al. 2015. An overview of a highly versatile forward and stable inverse algorithm for airborne, ground-based and borehole electromagnetic and electric data. *Exploration Geophysics*. 46(3):223–235. doi:10.1071/EG13097.

Auken E, Christiansen AV, Westergaard JH, Kirkegaard C, Foged N, Viezzoli A. 2009. An integrated processing scheme for high-resolution airborne electromagnetic surveys, the SkyTEM system. *Exploration Geophysics*. 40(2):184–192. doi:10.1071/EG08128.

Auken E, Foged N, Andersen KR, Nyboe NS, Christiansen AV. 2020. On-time modelling using system response convolution for improved shallow resolution of the subsurface in airborne TEM. *Exploration Geophysics*. 51(1):4–13. doi:10.1080/08123985.2019.1662292.

Christiansen AV, Auken E. 2012. A global measure for depth of investigation. *Geophysics*. 77(4):WB171–WB177. doi:10.1190/geo2011-0393.1.

Farrier T. 2020. 3D Aquifier Mapping Project DEM Version 2. Napier (NZ): Hawke's Bay Regional Council.

[HBRC] Hawke's Bay Regional Council. 2021. Napier (NZ): Hawke's Bay Regional Council. Site: HAWQi. Offshore monitoring; [accessed 2021 Sep]. https://data.hbrc.govt.nz/hydrotel/cgi-bin/hydwebserver.cgi/sites/details?site=2782&treecatchment=1818

Heron DW, custodian. 2018. Geological map of New Zealand 1:250,000. 2nd ed. Lower Hutt (NZ): GNS Science. 1 USB. (GNS Science geological map; 1).

[HGG] HydroGeophysics Group, Aarhus University. 2011. Guideline and standards for SkyTEM measurements, processing and inversion. Aarhus (DK): Aarhus University; [accessed 2020 Nov]. http://www.hgg.geo.au.dk/rapporter/SkyTEMGuideEN.pdf

[HGG] HydroGeophysics Group, Aarhus University. 2017. SkyTEM survey Drenthe. Aarhus (DK): Aarhus University. 25 p. + appendices. Report 15-06-2017.

Jørgensen F, Lykke-Andersen H, Sandersen PBE, Auken E, Nørmark E. 2003. Geophysical investigations of buried Quaternary valleys in Denmark: an integrated application of transient electromagnetic soundings, reflection seismic surveys and exploratory drillings. *Journal of Applied Geophysics*. 53(4):215–228. doi:10.1016/j.jappgeo.2003.08.017.

[LINZ] Toitū Te Whenua Land Information New Zealand. 2021. Wellington (NZ): LINZ. Topo250 maps; [updated 2021 Sep 9; accessed 2021 Sep]. http://www.linz.govt.nz/land/maps/linz-topographic-maps/topo250-maps

LINZ Data Service. 2021. Wellington (NZ): Toitū Te Whenua Land Information New Zealand. LINZ Data Service; [updated 2021 Sep 14; accessed 2021 Sep]. https://data.linz.govt.nz/

Nabighian MN, Macnae JC. 1991. Time domain electromagnetic prospecting methods. In: Nabighian MN, editor. *Electromagnetic methods in applied geophysics: volume 2, applications, part A and part B*. Tulsa (OK): Society of Exploration Geophysicists. p. 427–520.

Rawlinson ZJ, Westerhoff RS, Kellett RL, Pederson JB, Maurya JB, Foged N. 2021. Hawke's Bay 3D Aquifer Mapping Project: Poukawa and Otane Basin SkyTEM data processing and resistivity models. Wairakei (NZ): GNS Science. 76 p. Consultancy Report 2020/138. Prepared for Hawke's Bay Regional Council.

SkyTEM Australia Pty Ltd. 2020. Acquisition and processing report: SkyTEM helicopter EM survey, Hawkes Bay, NZ. Malaga (AU): SkyTEM Australia Pty Ltd. 33 p. Report AUS 10056. Prepared for Hawke's Bay Regional Council.

Sørensen KI, Auken E. 2004. SkyTEM – a new high-resolution helicopter transient electromagnetic system. *Exploration Geophysics*. 35(3):194–202. doi:10.1071/EG04194.

This page left intentionally blank.

APPENDICES

This page left intentionally blank.

APPENDIX 1 LOCATION MAPS, QUALITY CONTROL MAPS

This appendix includes maps of:

- Model location and flight lines
- Model moment indication
- Flight altitude
- Data residual
- Number of datapoints
- Depth of investigation, in elevation and depth.

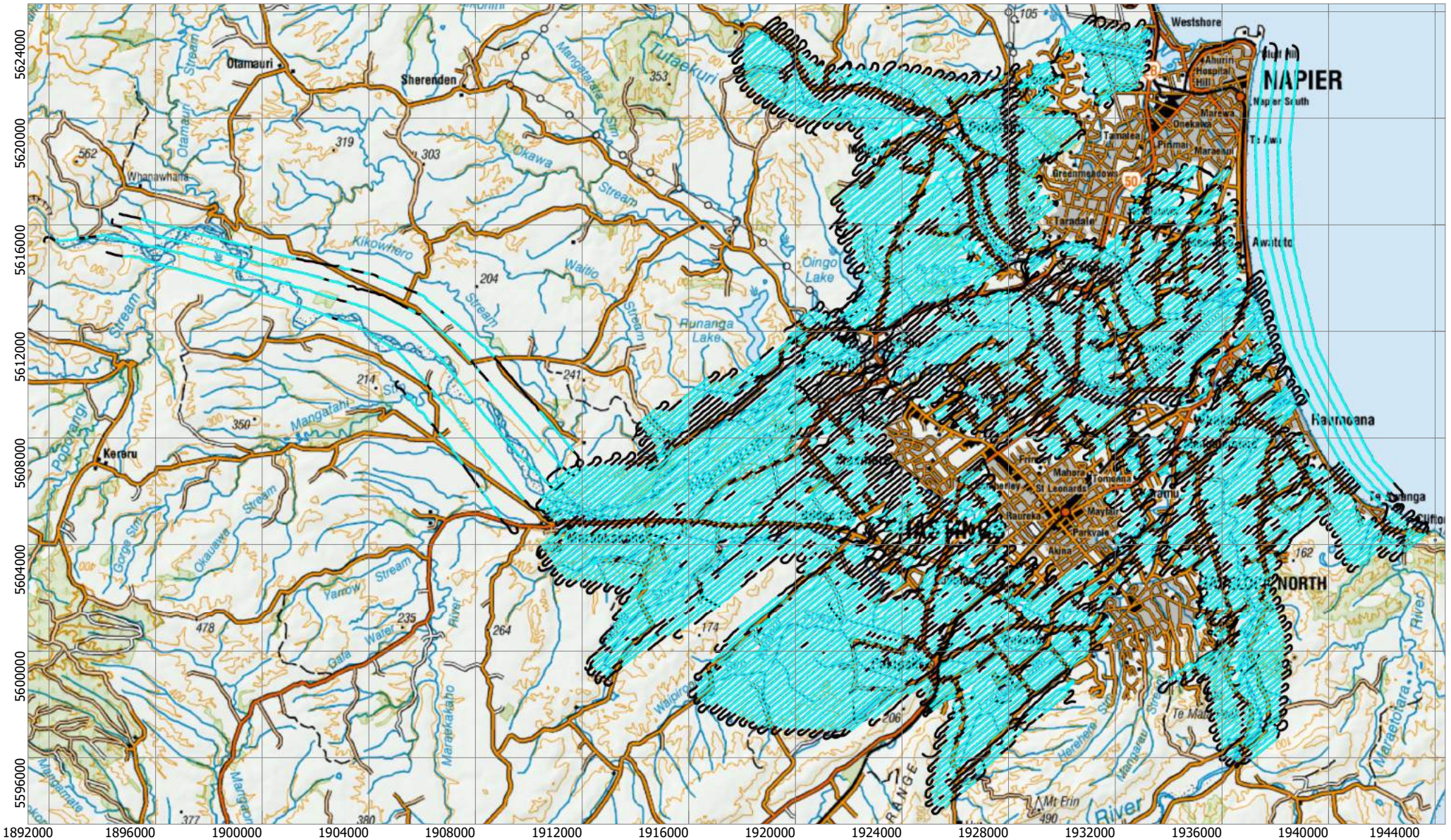

Confidential 2021

GNS SCIENCE TE PŪ AO

GNS Science Consultancy Report 2021/93

SkyTEM Survey Heretaunga 2020

Location, flight lines

Blue: 1D model; Black: Discarded data

NZTM2000

15 km

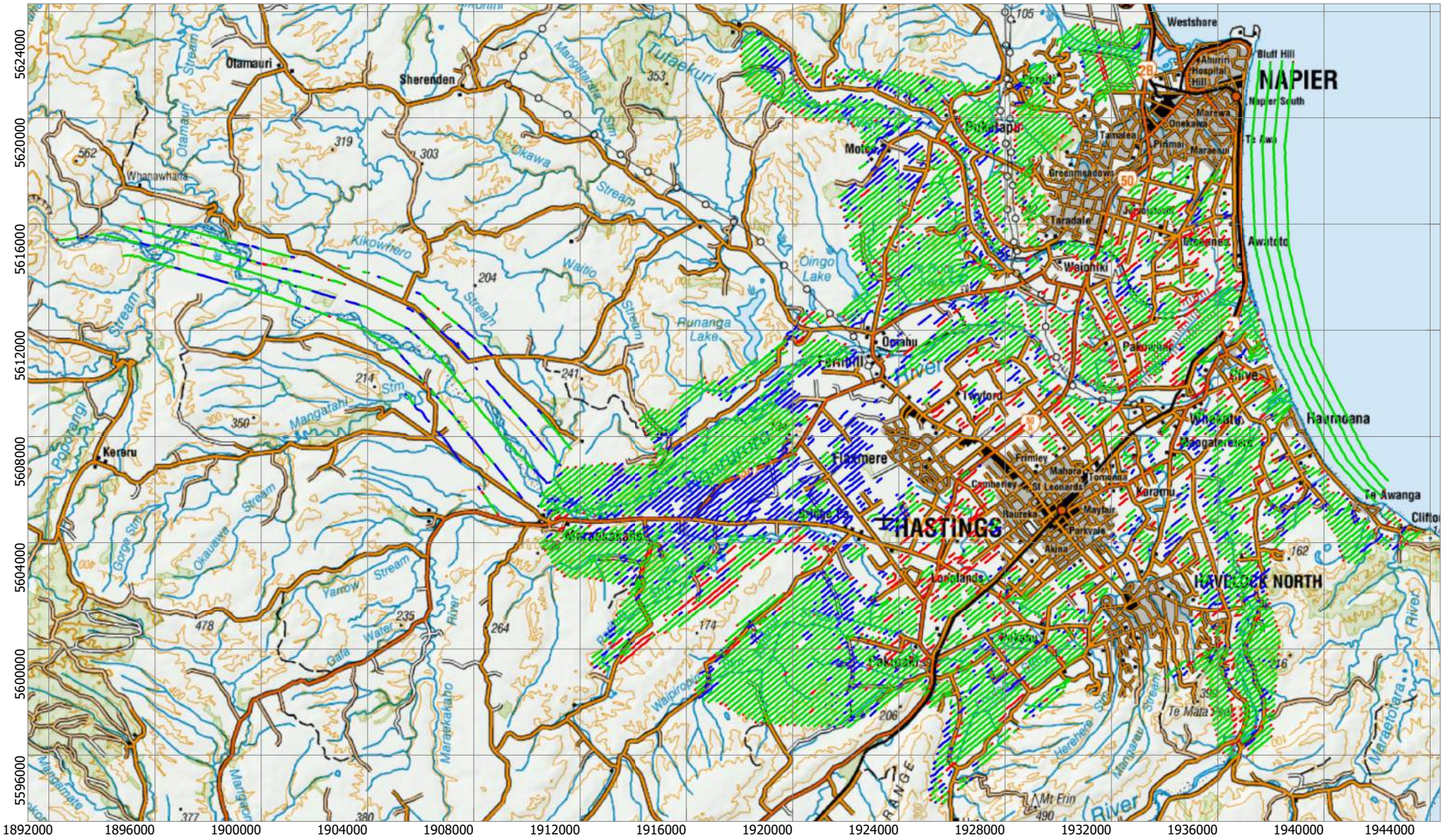

Confidential 2021

GNS SCIENCE TE PŪ AO

GNS Science Consultancy Report 2021/93

SkyTEM Survey Heretaunga 2020

Model Moment Indications

Green: LM and HM; Red: LM only; Blue: HM only

NZTM2000

15 km

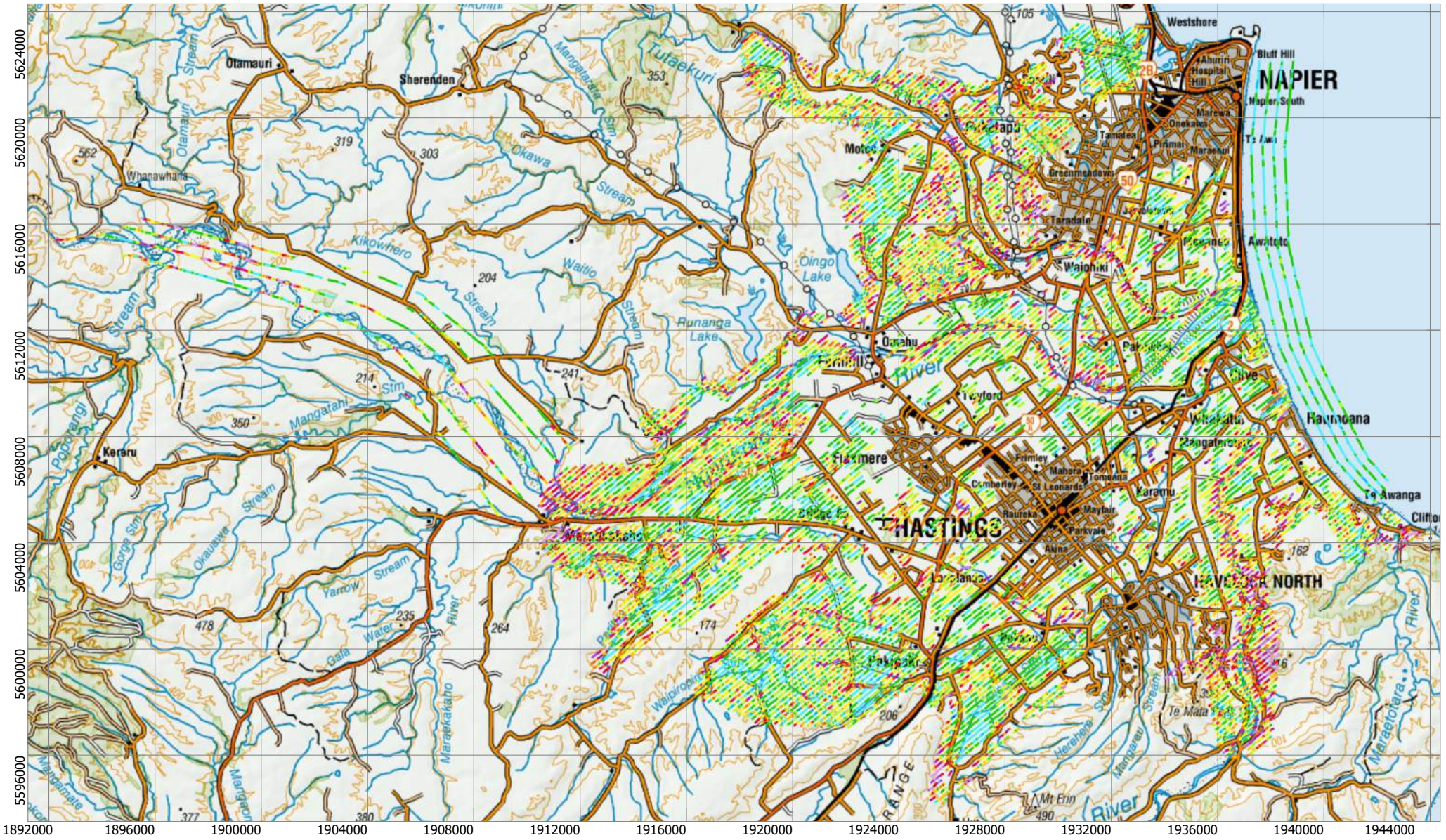

Confidential 2021

GNS SCIENCE TE PŪ AO

GNS Science Consultancy Report 2021/93

SkyTEM Survey Heretaunga 2020

10.0 20.0 30.0 40.0 50.0 60.0 70.0 80.0 90.0 100.0

Altitude [m]

Flight Altitude

Elevation, metres

NZTM2000

15 km

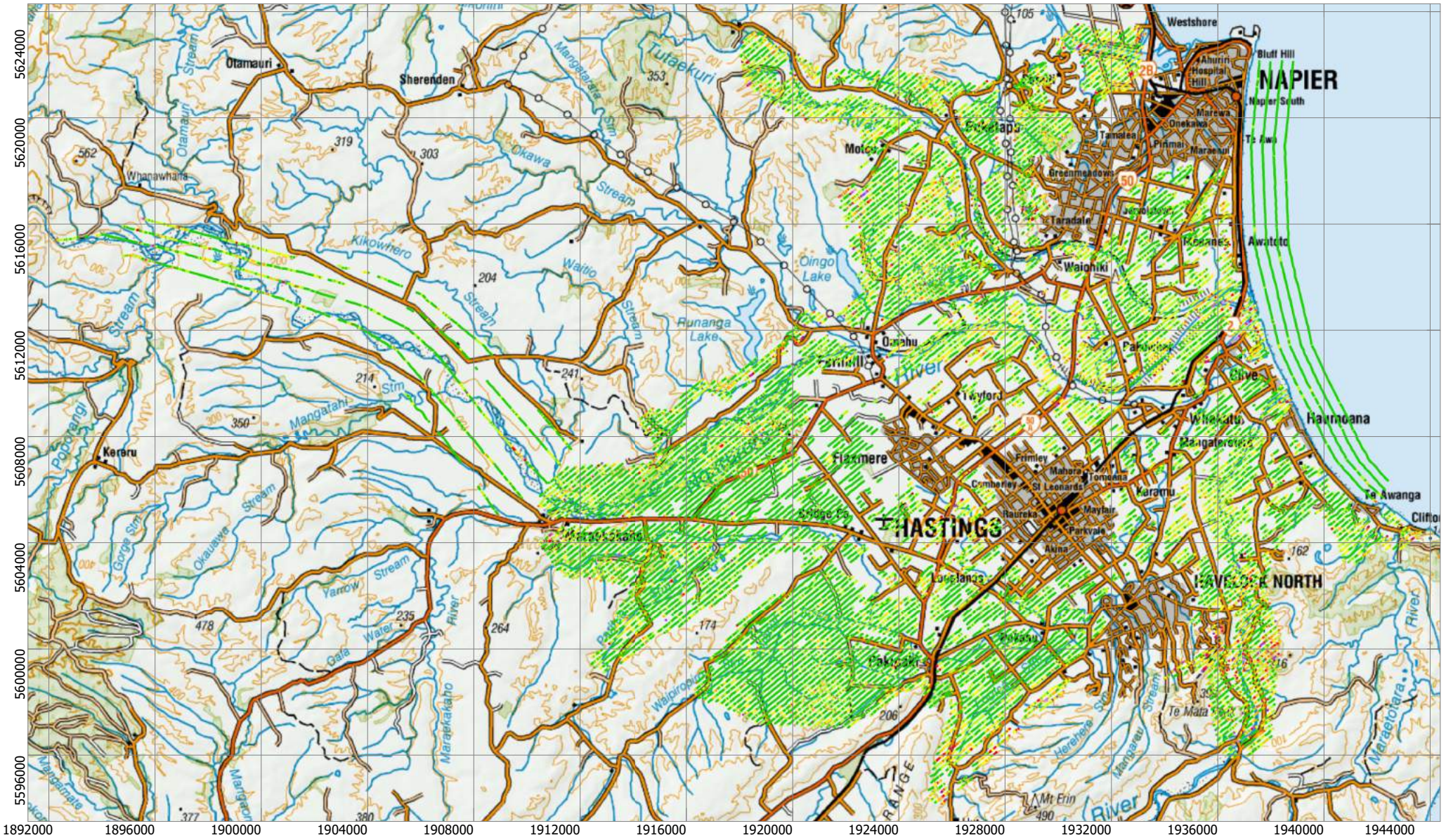

Confidential 2021

GNS SCIENCE TE PŪ AO

GNS Science Consultancy Report 2021/93

SkyTEM Survey Heretaunga 2020

0.2 0.4 0.6 0.8 1.0 1.2 1.4 1.6 1.8 2.0 2.2 2.4 2.6 2.8 3.0 3.2 3.4

Data Residual

Below one corresponds to a fit within one standard deviation

NZTM2000

15 km

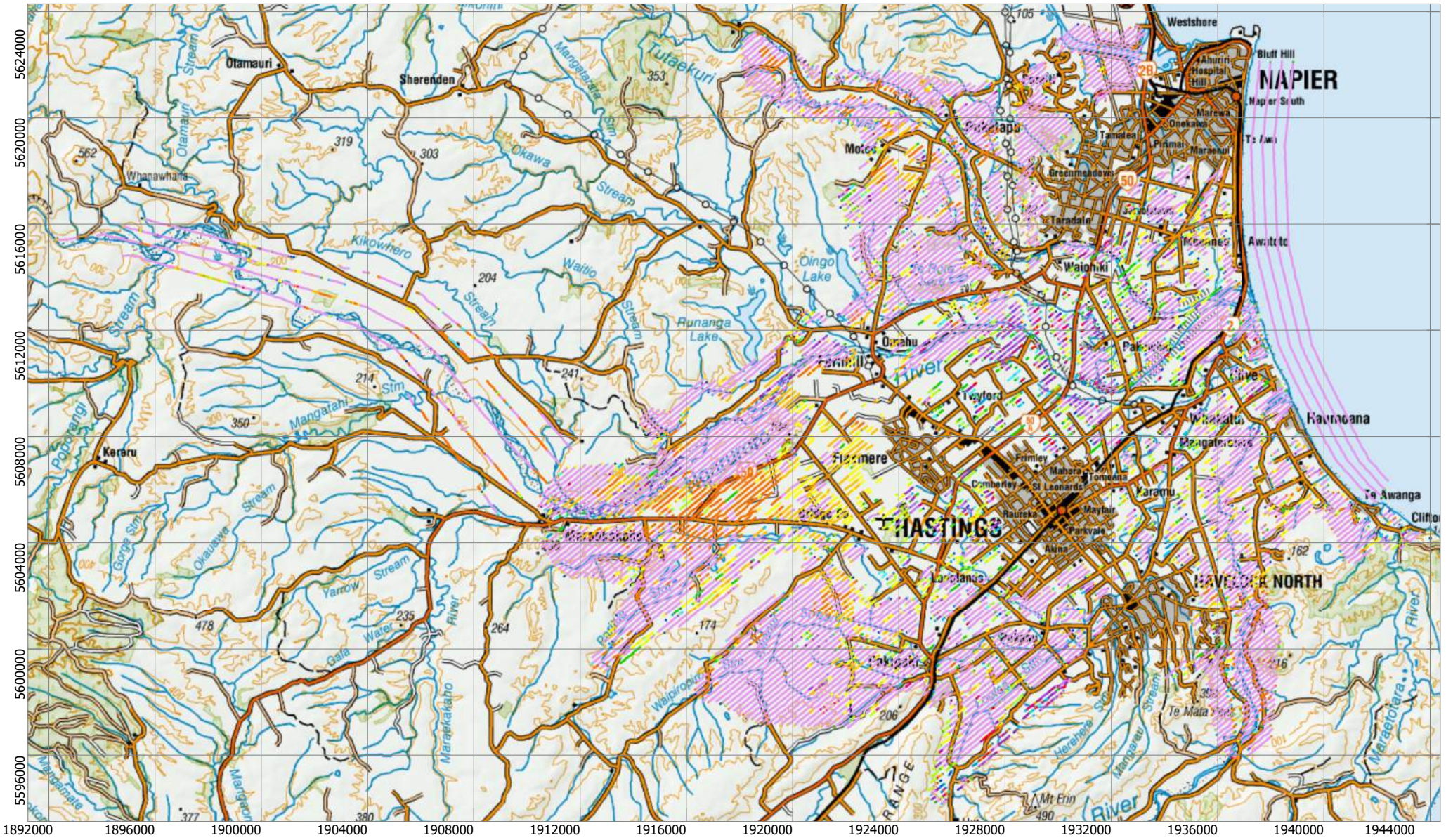

Confidential 2021

GNS SCIENCE TE PŪ AO

GNS Science Consultancy Report 2021/93

SkyTEM Survey Heretaunga 2020

0.0 2.0 4.0 6.0 8.0 10.0 12.0 14.0 16.0 18.0 20.0 22.0 24.0 26.0 28.0 30.0 32.0 34.0 36.0

Number of data points

Time gates used for inversion

NZTM2000

15 km

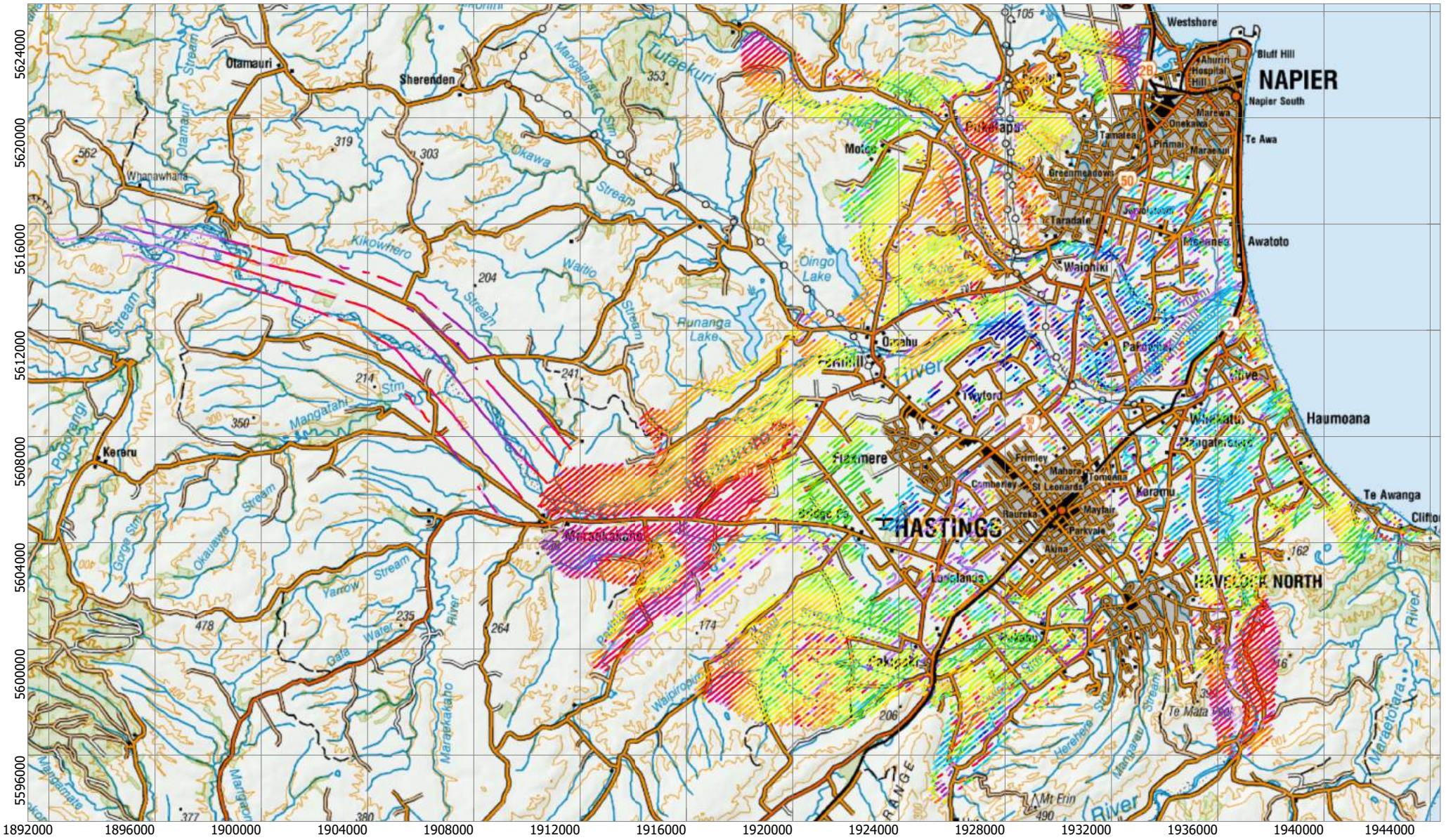

Confidential 2021

GNS SCIENCE TE PŪ AO

GNS Science Consultancy Report 2021/93

SkyTEM Survey Heretaunga 2020

-500.0 -450.0 -400.0 -350.0 -300.0 -250.0 -200.0 -150.0 -100.0 -50.0 0.0

Elevation [m]

Depth of Investigation, Standard

Elevation, metres

NZTM2000

15 km

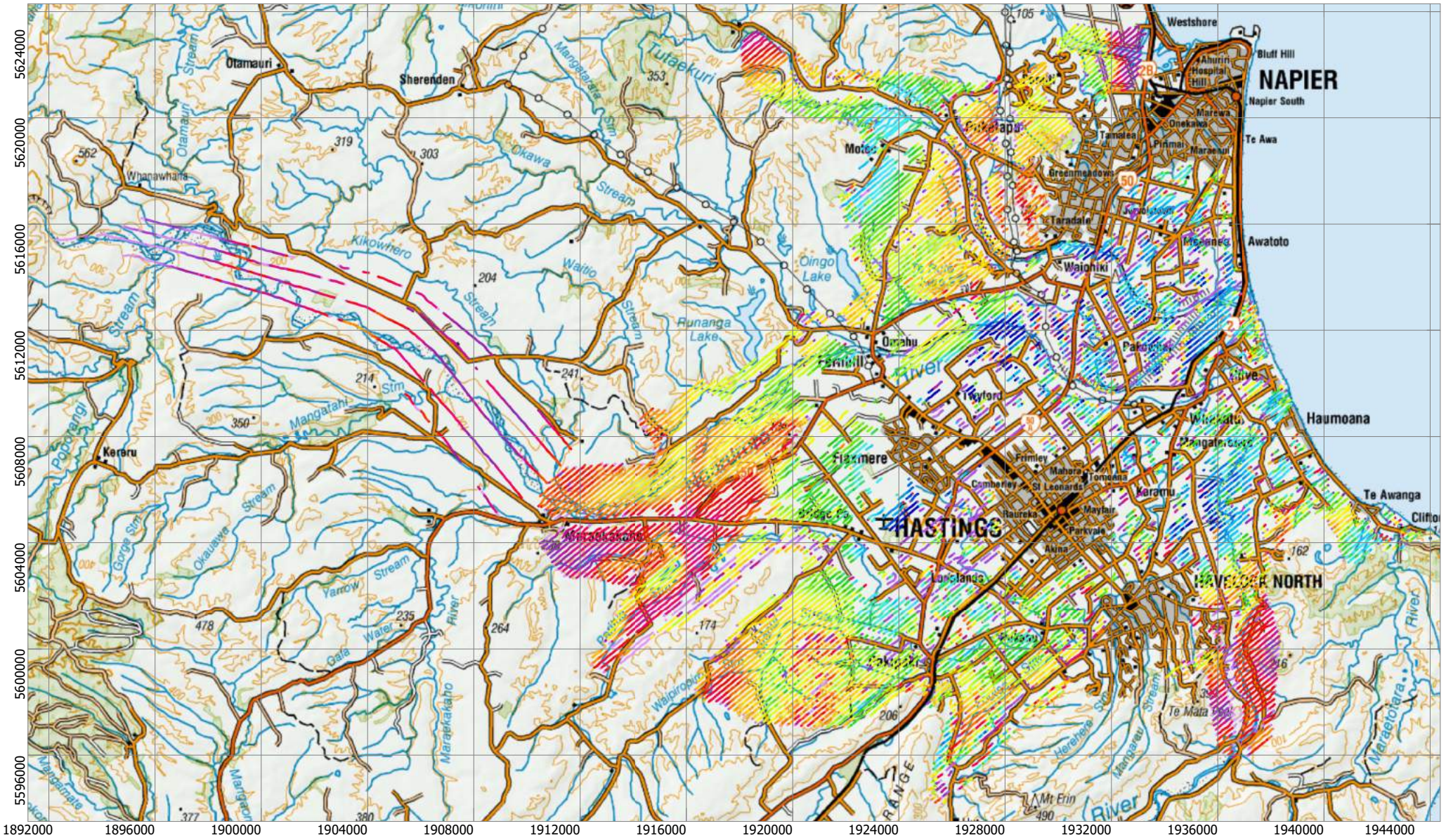

Confidential 2021

GNS SCIENCE TE PŪ AO

GNS Science Consultancy Report 2021/93

SkyTEM Survey Heretaunga 2020

-350.0 -300.0 -250.0 -200.0 -150.0 -100.0 -50.0 0.0

Elevation [m]

Depth of Investigation, Conservative

Elevation, metres

NZTM2000

15 km

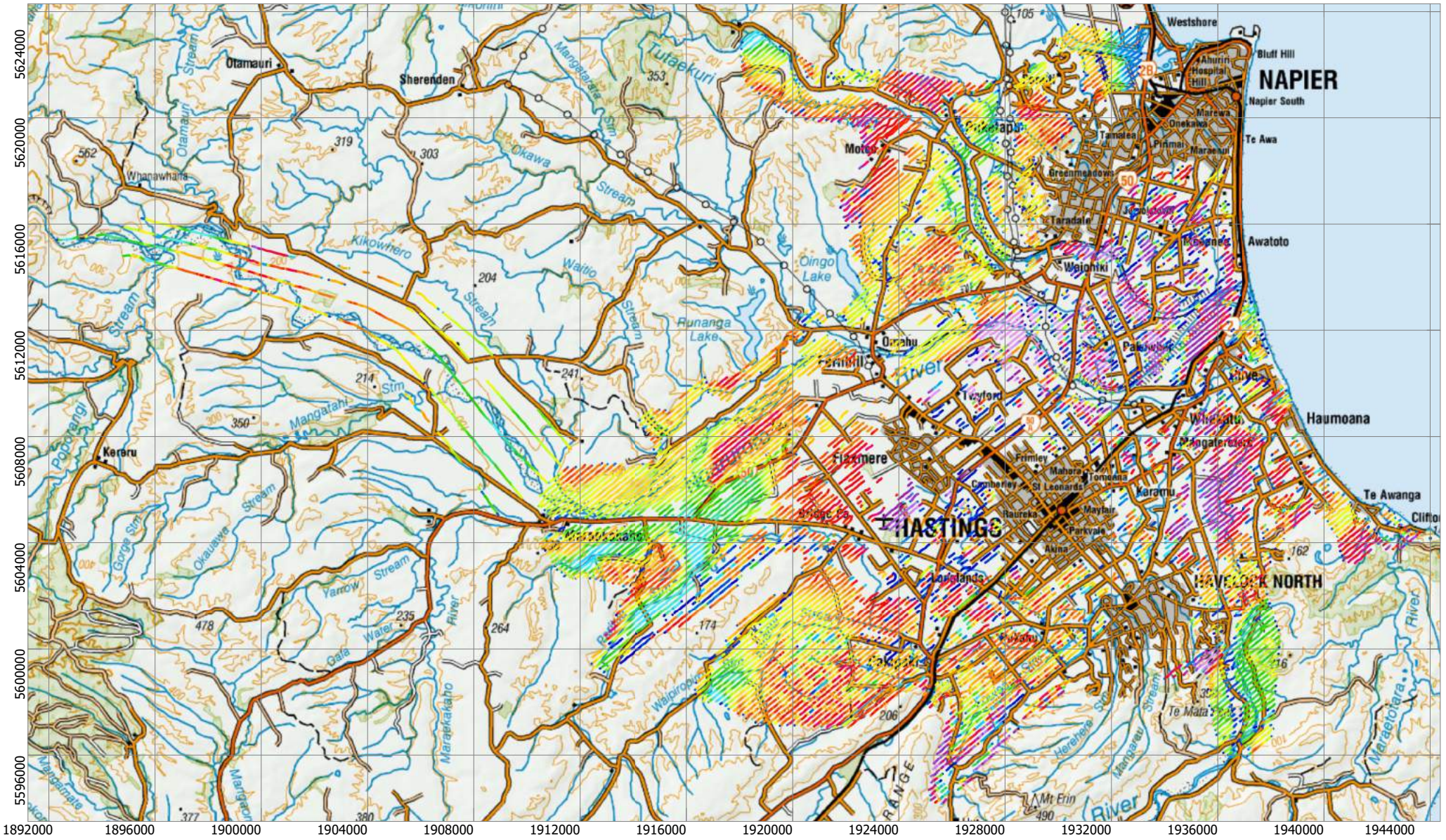

Confidential 2021

GNS SCIENCE TE PŪ AO

GNS Science Consultancy Report 2021/93

SkyTEM Survey Heretaunga 2020

50.0 100.0 150.0 200.0 250.0 300.0 350.0 400.0 450.0 500.0

Depth [m]

Depth of Investigation, Standard

Depth, metres

NZTM2000

15 km

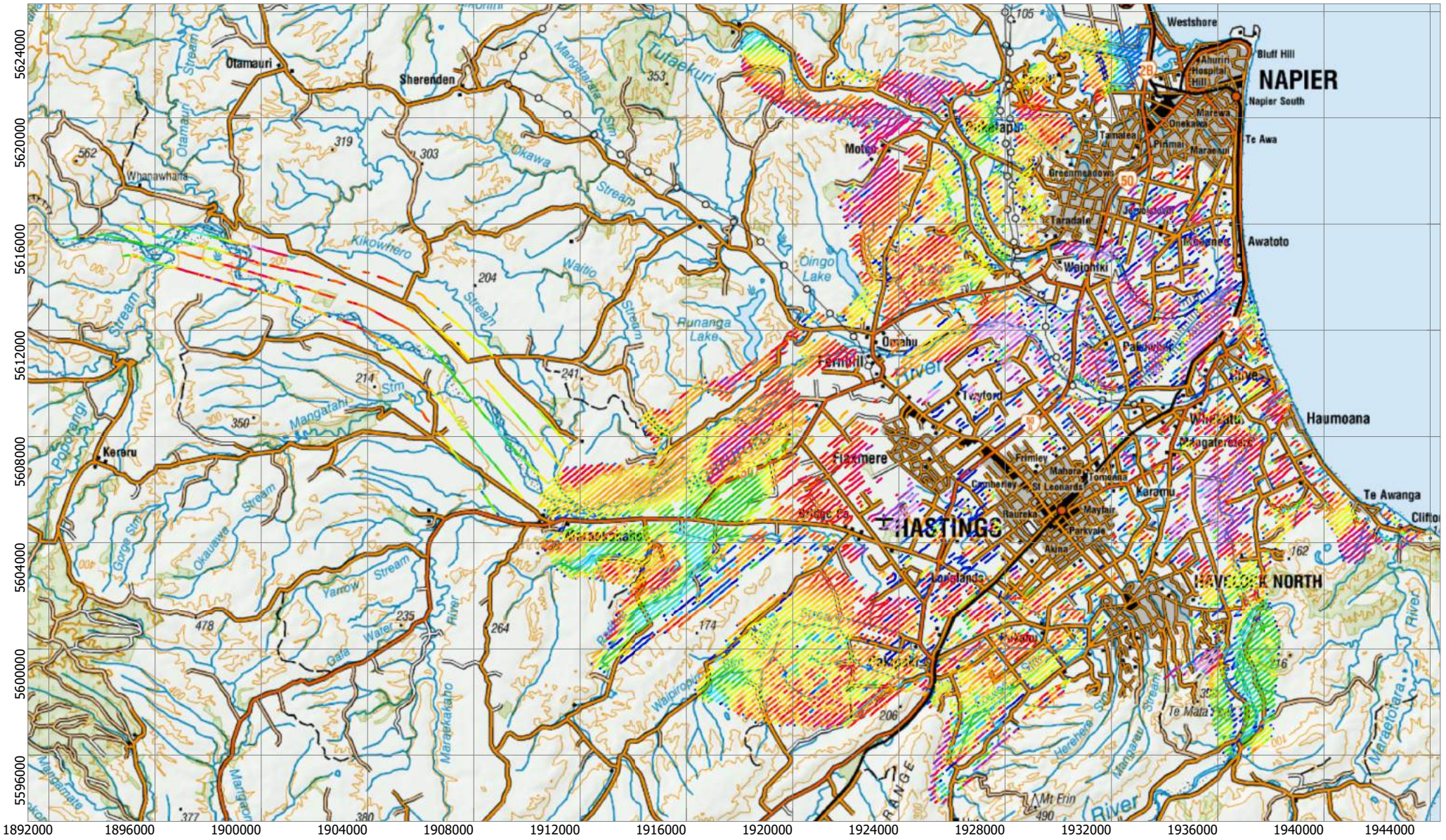

Confidential 2021

GNS SCIENCE TE PŪ AO

GNS Science Consultancy Report 2021/93

SkyTEM Survey Heretaunga 2020

50.0 100.0 150.0 200.0 250.0 300.0 350.0 400.0

Depth [m]

Depth of Investigation, Conservative

Depth, metres

NZTM2000

15 km

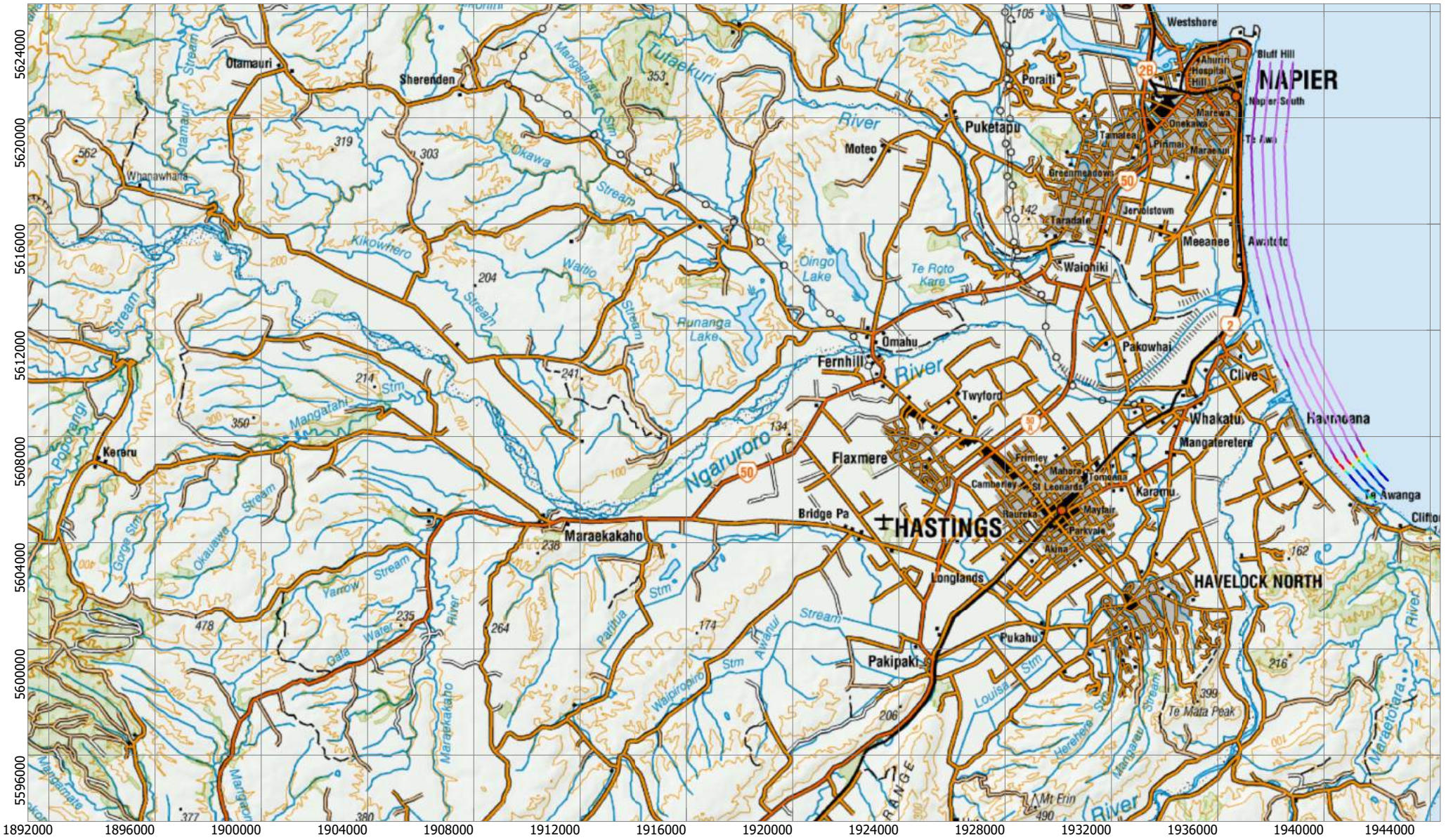

Confidential 2021

GNS SCIENCE TE PŪ AO

GNS Science Consultancy Report 2021/93

SkyTEM Survey Heretaunga 2020

-65.0 -60.0 -55.0 -50.0 -45.0 -40.0 -35.0 -30.0 -25.0

Elevation [m]

Depth of Investigation, Standard

Elevation, metres

NZTM2000

15 km

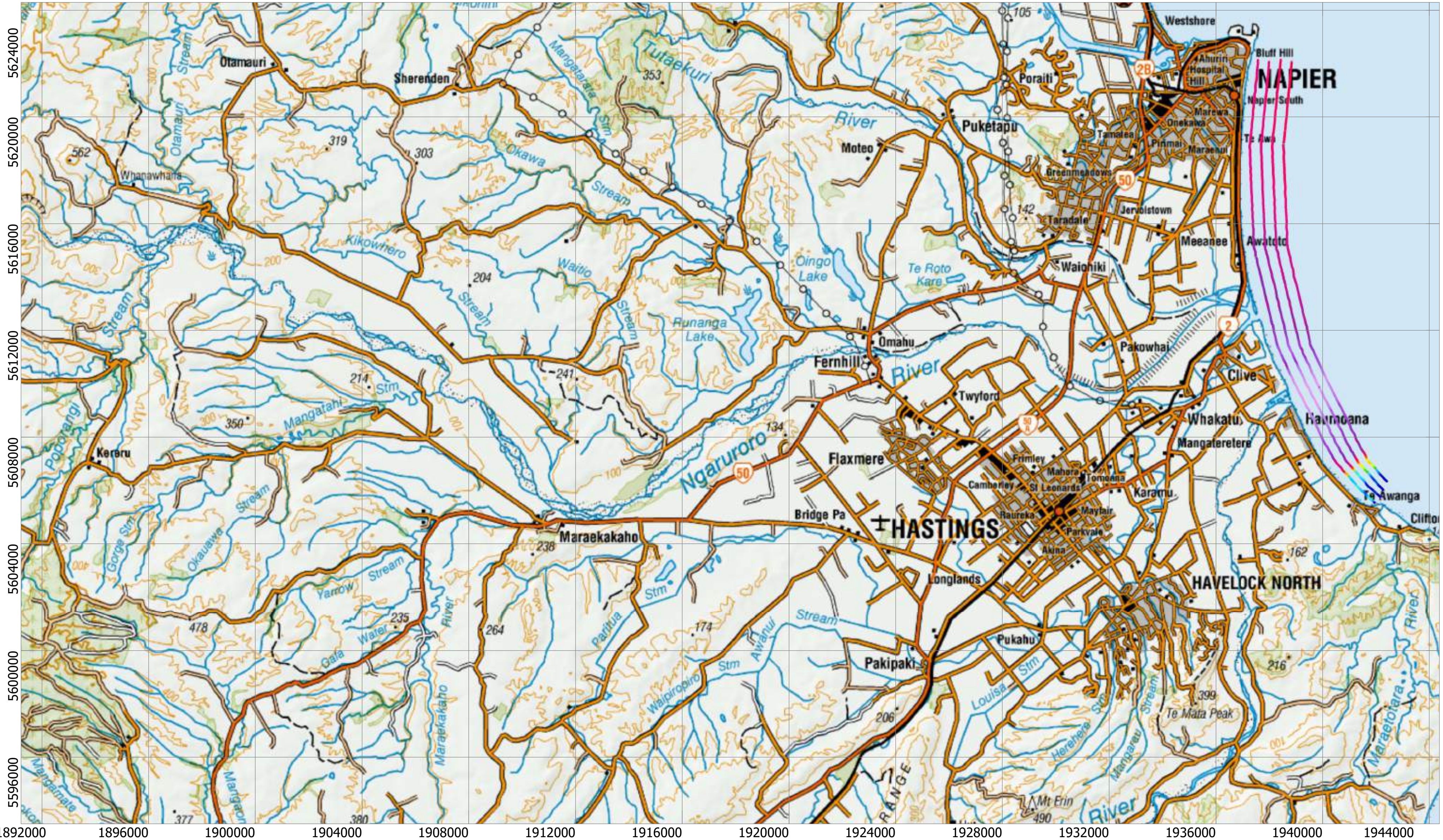

Confidential 2021

GNS SCIENCE TE PŪ AO

GNS Science Consultancy Report 2021/93

SkyTEM Survey Heretaunga 2020

-45.0 -40.0 -35.0 -30.0 -25.0 -20.0
Elevation [m]

Depth of Investigation, Conservative

Elevation, metres

NZTM2000

15 km

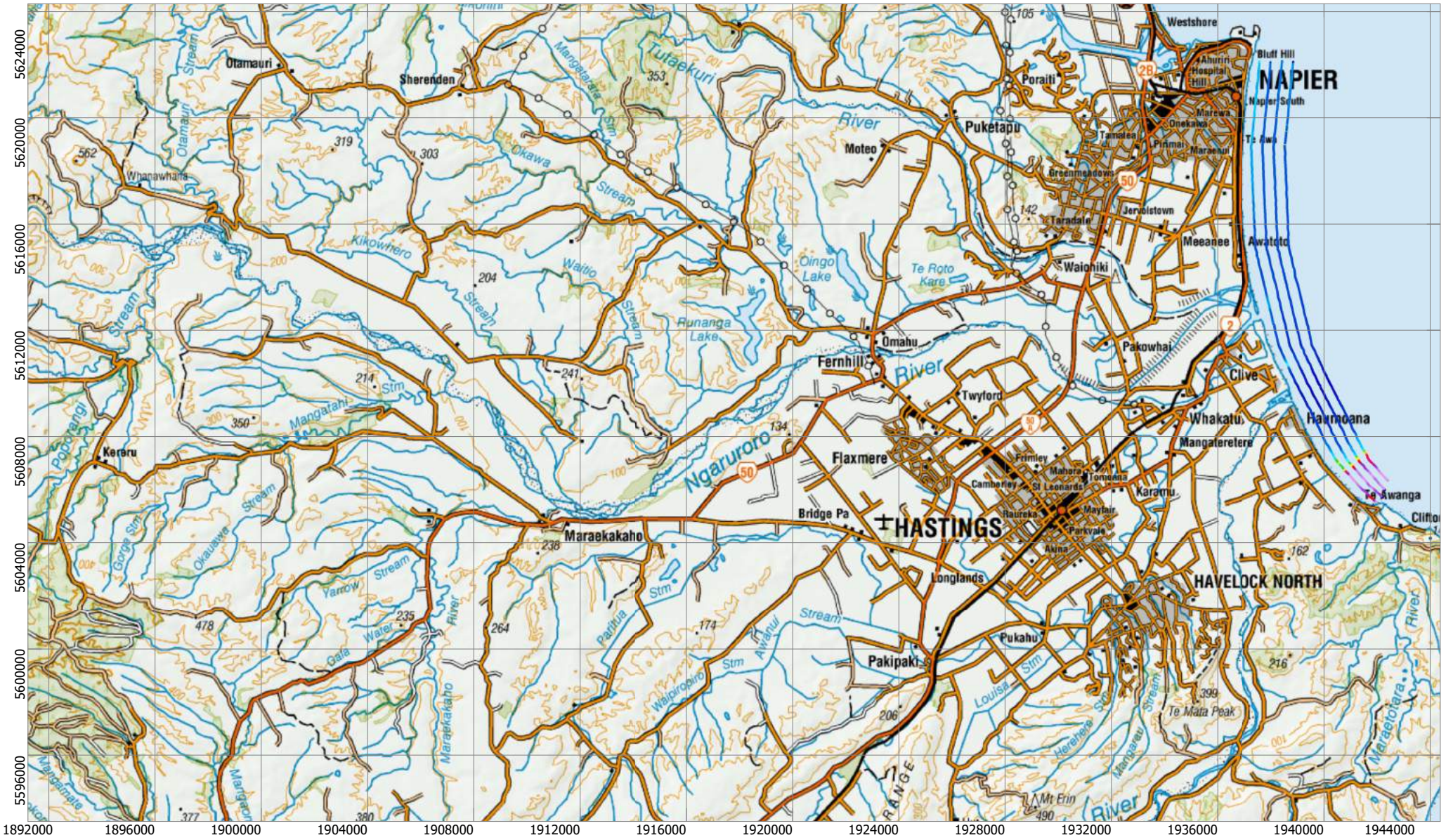

Confidential 2021

GNS SCIENCE TE PŪ AO

GNS Science Consultancy Report 2021/93

SkyTEM Survey Heretaunga 2020

25.0 30.0 35.0 40.0 45.0 50.0 55.0 60.0 65.0

Depth [m]

Depth of Investigation, Standard

Depth, metres

NZTM2000

15 km

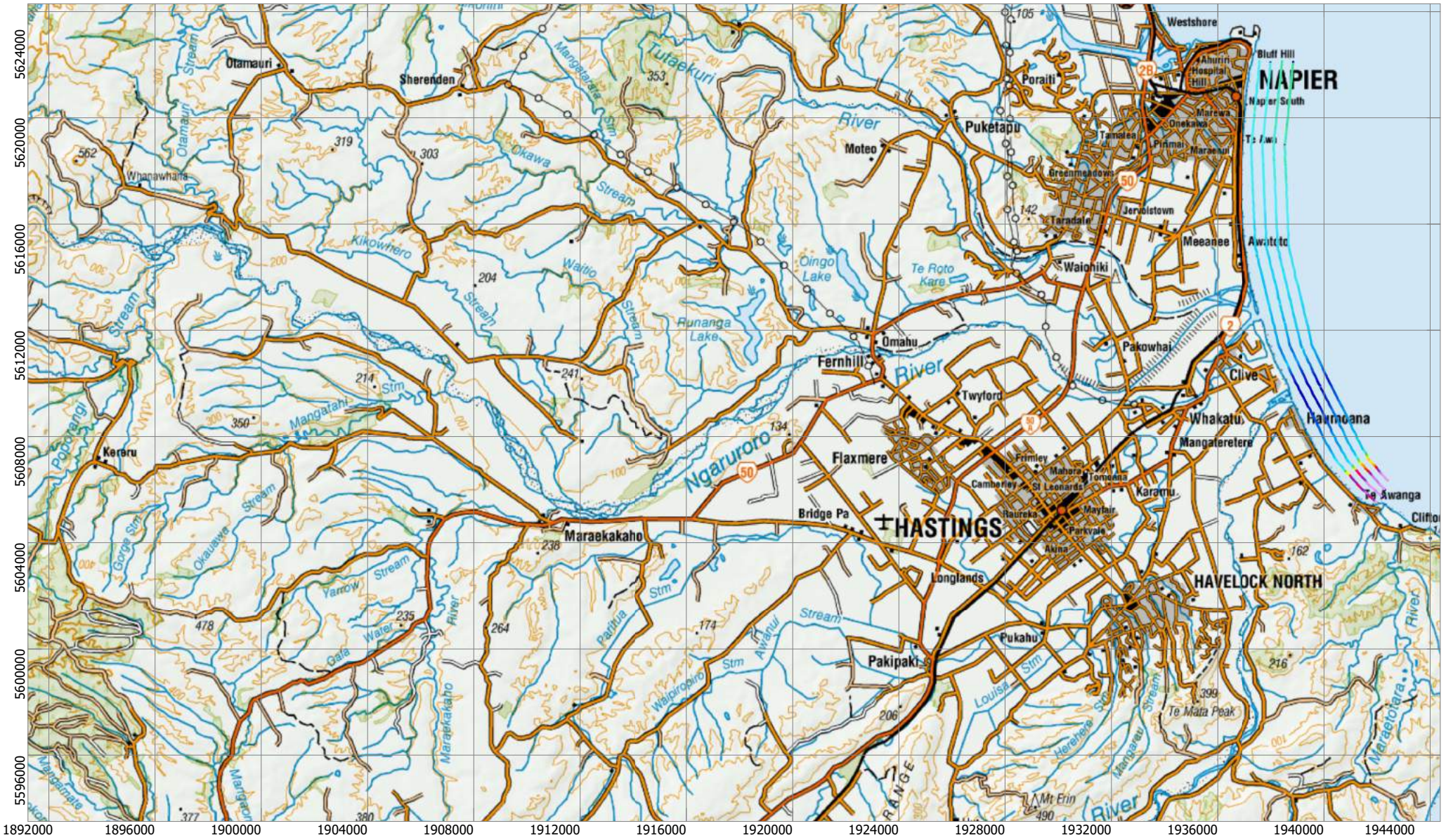

Confidential 2021

GNS SCIENCE TE PŪ AO

GNS Science Consultancy Report 2021/93

SkyTEM Survey Heretaunga 2020

20.0 25.0 30.0 35.0 40.0 45.0

Depth [m]

Depth of Investigation, Conservative

Depth, metres

NZTM2000

15 km

APPENDIX 2 CROSS-SECTIONS

Selected cross-sections for the smooth inversion are included. Each section shows the 1D models blanked at the depth of investigation standard value. Sections for all flight lines are available in the delivered Aarhus Workbench workspace.

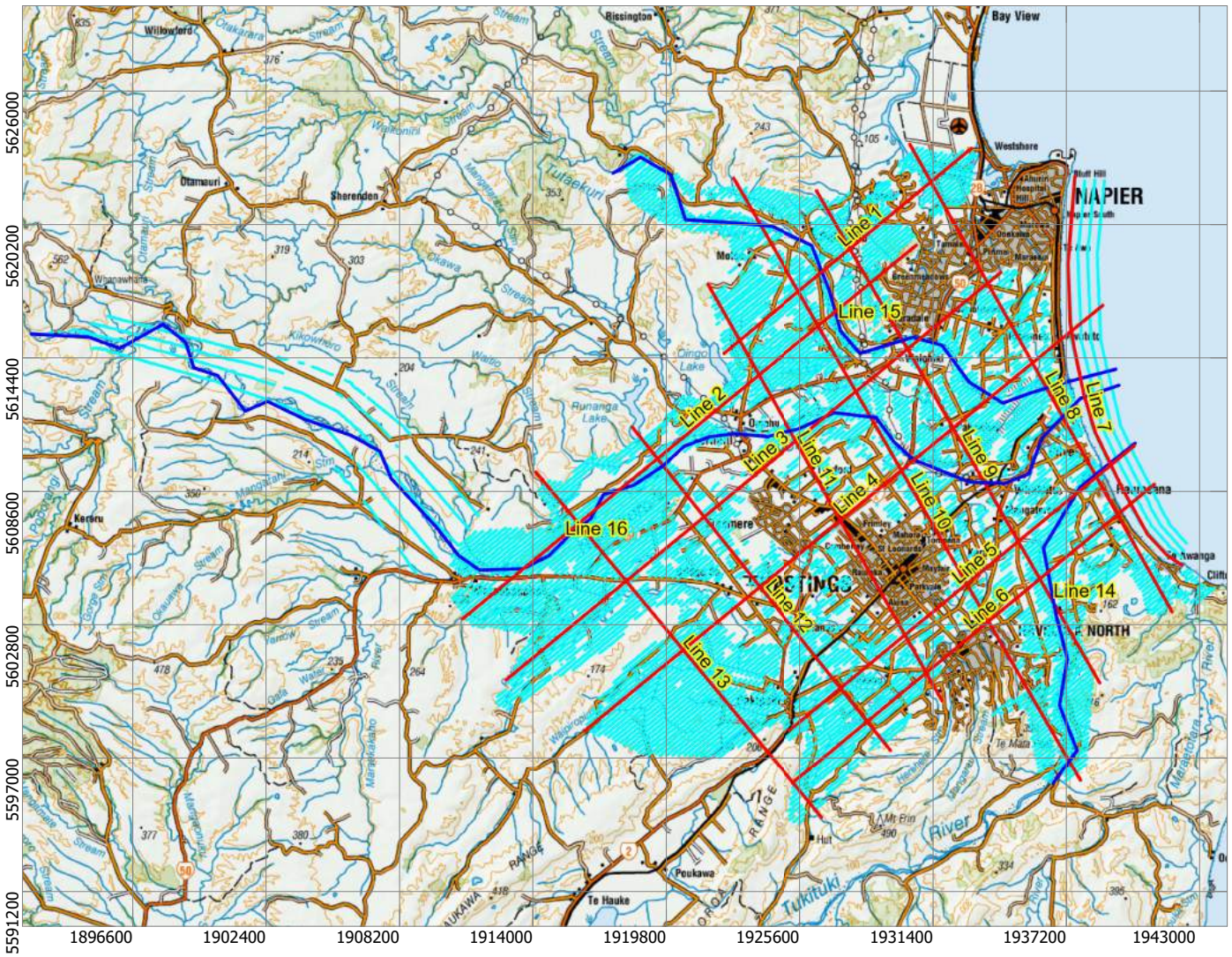

Line 1 (SW-NE)

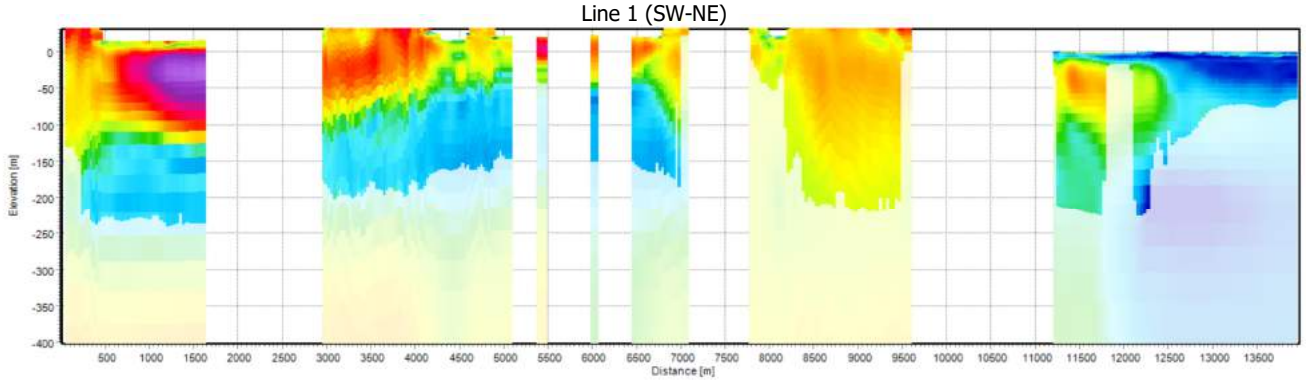

Line 2 (SW-NE)

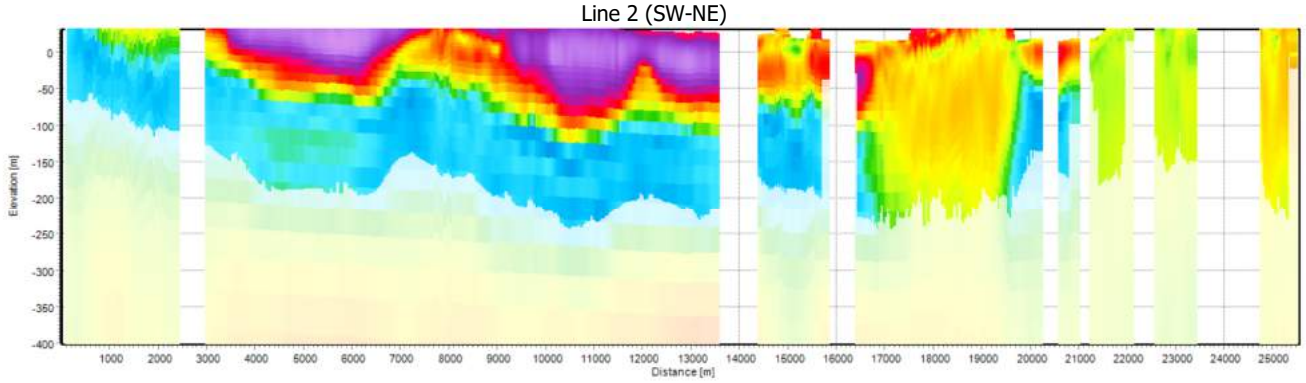

Confidential 2021

GNS SCIENCE TE PŪ AO

GNS Science Consultancy Report 2021/93

SkyTEM Survey Heretaunga 2020

Resistivity Profiles (ohm-m)

Smooth SCI Model

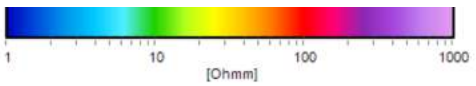

The profiles display model bars from the smooth inversion results. Models have been blanked by 90% below the DOI Standard.

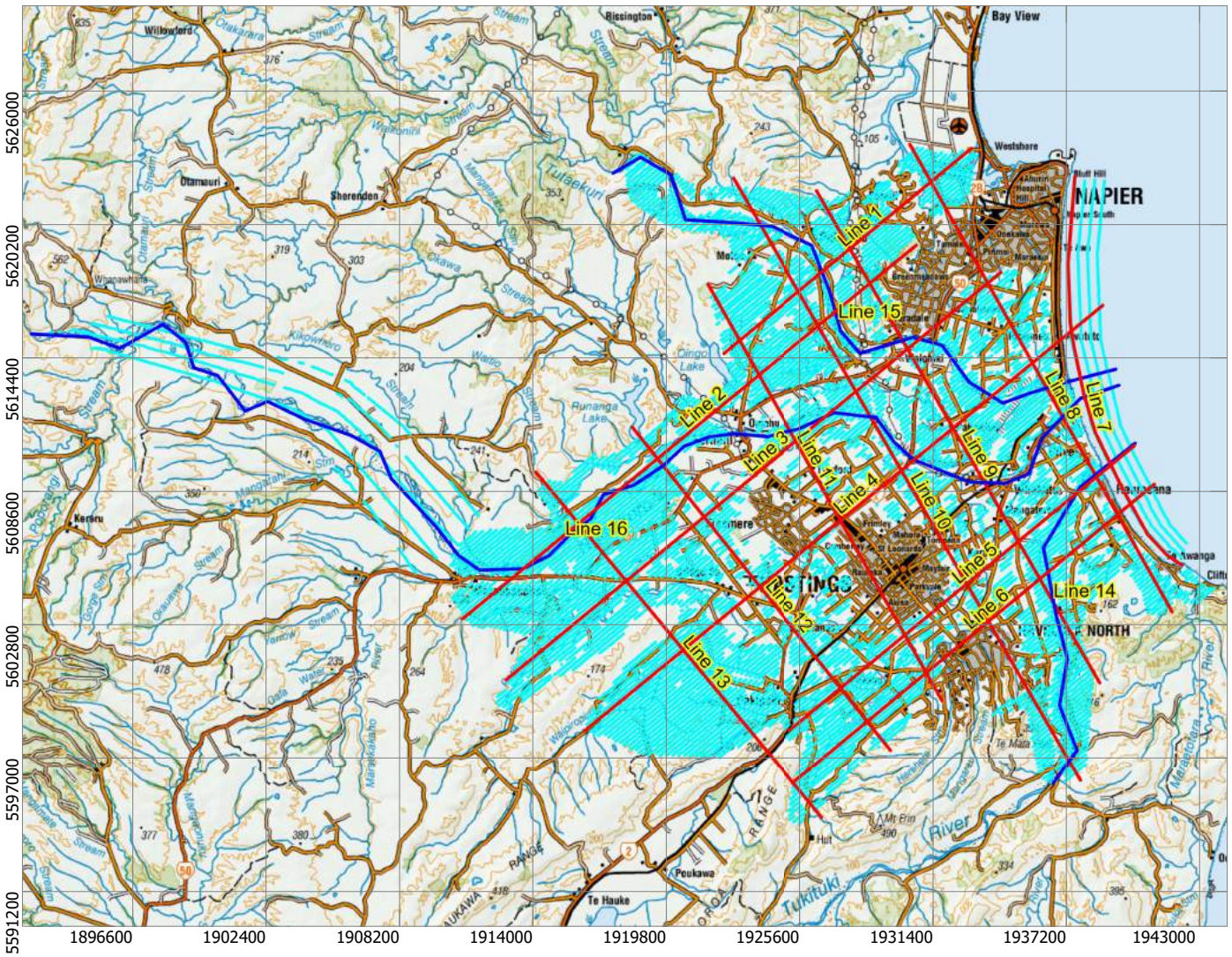

Line 3 (SW-NE)

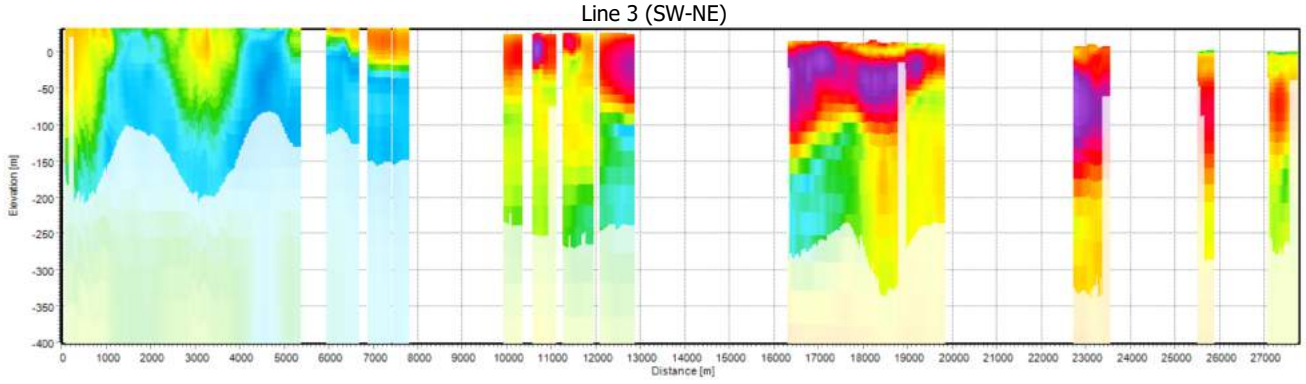

Line 4 (SW-NE)

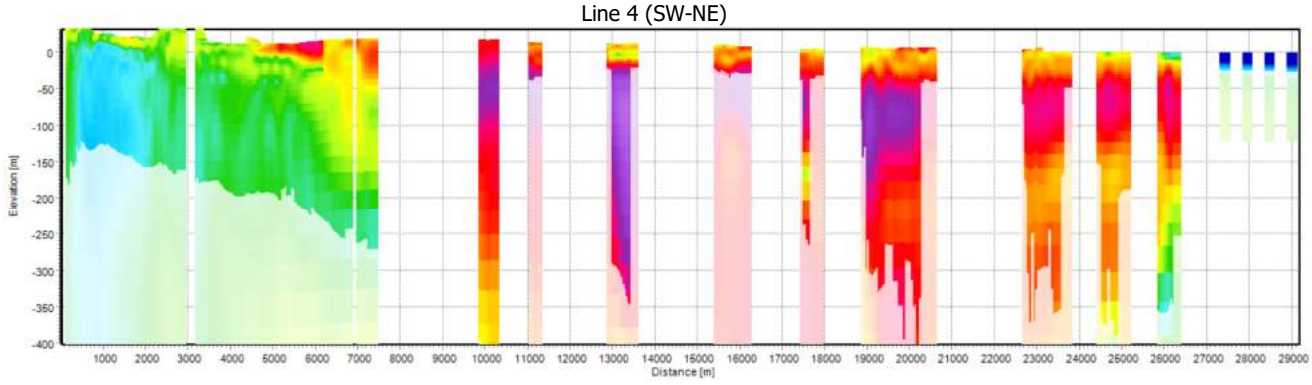

Confidential 2021

GNS SCIENCE TE PŪ AO

GNS Science Consultancy Report 2021/93

SkyTEM Survey Heretaunga 2020

Resistivity Profiles (ohm-m)

Smooth SCI Model

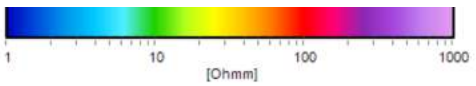

The profiles display model bars from the smooth inversion results. Models have been blanked by 90% below the DOI Standard.

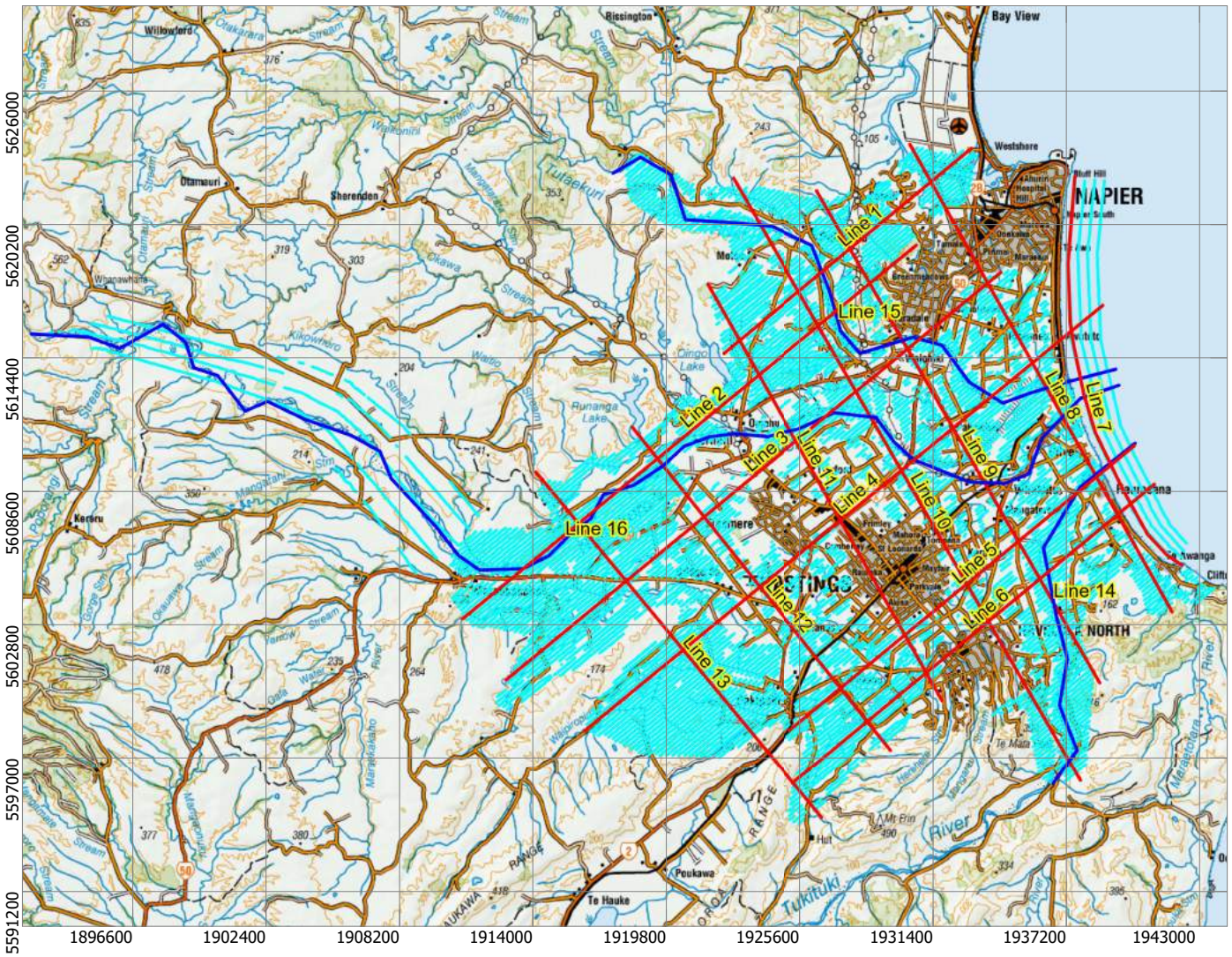

Line 5 (SW-NE)

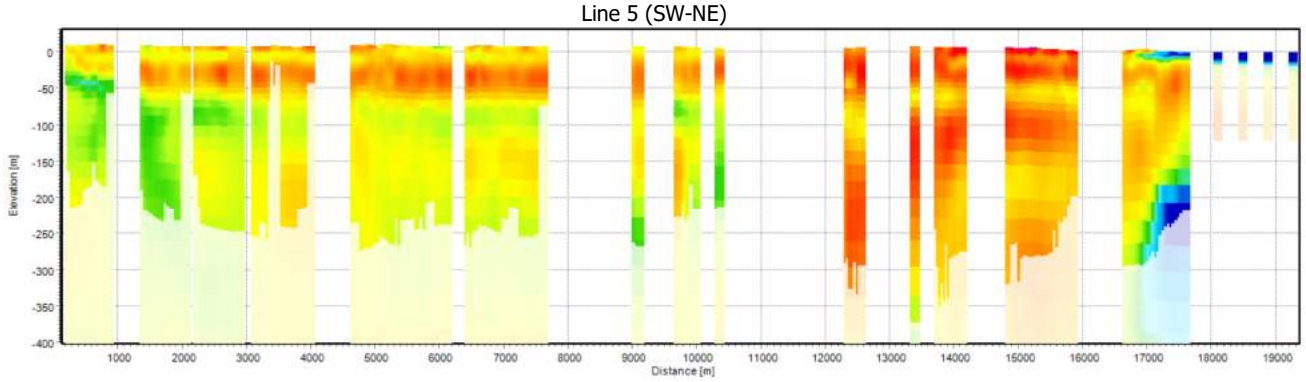

Line 6 (SW-NE)

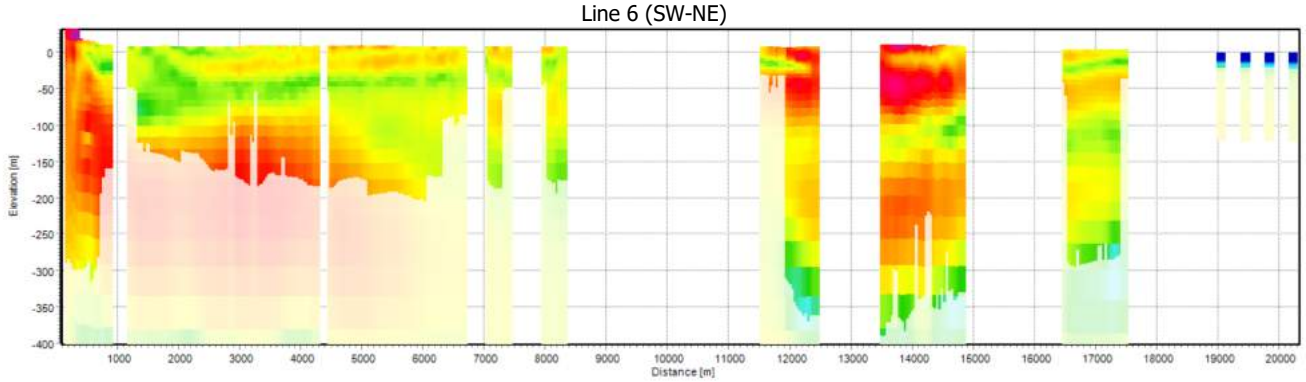

Confidential 2021

GNS SCIENCE TE PŪ AO

GNS Science Consultancy Report 2021/93

SkyTEM Survey Heretaunga 2020

Resistivity Profiles (ohm-m)

Smooth SCI Model

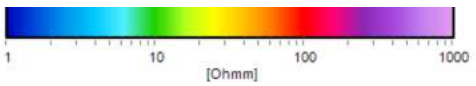

The profiles display model bars from the smooth inversion results. Models have been blanked by 90% below the DOI Standard.

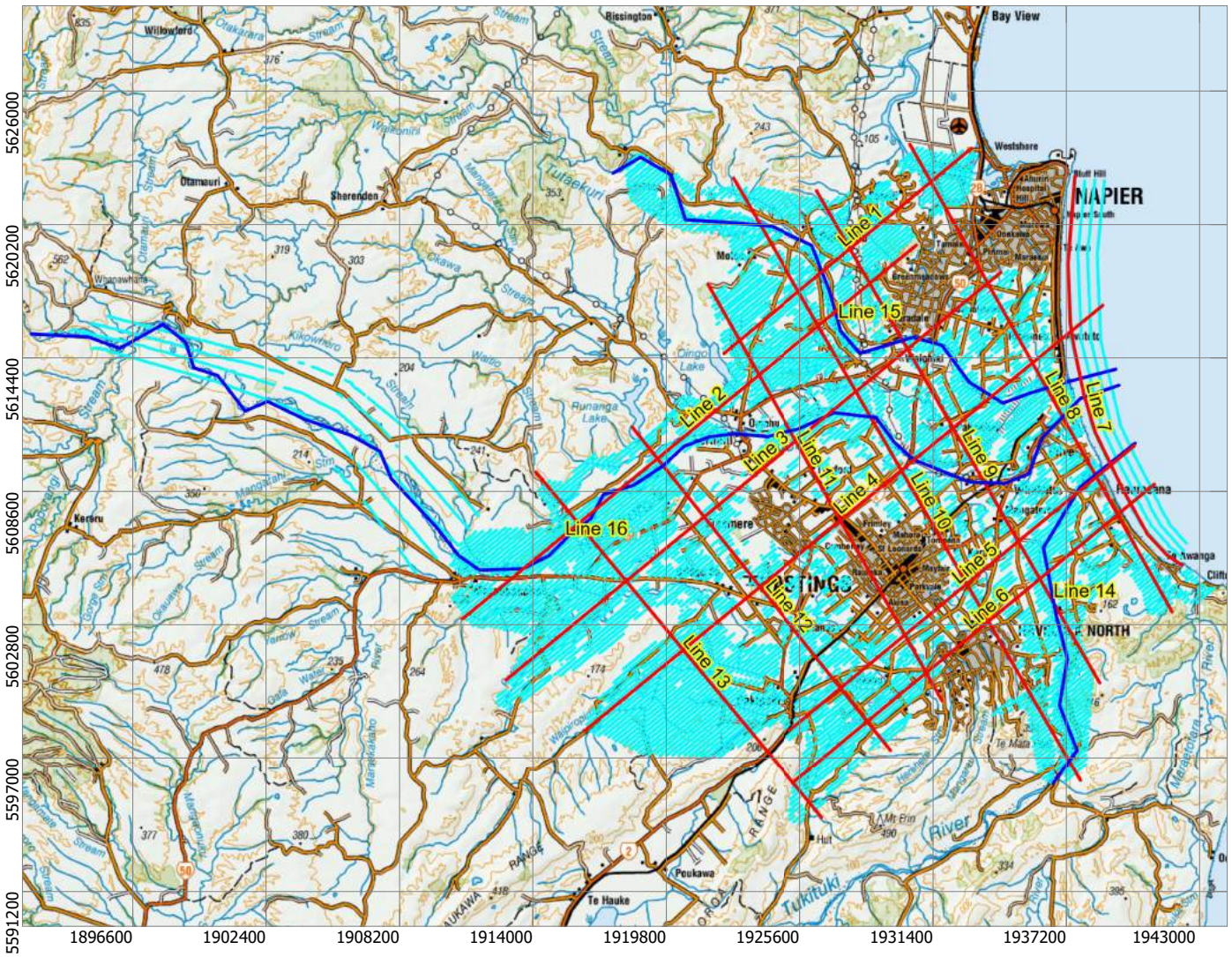

Line 7 (N-S)

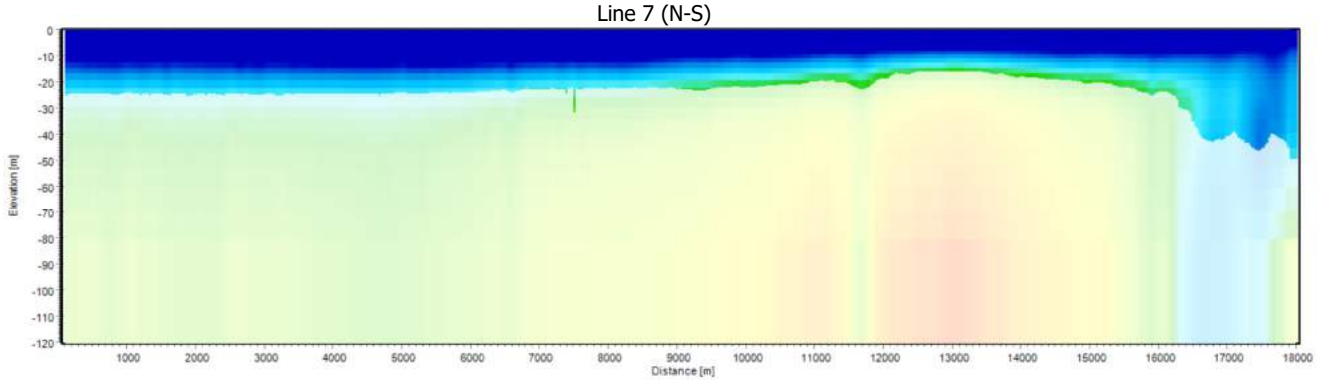

Line 8 (NW-SE)

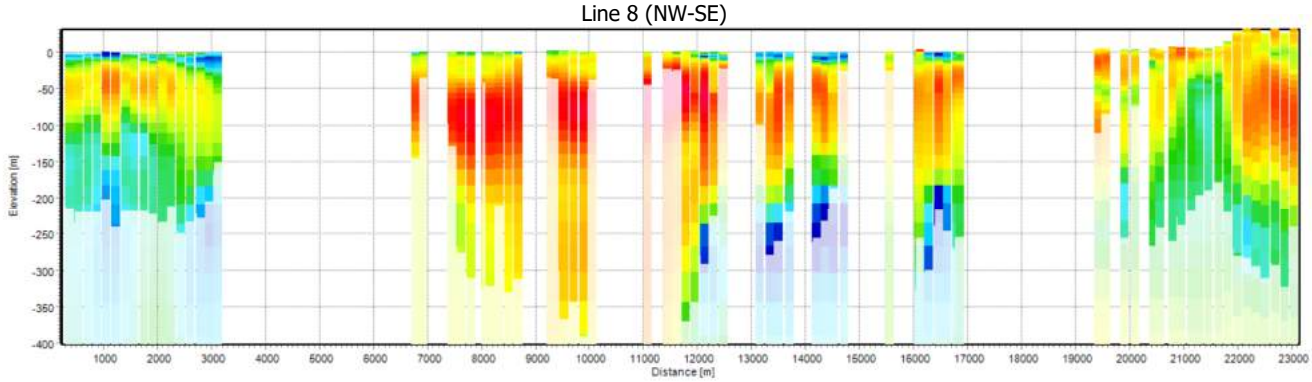

Confidential 2021

GNS SCIENCE TE PŪ AO

GNS Science Consultancy Report 2021/93

SkyTEM Survey Heretaunga 2020

Resistivity Profiles (ohm-m)

Smooth SCI Model

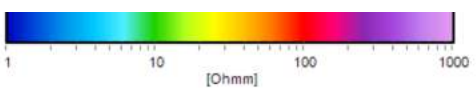

The profiles display model bars from the smooth inversion results. Models have been blanked by 90% below the DOI Standard.

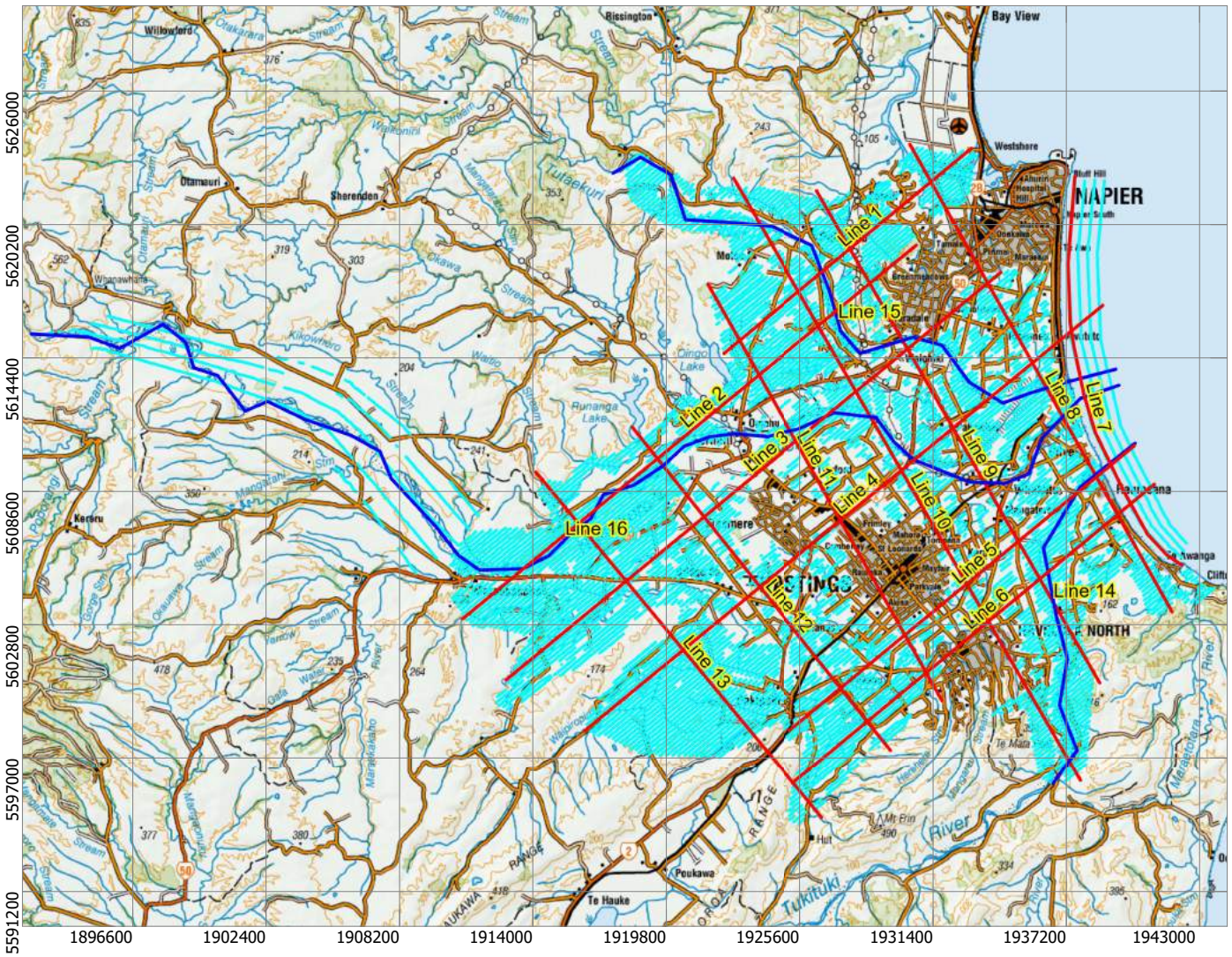

Line 9 (NW-SE)

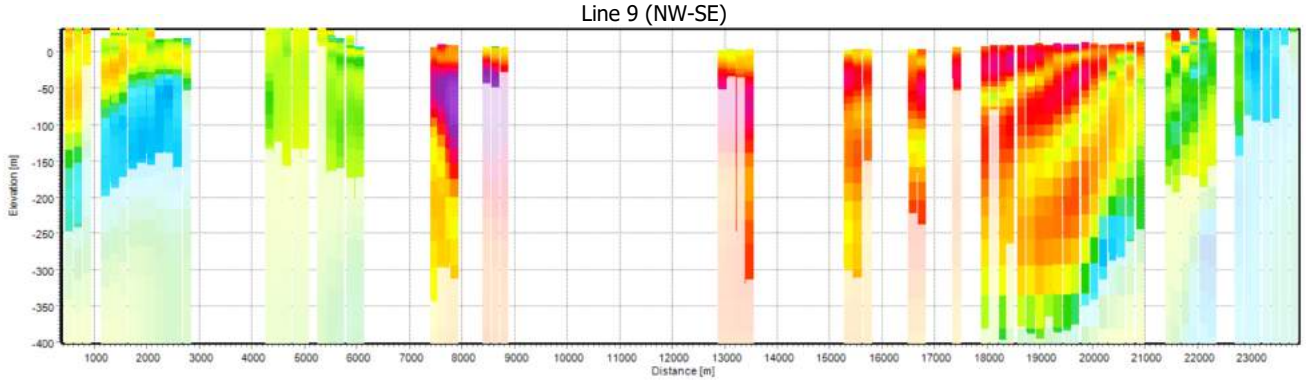

Line 10 (NW-SE)

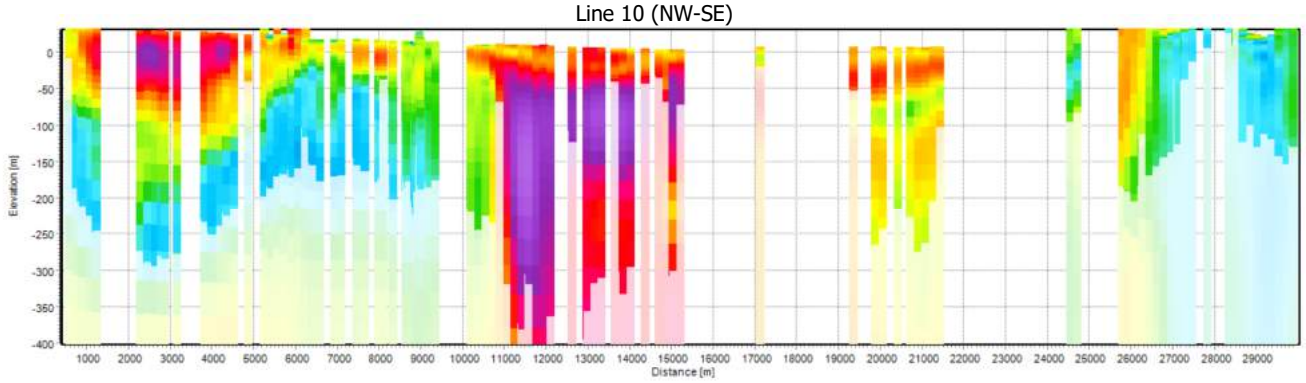

Confidential 2021

GNS SCIENCE TE PŪ AO

GNS Science Consultancy Report 2021/93

SkyTEM Survey Heretaunga 2020

Resistivity Profiles (ohm-m)

Smooth SCI Model

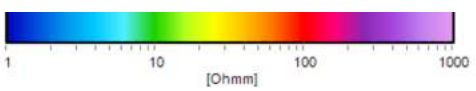

The profiles display model bars from the smooth inversion results. Models have been blanked by 90% below the DOI Standard.

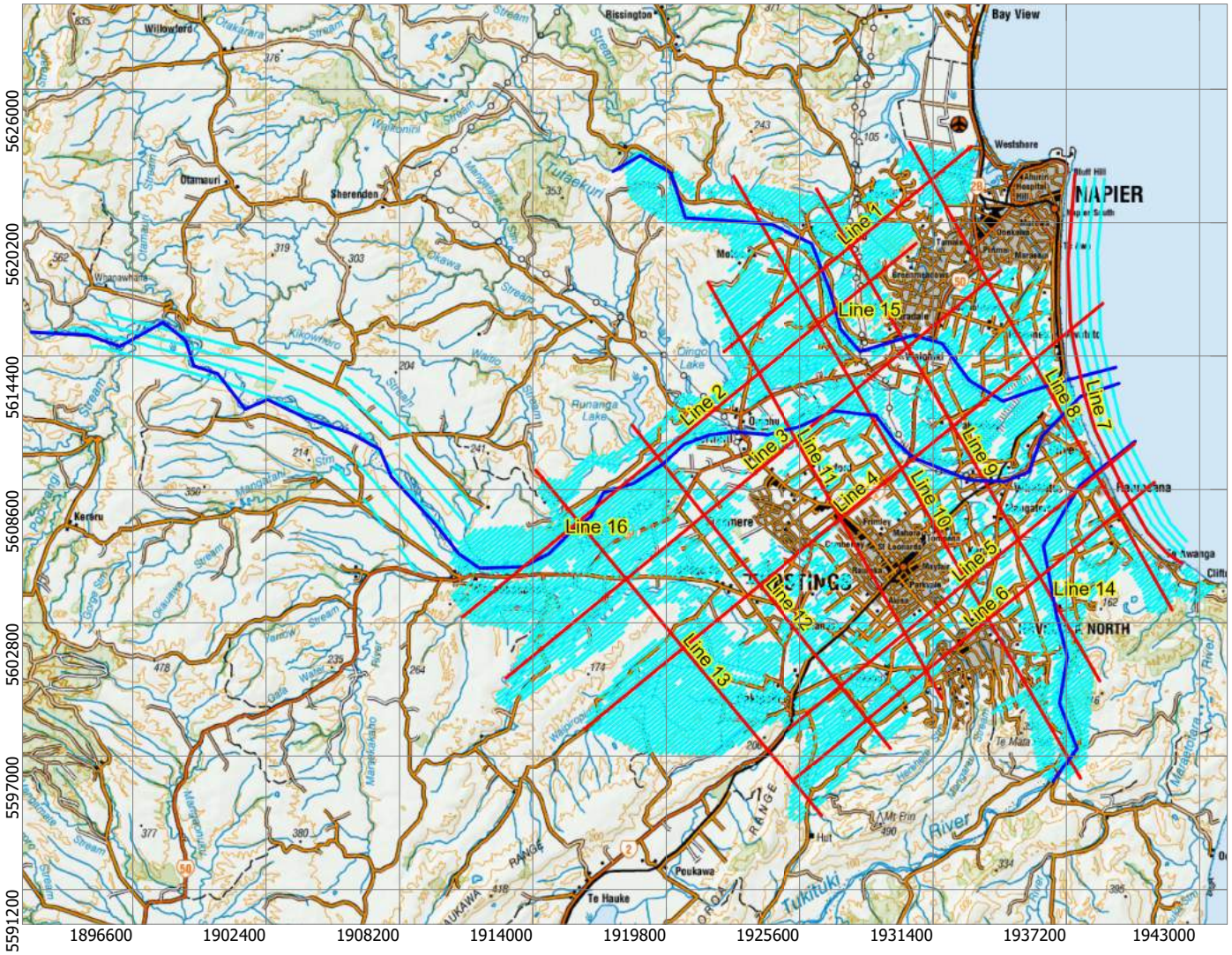

Line 11 (NW-SE)

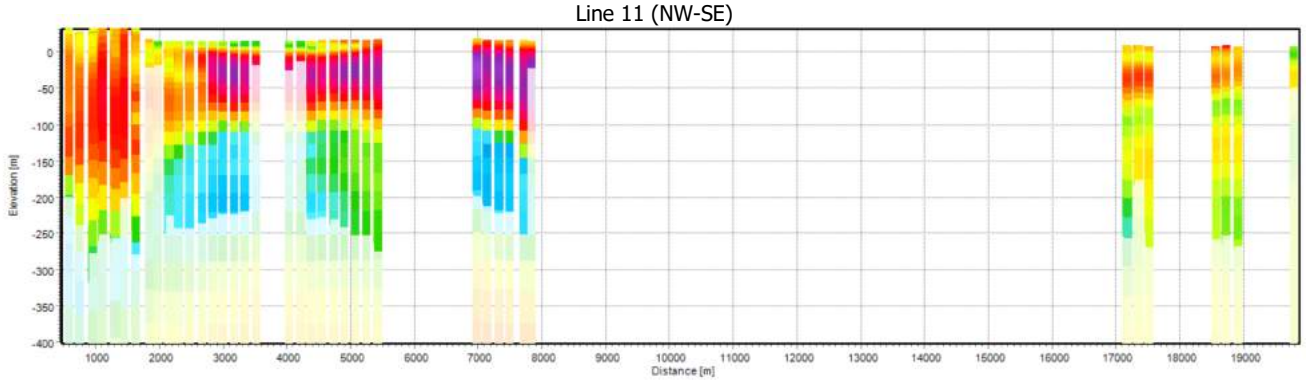

Line 12 (NW-SE)

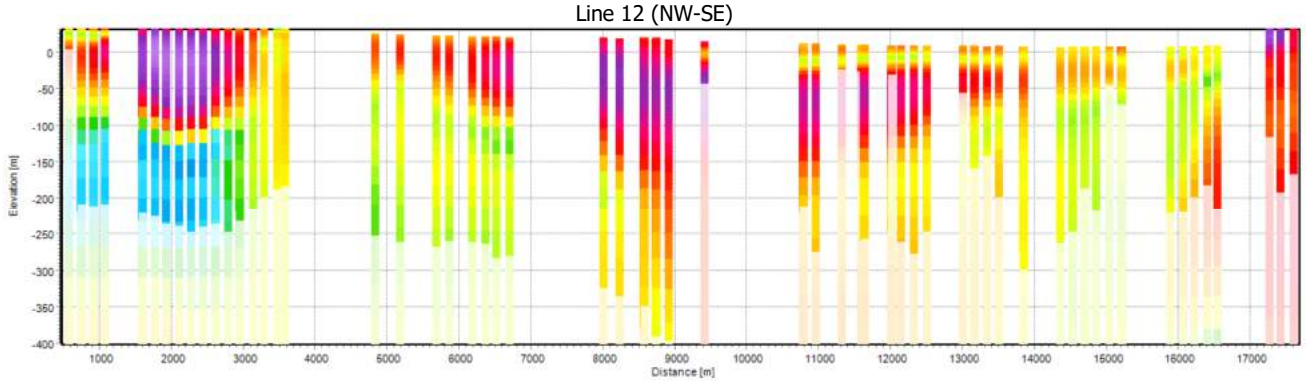

Confidential 2021

GNS SCIENCE TE PŪ AO

GNS Science Consultancy Report 2021/93

SkyTEM Survey Heretaunga 2020

Resistivity Profiles (ohm-m)

Smooth SCI Model

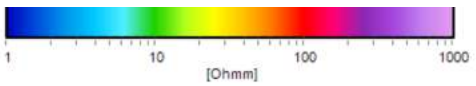

The profiles display model bars from the smooth inversion results. Models have been blanked by 90% below the DOI Standard.

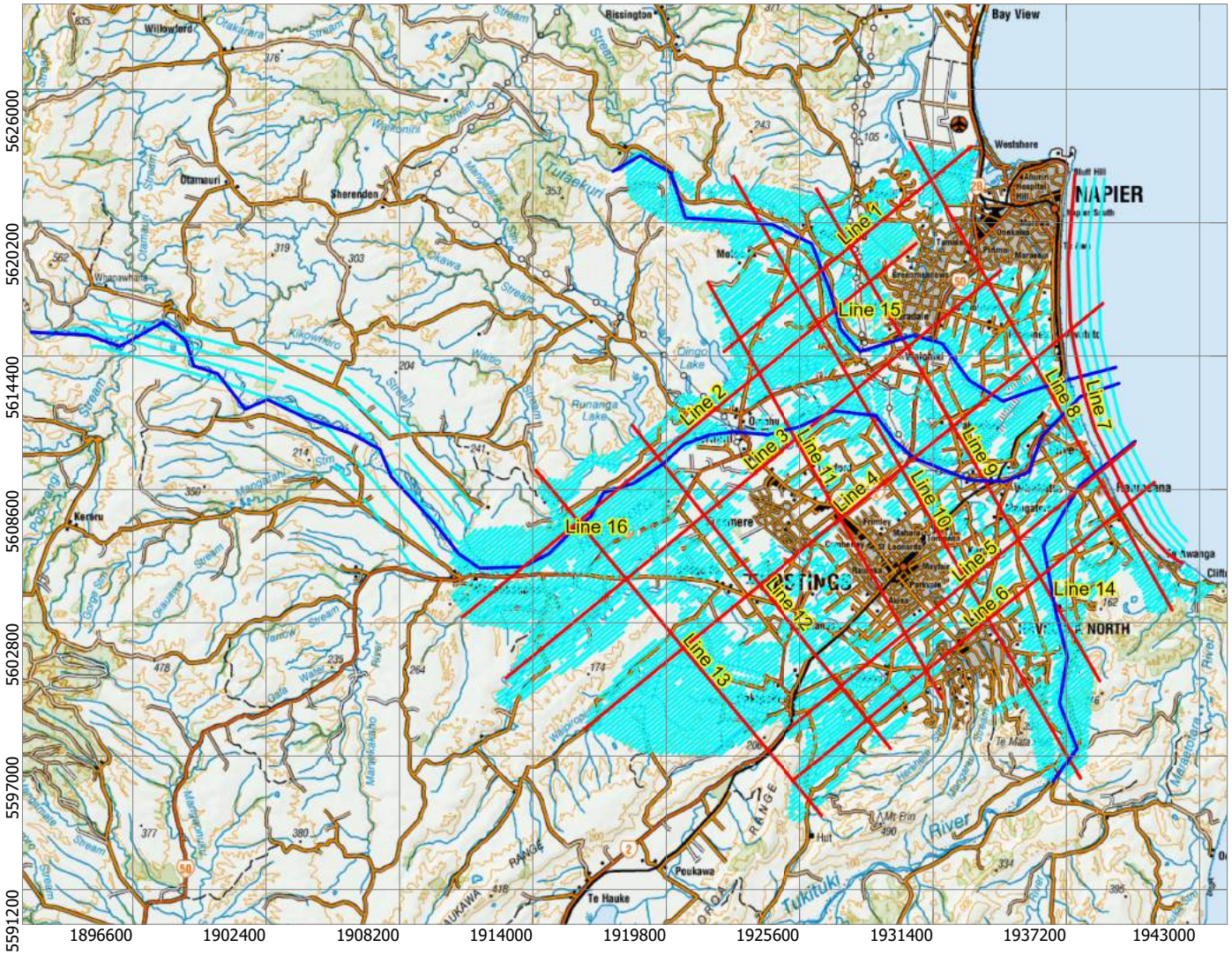

Line 13 (NW-SE)

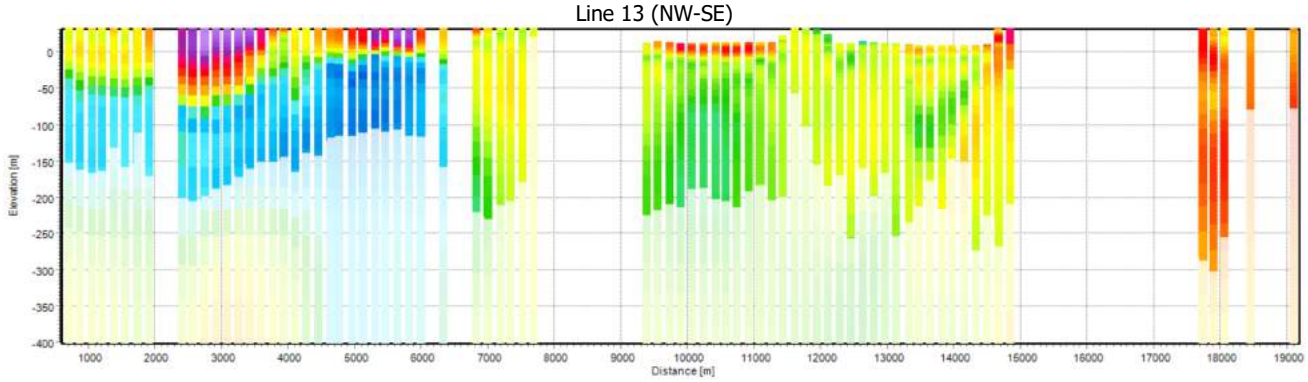

Line 14 (SW-NE)

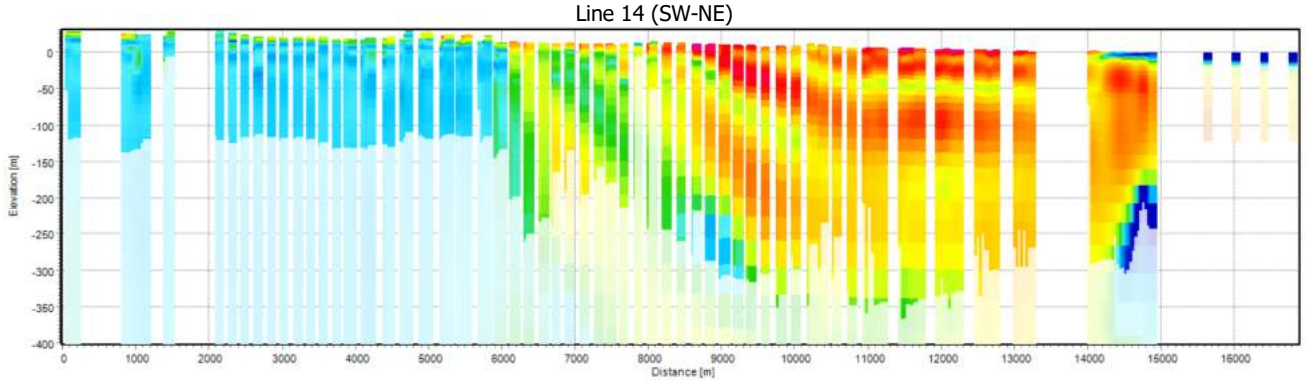

Confidential 2021

GNS SCIENCE TE PŪ AO

GNS Science Consultancy Report 2021/93

SkyTEM Survey Heretaunga 2020

Resistivity Profiles (ohm-m)

Smooth SCI Model

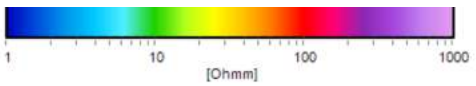

The profiles display model bars from the smooth inversion results. Models have been blanked by 90% below the DOI Standard.

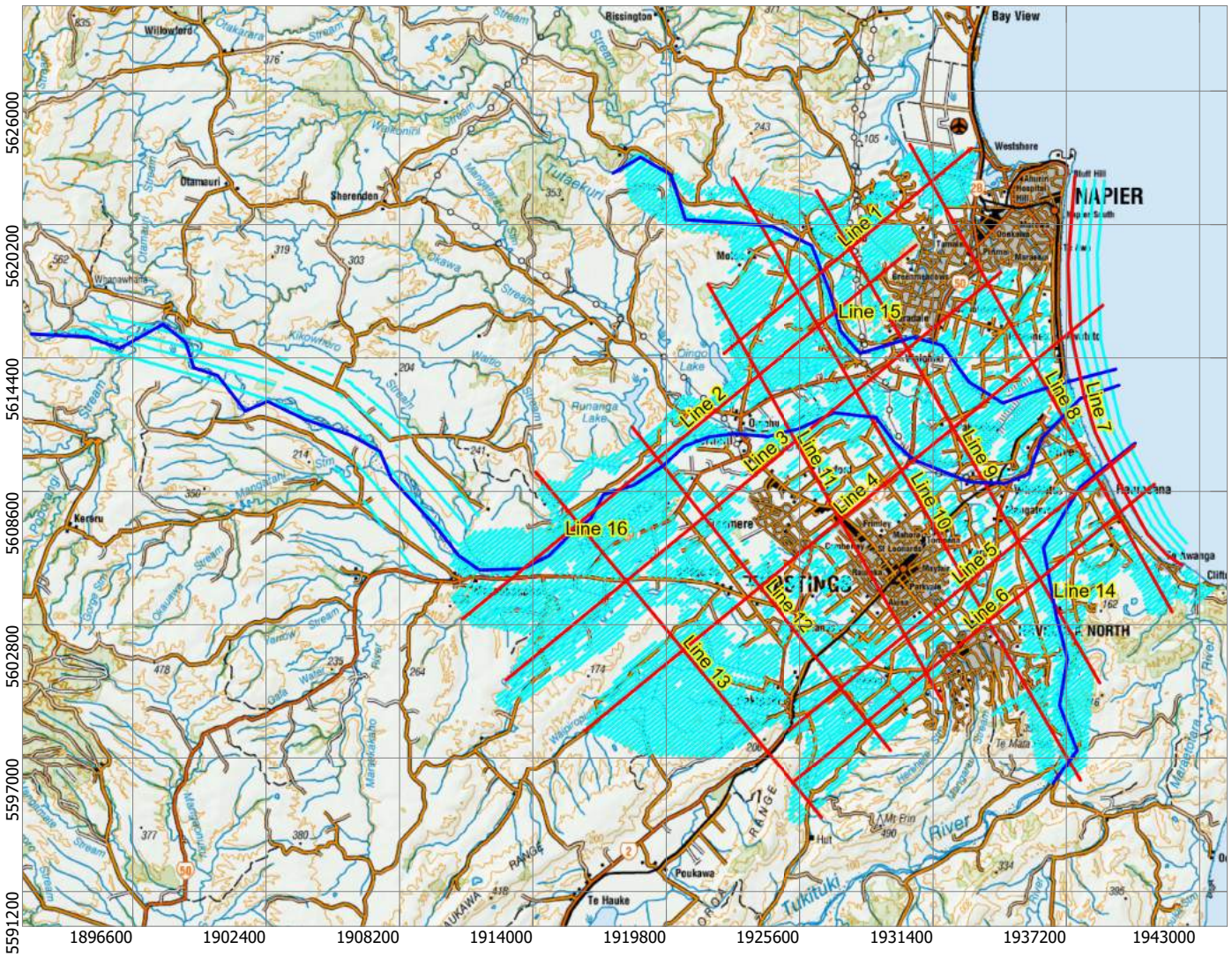

Line 15 (NW-SE)

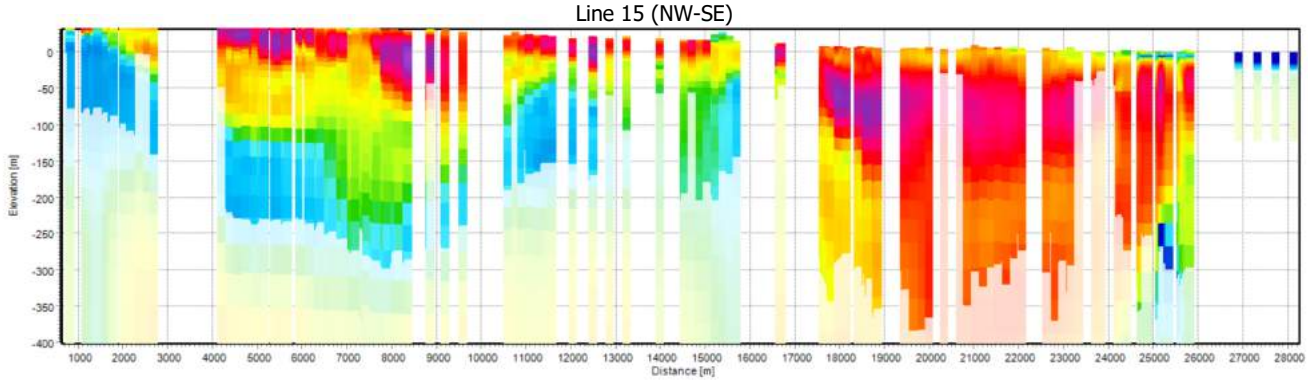

Line 16 (W-E)

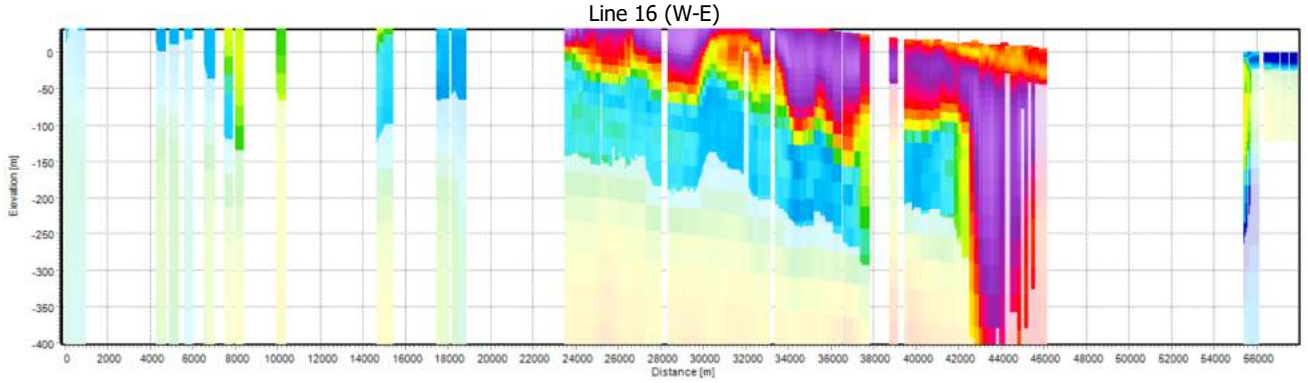

Confidential 2021

GNS SCIENCE TE PŪ AO

GNS Science Consultancy Report 2021/93

SkyTEM Survey Heretaunga 2020

Resistivity Profiles (ohm-m)

Smooth SCI Model

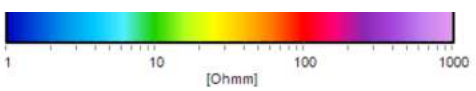

The profiles display model bars from the smooth inversion results. Models have been blanked by 90% below the DOI Standard.

APPENDIX 3 MEAN RESISTIVITY MAPS

This appendix includes mean resistivity maps generated from the smooth model inversion result in 5 m depth intervals from 0 to 50 m, in 10 m intervals from 50 to 100 m and in 50 m intervals from 100 to 500 m. The resistivity models have been blanked at the depth of investigation standard value prior to interpolation to the regular mean resistivity grids.

The interpolation of the mean resistivity values was performed by Kriging interpolation, with a node spacing of 40 m, a search radius of 400 m and additional pixel smoothing in the presented bitmap images.

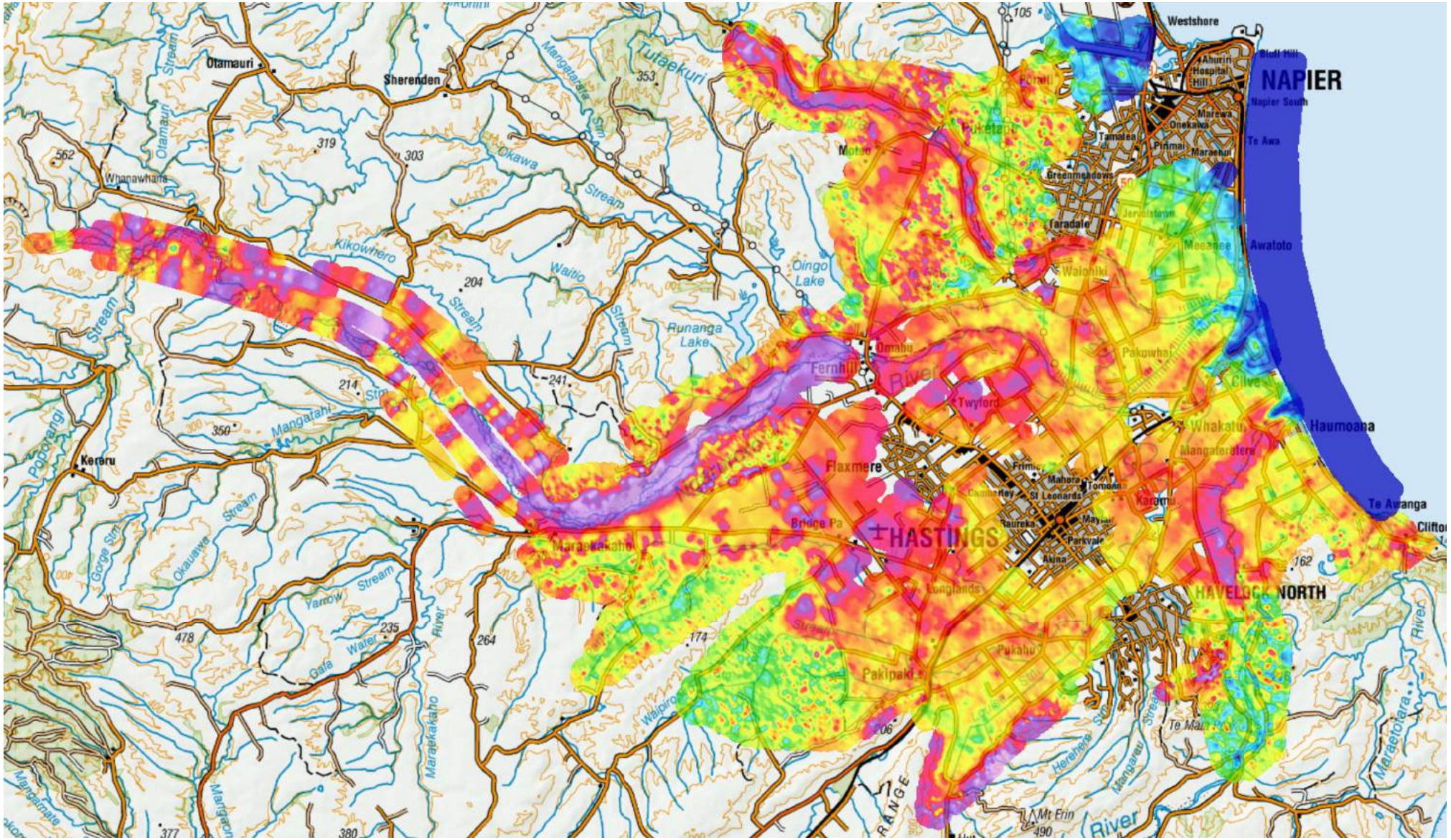

Confidential 2021

GNS SCIENCE TE PŪ AO

GNS Science Consultancy Report 2021/93

SkyTEM Survey Heretaunga 2020

2 4 6 12 21 38 68 123 222 400

Resistivity [Ohmm]

Mean Resistivity, Depth 0-5 m (ohm-m)

SCI Smooth Model - Kriging, Search Radius 400 m

NZTM2000

15 km

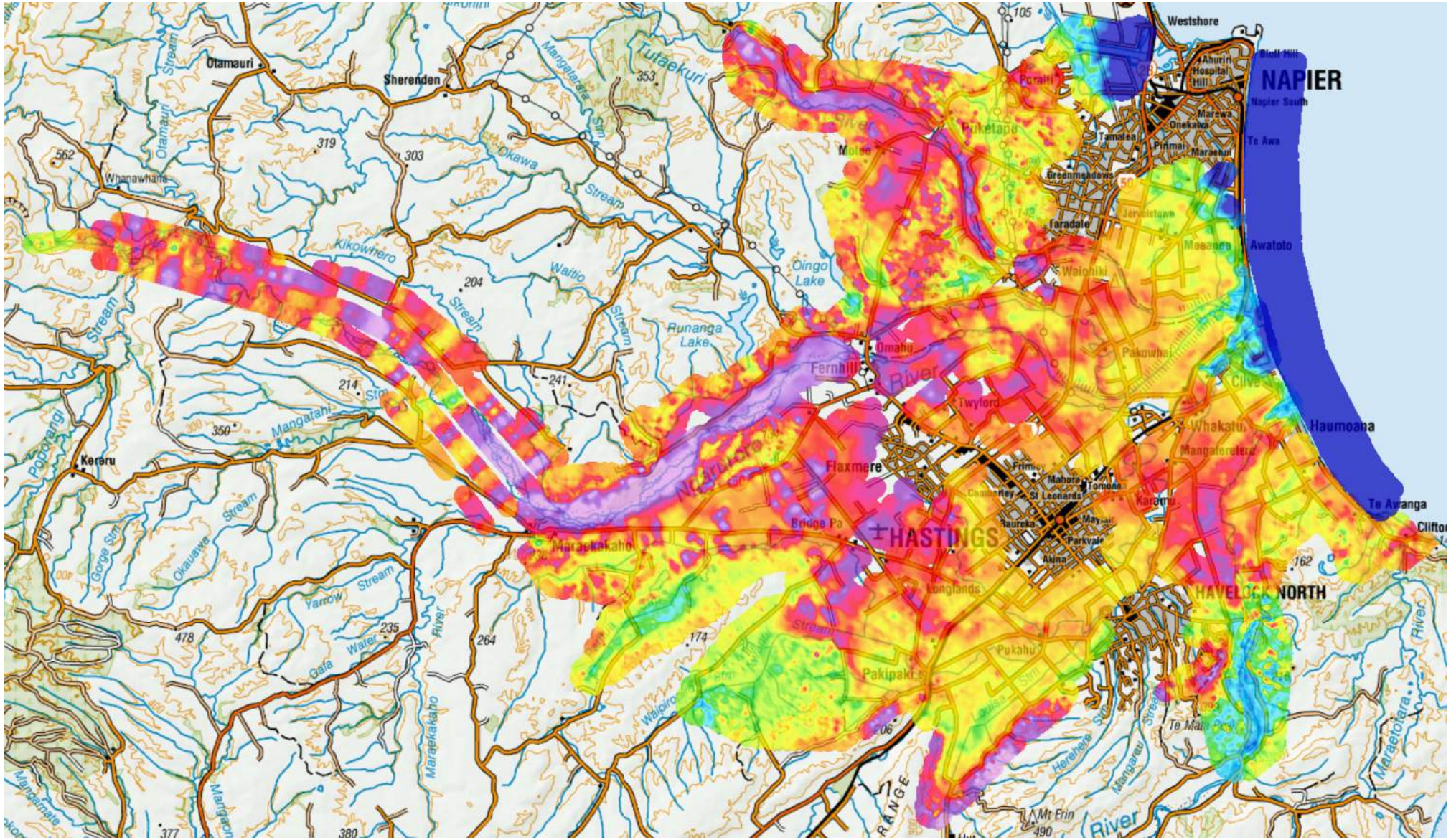

Confidential 2021

GNS SCIENCE TE PŪ AO

GNS Science Consultancy Report 2021/93

SkyTEM Survey Heretaunga 2020

2 4 6 12 21 38 68 123 222 400

Resistivity [Ohmm]

Mean Resistivity, Depth 5-10 m (ohm-m)

SCI Smooth Model - Kriging, Search Radius 400 m

NZTM2000

15 km

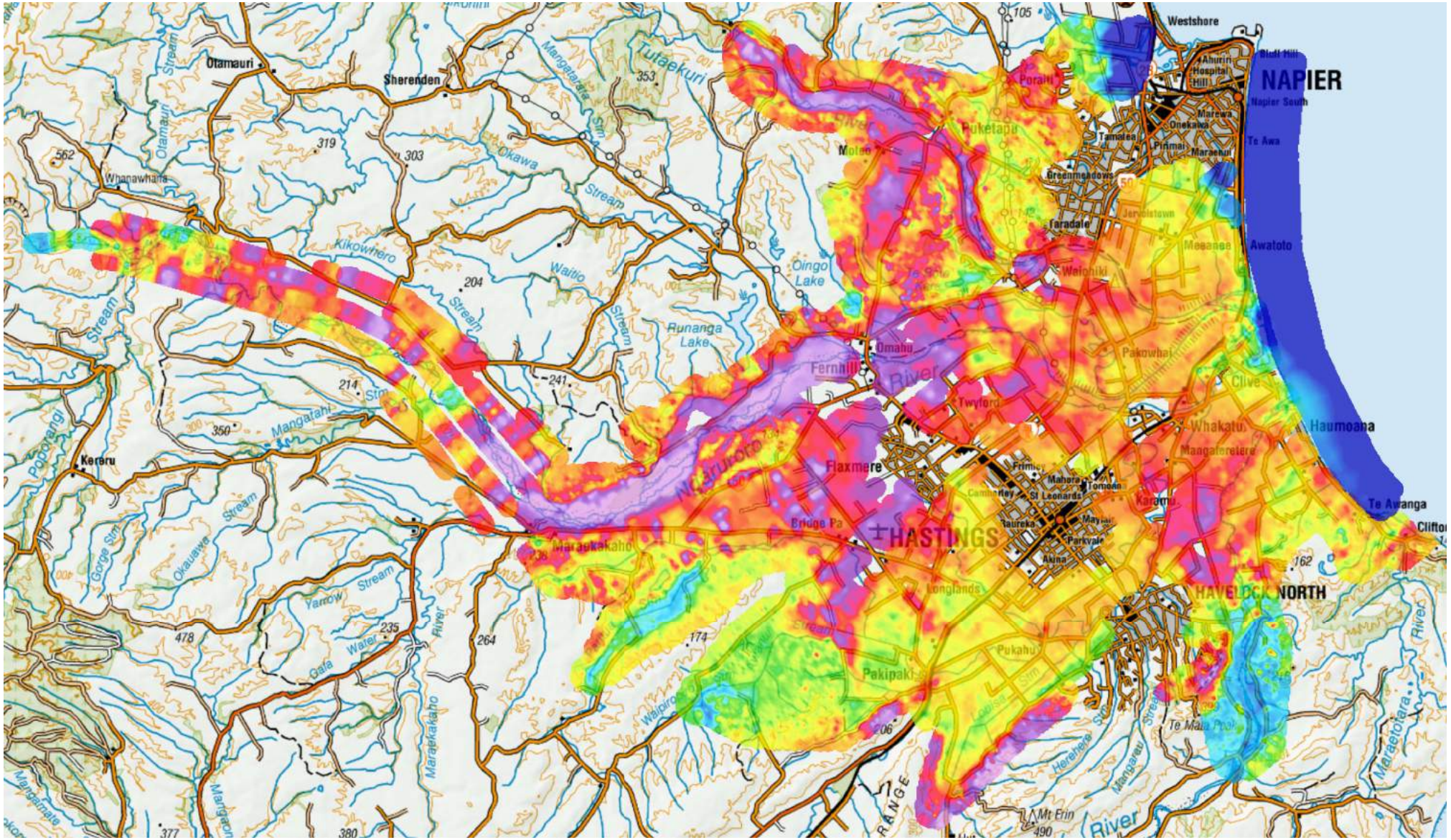

Confidential 2021

GNS SCIENCE TE PŪ AO

GNS Science Consultancy Report 2021/93

SkyTEM Survey Heretaunga 2020

2 4 6 12 21 38 68 123 222 400

Resistivity [Ohmm]

Mean Resistivity, Depth 10-15 m (ohm-m)

SCI Smooth Model - Kriging, Search Radius 400 m

NZTM2000

15 km

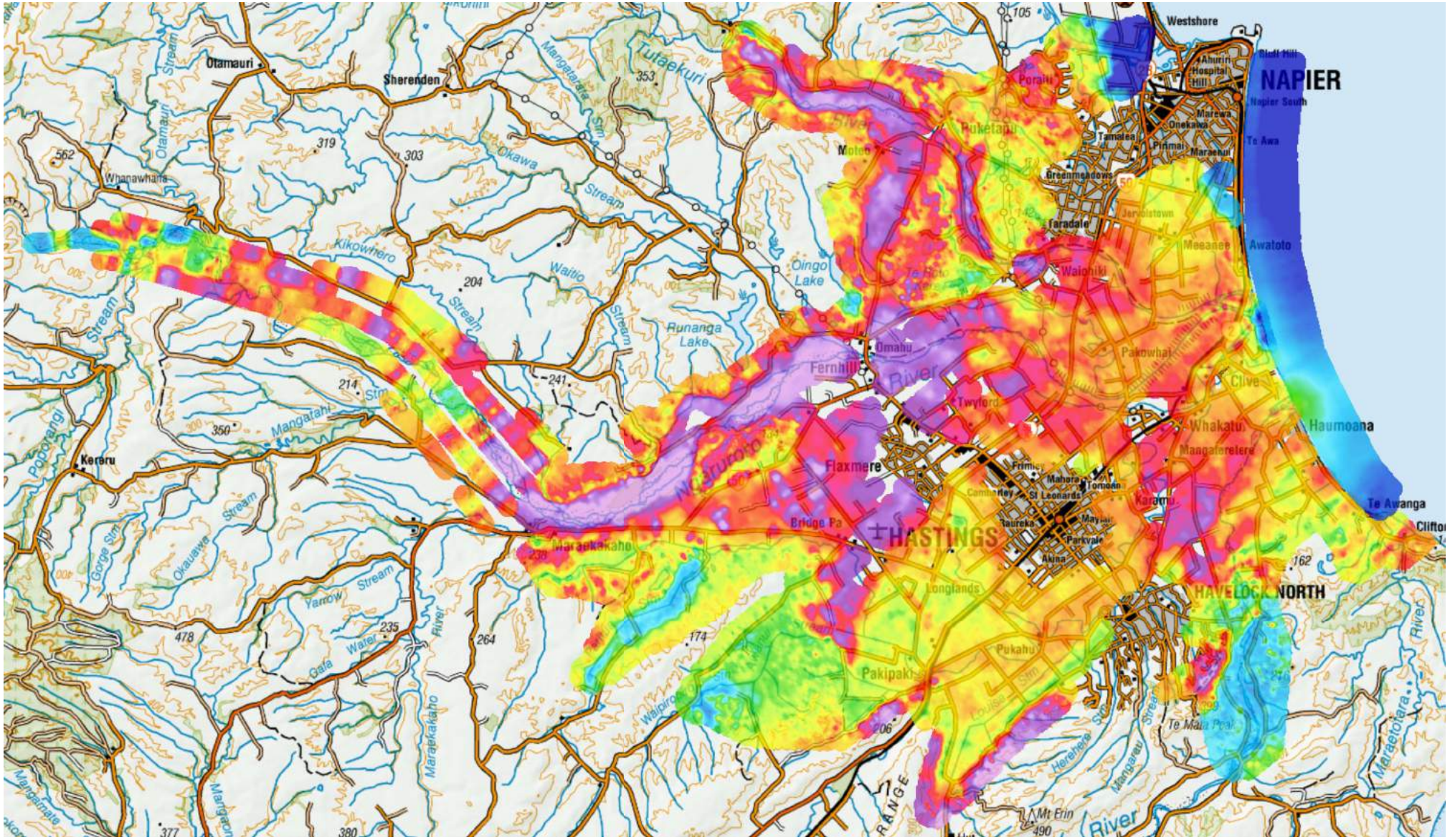

Confidential 2021

GNS SCIENCE TE PŪ AO

GNS Science Consultancy Report 2021/93

SkyTEM Survey Heretaunga 2020

Mean Resistivity, Depth 15-20 m (ohm-m)

SCI Smooth Model - Kriging, Search Radius 400 m

NZTM2000

15 km

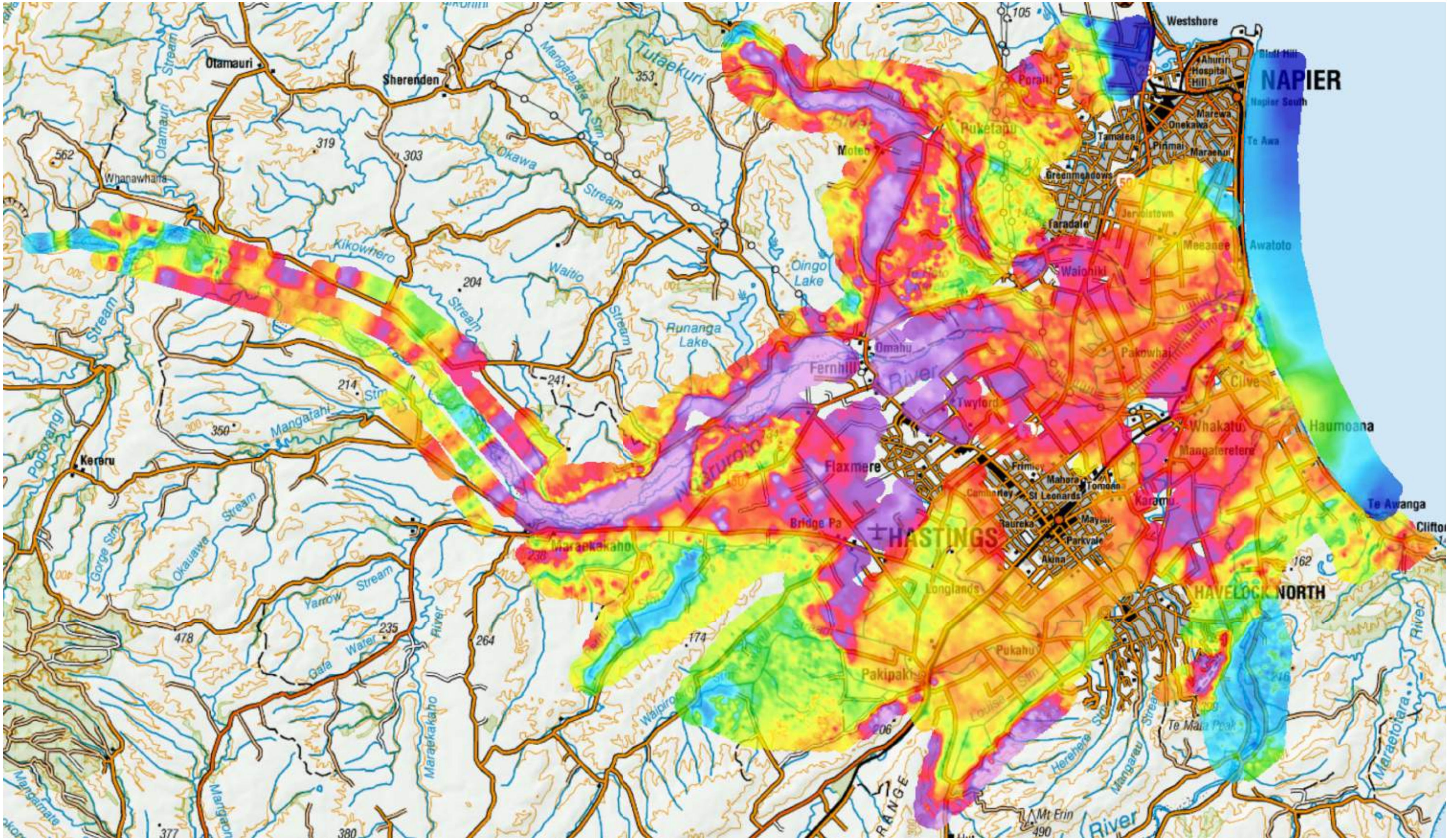

Confidential 2021	SkyTEM Survey Heretaunga 2020	Mean Resistivity, Depth 20-25 m (ohm-m) SCI Smooth Model - Kriging, Search Radius 400 m
GNS SCIENCE TE PŪ AO	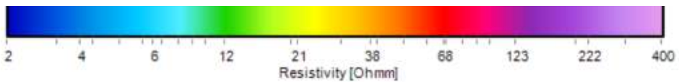	NZTM2000 15 km
GNS Science Consultancy Report 2021/93		

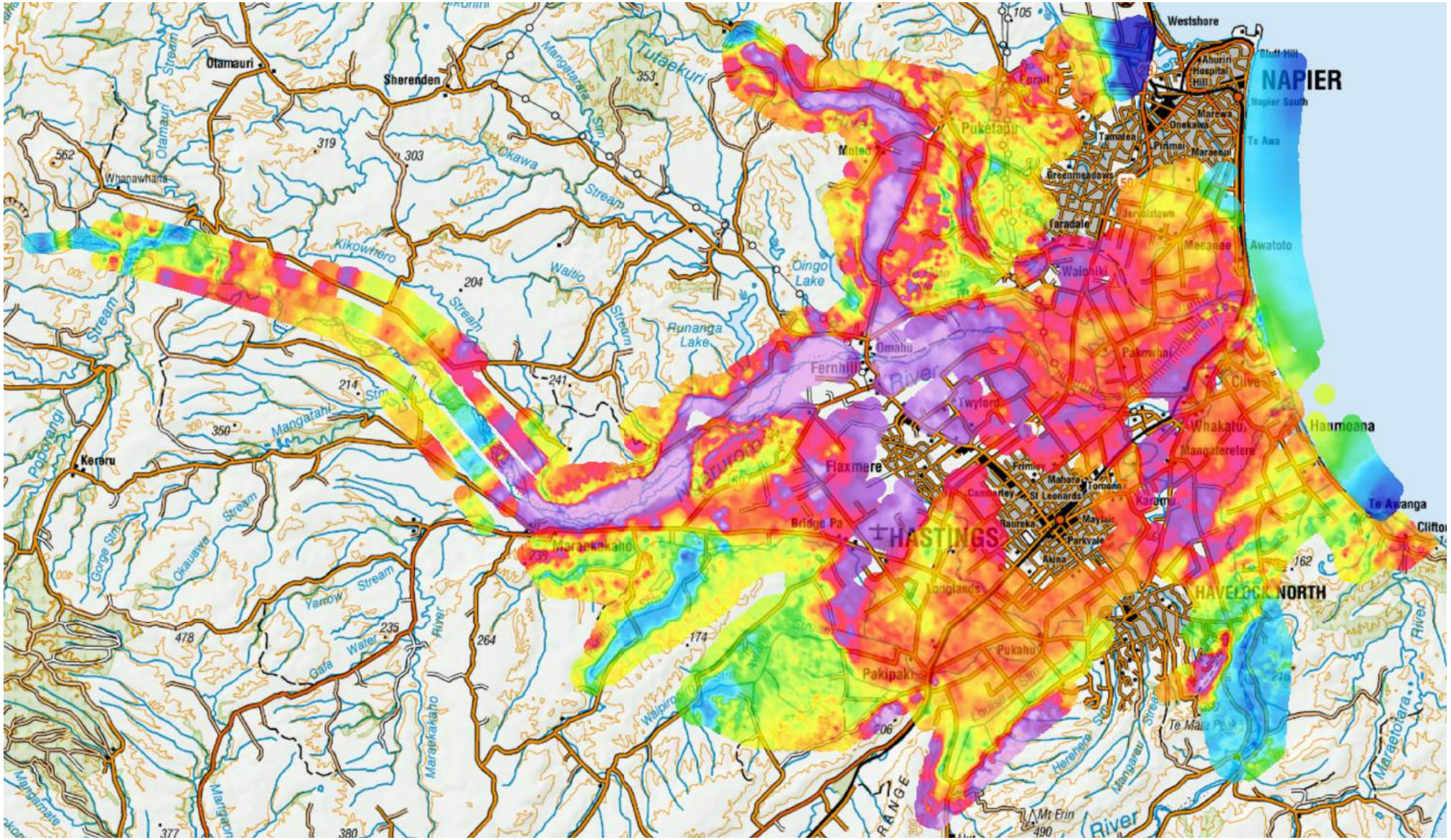

Confidential 2021

GNS SCIENCE TE PŪ AO

GNS Science Consultancy Report 2021/93

SkyTEM Survey Heretaunga 2020

2 4 6 12 21 38 68 123 222 400

Resistivity [Ohmm]

Mean Resistivity, Depth 25-30 m (ohm-m)

SCI Smooth Model - Kriging, Search Radius 400 m

NZTM2000

15 km

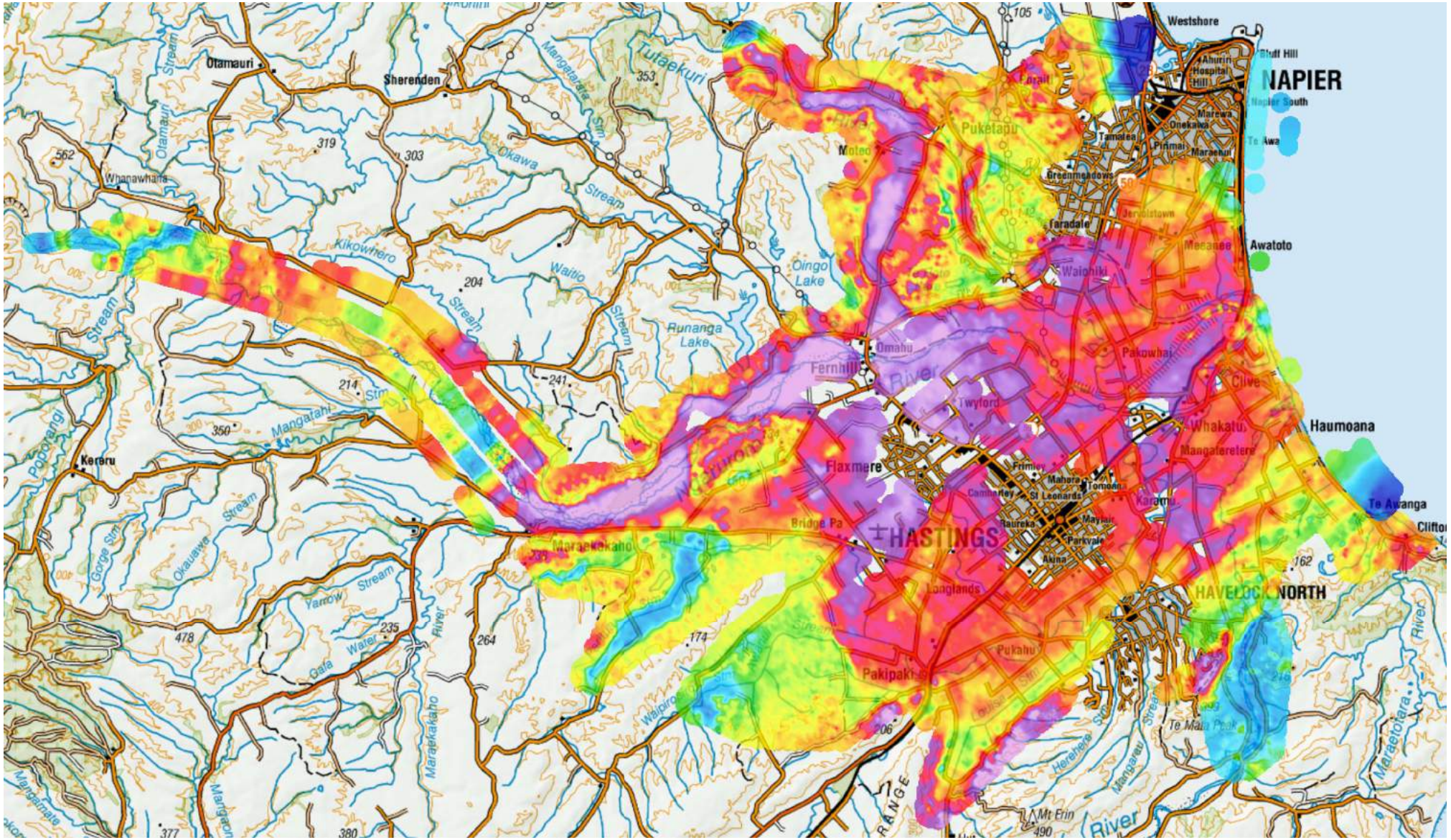

Confidential 2021

GNS SCIENCE TE PŪ AO

GNS Science Consultancy Report 2021/93

SkyTEM Survey Heretaunga 2020

2 4 6 12 21 38 68 123 222 400

Resistivity [Ohmm]

Mean Resistivity, Depth 30-35 m (ohm-m)

SCI Smooth Model - Kriging, Search Radius 400 m

NZTM2000

15 km

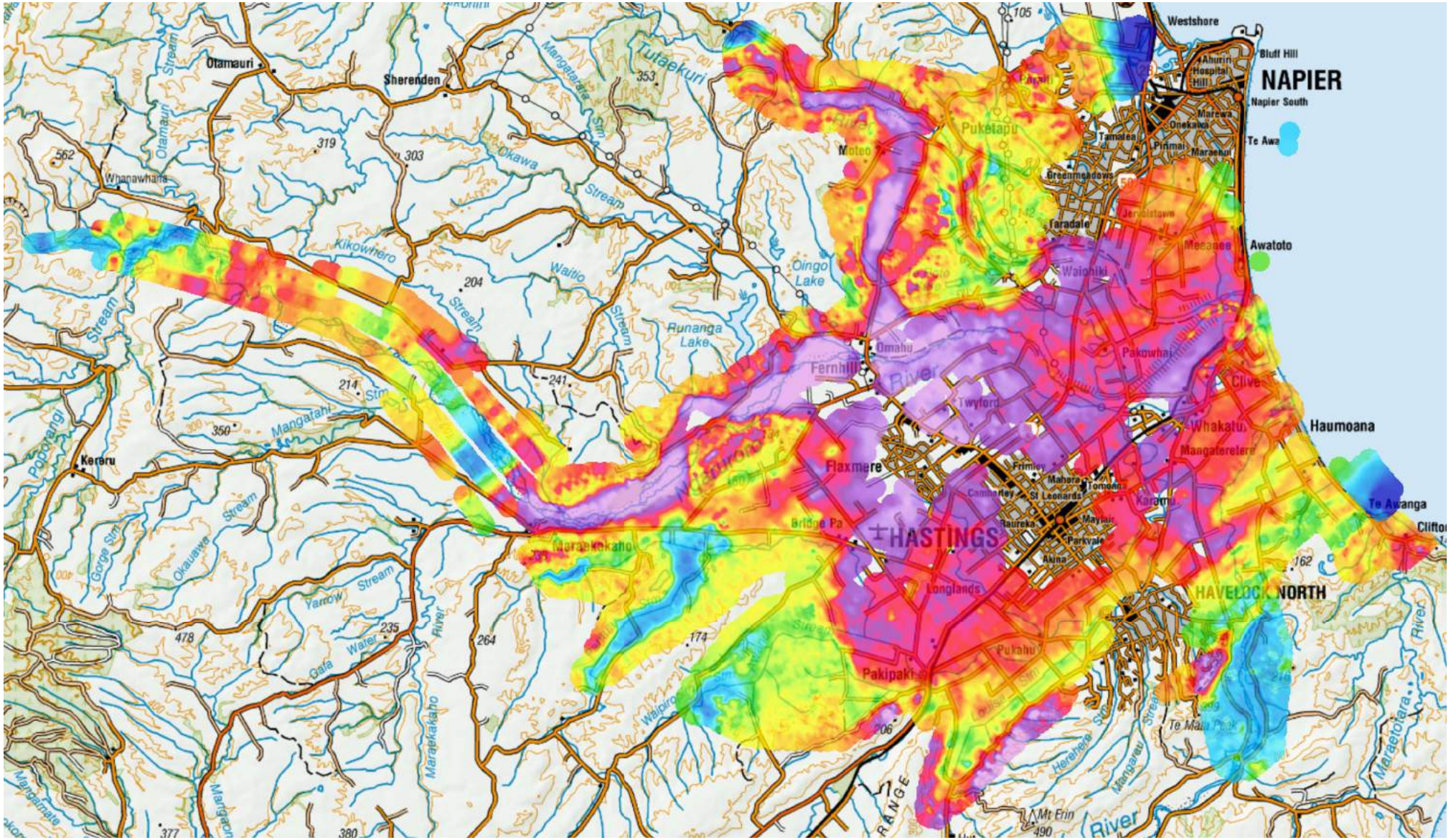

Confidential 2021

GNS SCIENCE TE PŪ AO

GNS Science Consultancy Report 2021/93

SkyTEM Survey Heretaunga 2020

2 4 6 12 21 38 68 123 222 400

Resistivity [Ohmm]

Mean Resistivity, Depth 35-40 m (ohm-m)

SCI Smooth Model - Kriging, Search Radius 400 m

NZTM2000

15 km

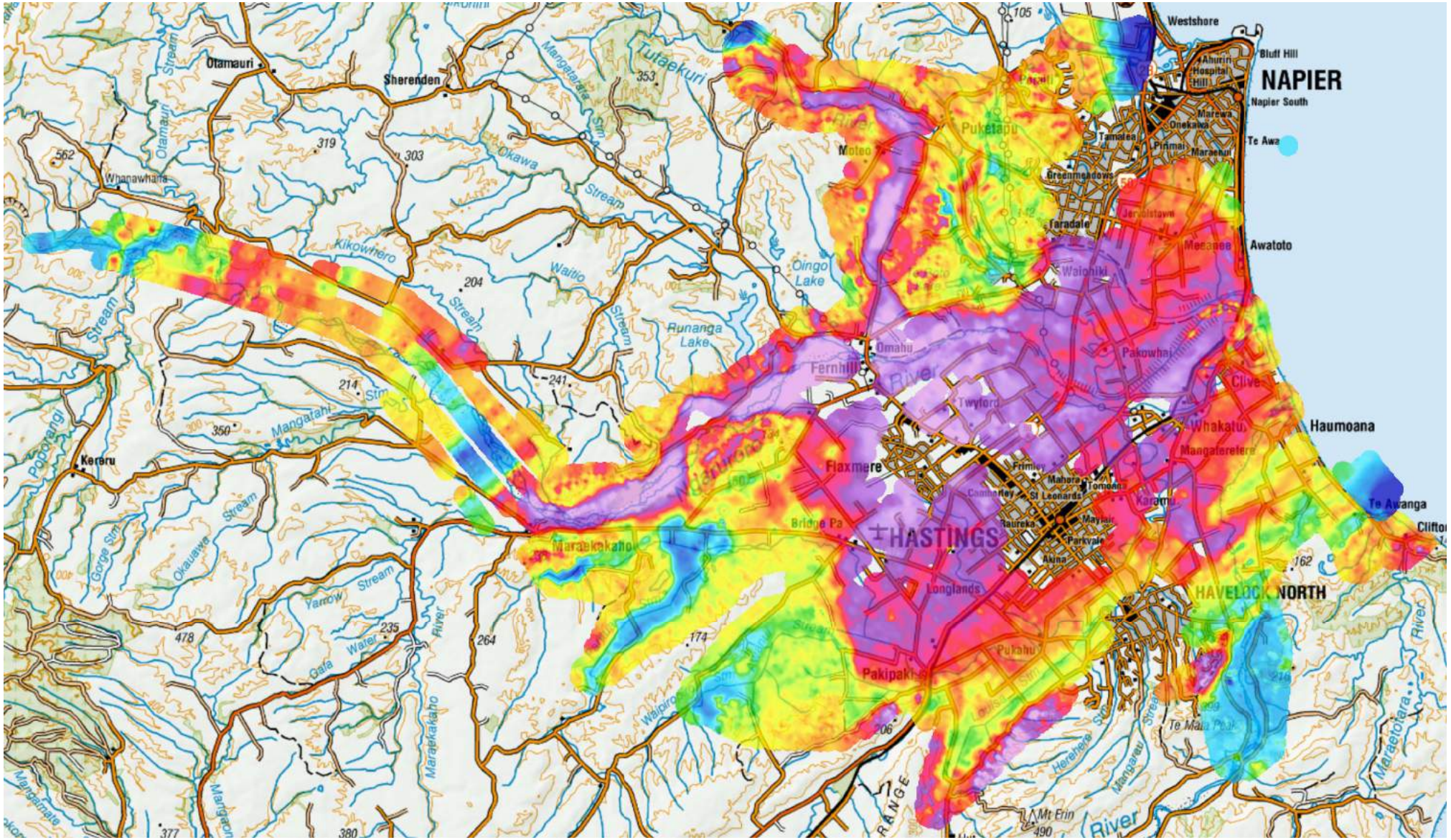

Confidential 2021

GNS SCIENCE TE PŪ AO

GNS Science Consultancy Report 2021/93

SkyTEM Survey Heretaunga 2020

2 4 6 12 21 38 68 123 222 400

Resistivity [Ohmm]

Mean Resistivity, Depth 40-45 m (ohm-m)

SCI Smooth Model - Kriging, Search Radius 400 m

NZTM2000

15 km

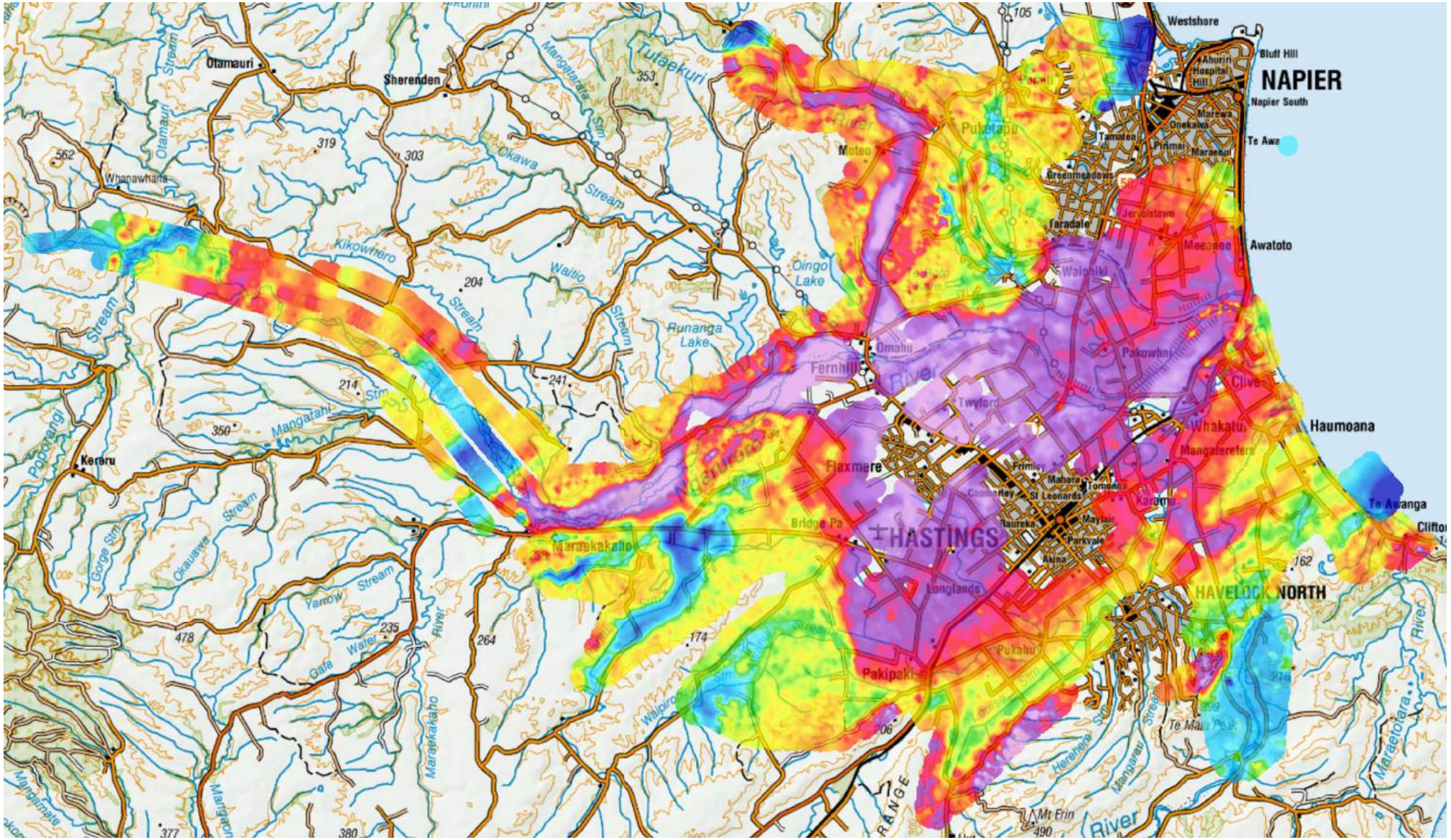

Confidential 2021

GNS SCIENCE TE PŪ AO

GNS Science Consultancy Report 2021/93

SkyTEM Survey Heretaunga 2020

Mean Resistivity, Depth 45-50 m (ohm-m)

SCI Smooth Model - Kriging, Search Radius 400 m

NZTM2000

15 km

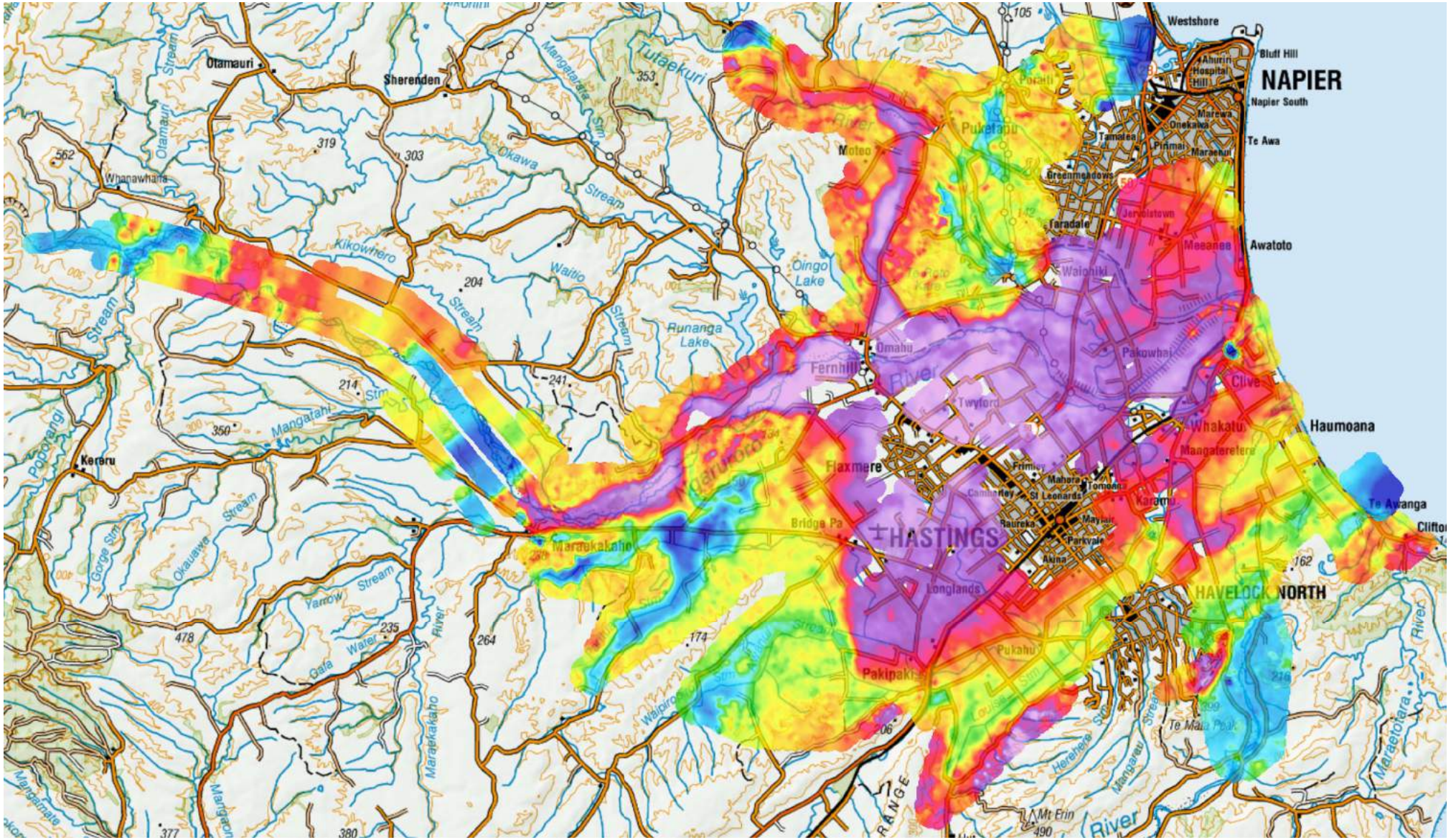

Confidential 2021

GNS SCIENCE TE PŪ AO

GNS Science Consultancy Report 2021/93

SkyTEM Survey Heretaunga 2020

Mean Resistivity, Depth 50-60 m (ohm-m)

SCI Smooth Model - Kriging, Search Radius 400 m

NZTM2000

15 km

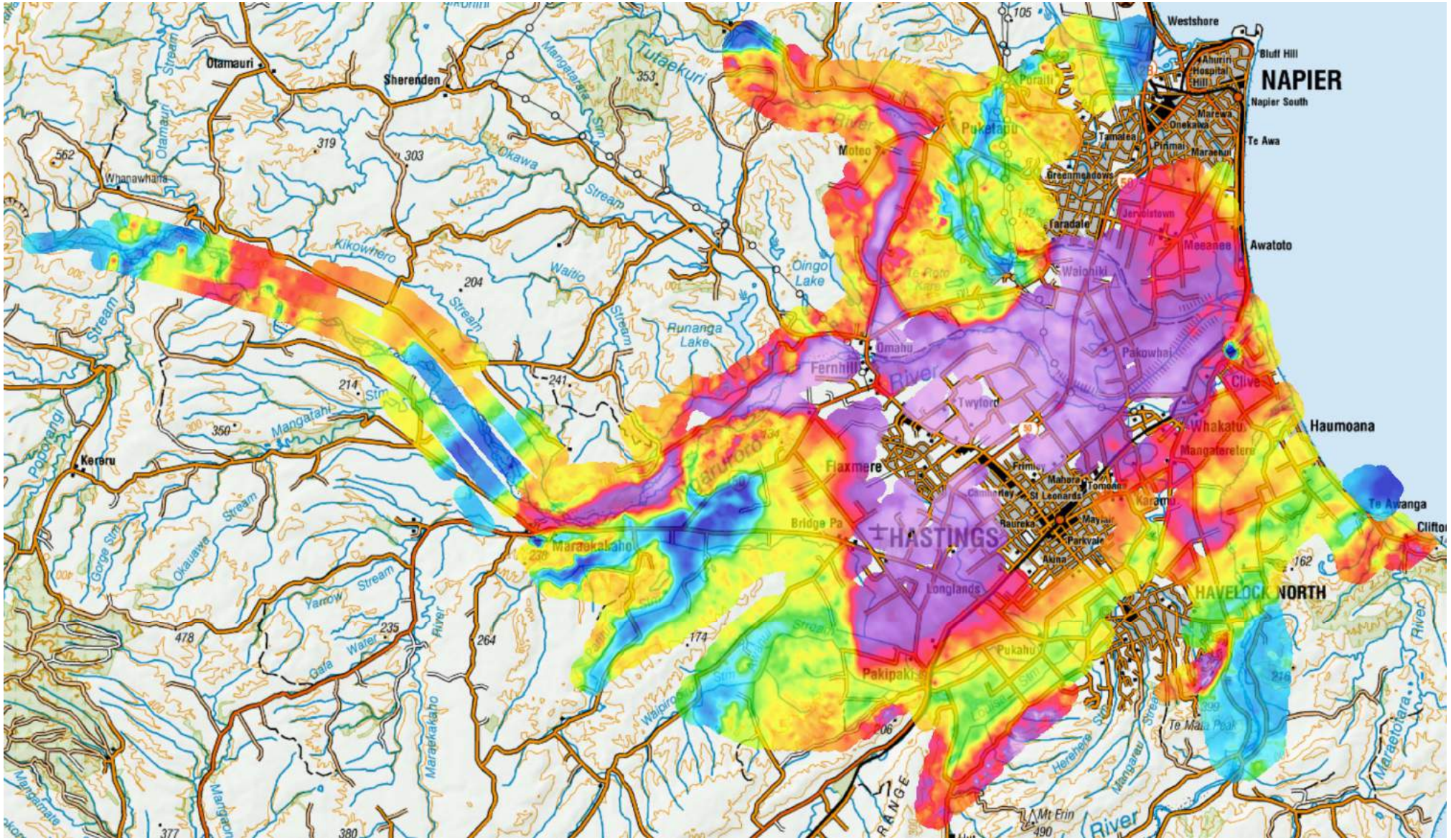

Confidential 2021

GNS SCIENCE TE PŪ AO

GNS Science Consultancy Report 2021/93

SkyTEM Survey Heretaunga 2020

2 4 6 12 21 38 68 123 222 400

Resistivity [Ohmm]

Mean Resistivity, Depth 60-70 m (ohm-m)

SCI Smooth Model - Kriging, Search Radius 400 m

NZTM2000

15 km

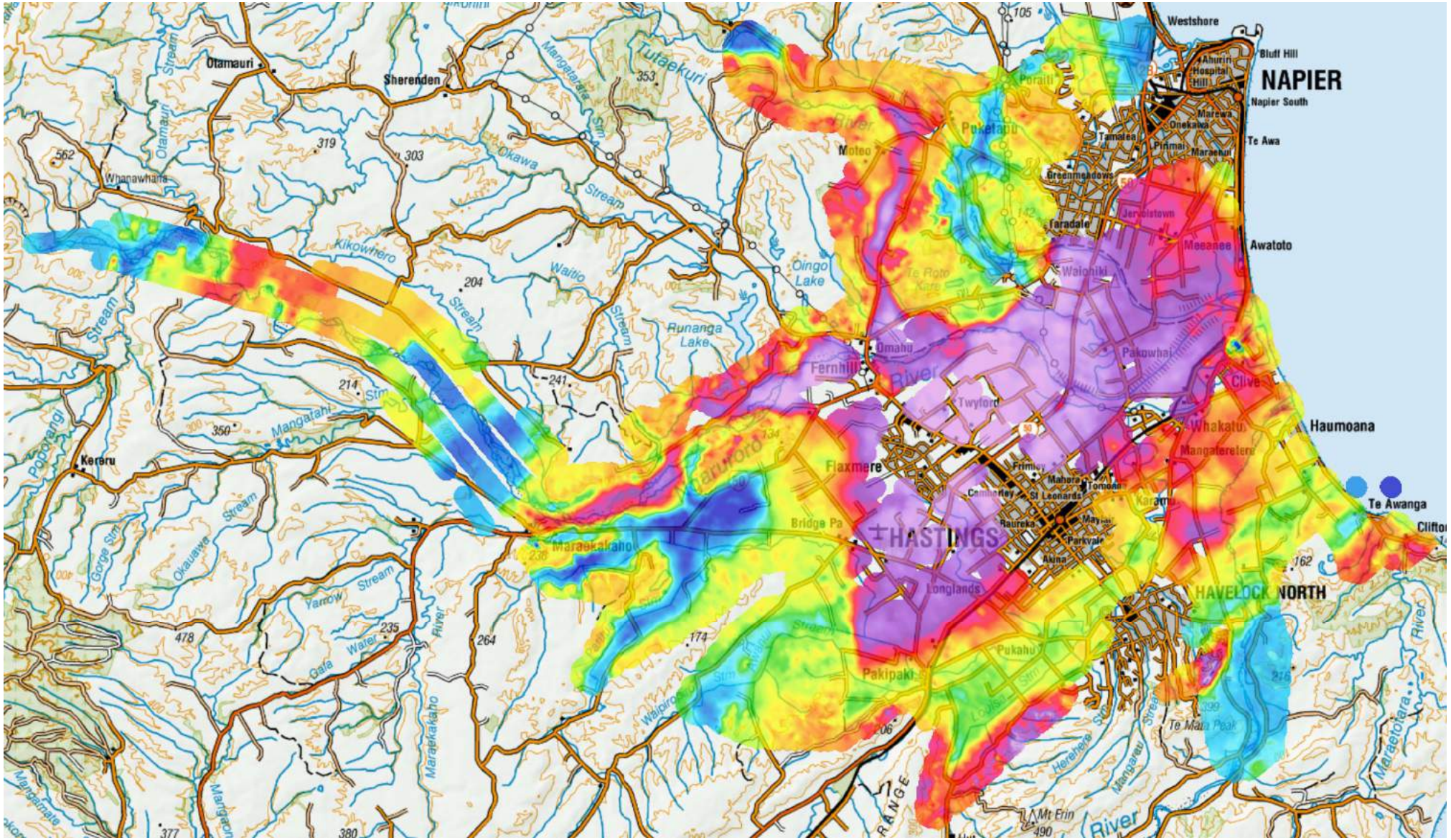

Confidential 2021

GNS SCIENCE TE PŪ AO

GNS Science Consultancy Report 2021/93

SkyTEM Survey Heretaunga 2020

2 4 6 12 21 38 68 123 222 400

Resistivity [Ohmm]

Mean Resistivity, Depth 70-80 m (ohm-m)

SCI Smooth Model - Kriging, Search Radius 400 m

NZTM2000

15 km

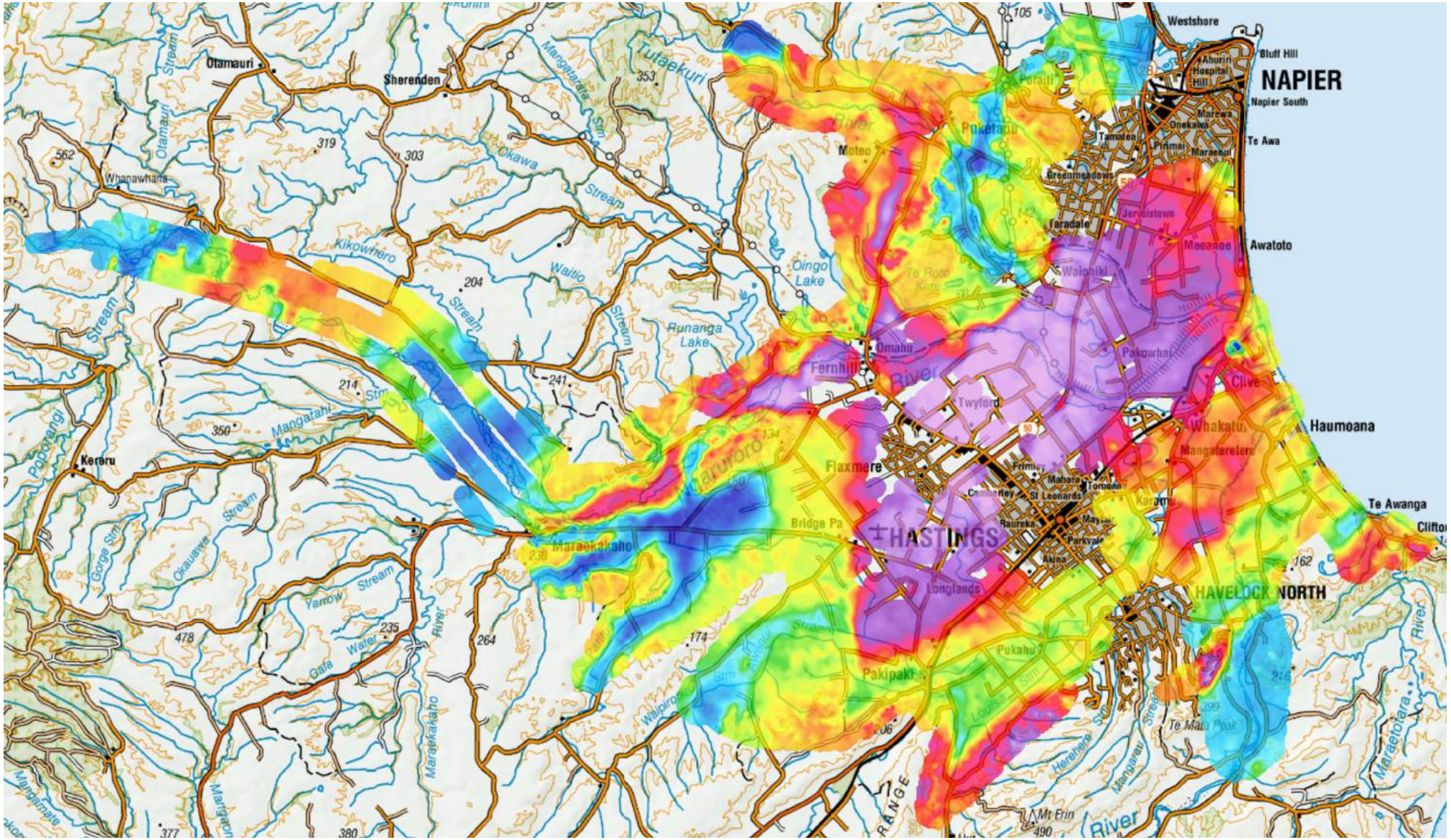

Confidential 2021

GNS SCIENCE TE PŪ AO

GNS Science Consultancy Report 2021/93

SkyTEM Survey Heretaunga 2020

2 4 6 12 21 38 68 123 222 400

Resistivity [Ohmm]

Mean Resistivity, Depth 80-90 m (ohm-m)

SCI Smooth Model - Kriging, Search Radius 400 m

NZTM2000

15 km

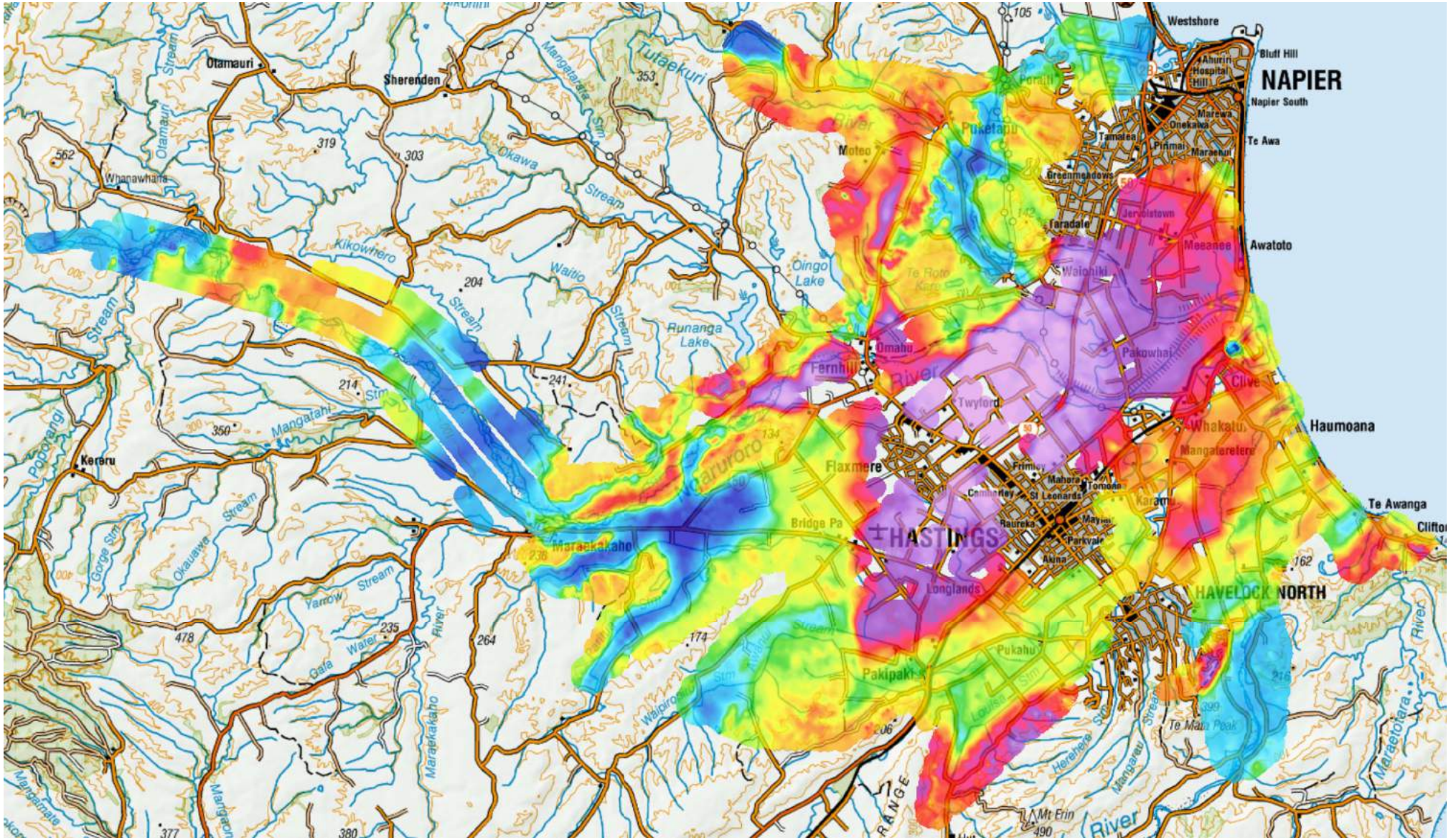

Confidential 2021

GNS SCIENCE TE PŪ AO

GNS Science Consultancy Report 2021/93

SkyTEM Survey Heretaunga 2020

2 4 6 12 21 38 68 123 222 400

Resistivity [Ohmm]

Mean Resistivity, Depth 90-100 m (ohm-m)

SCI Smooth Model - Kriging, Search Radius 400 m

NZTM2000

15 km

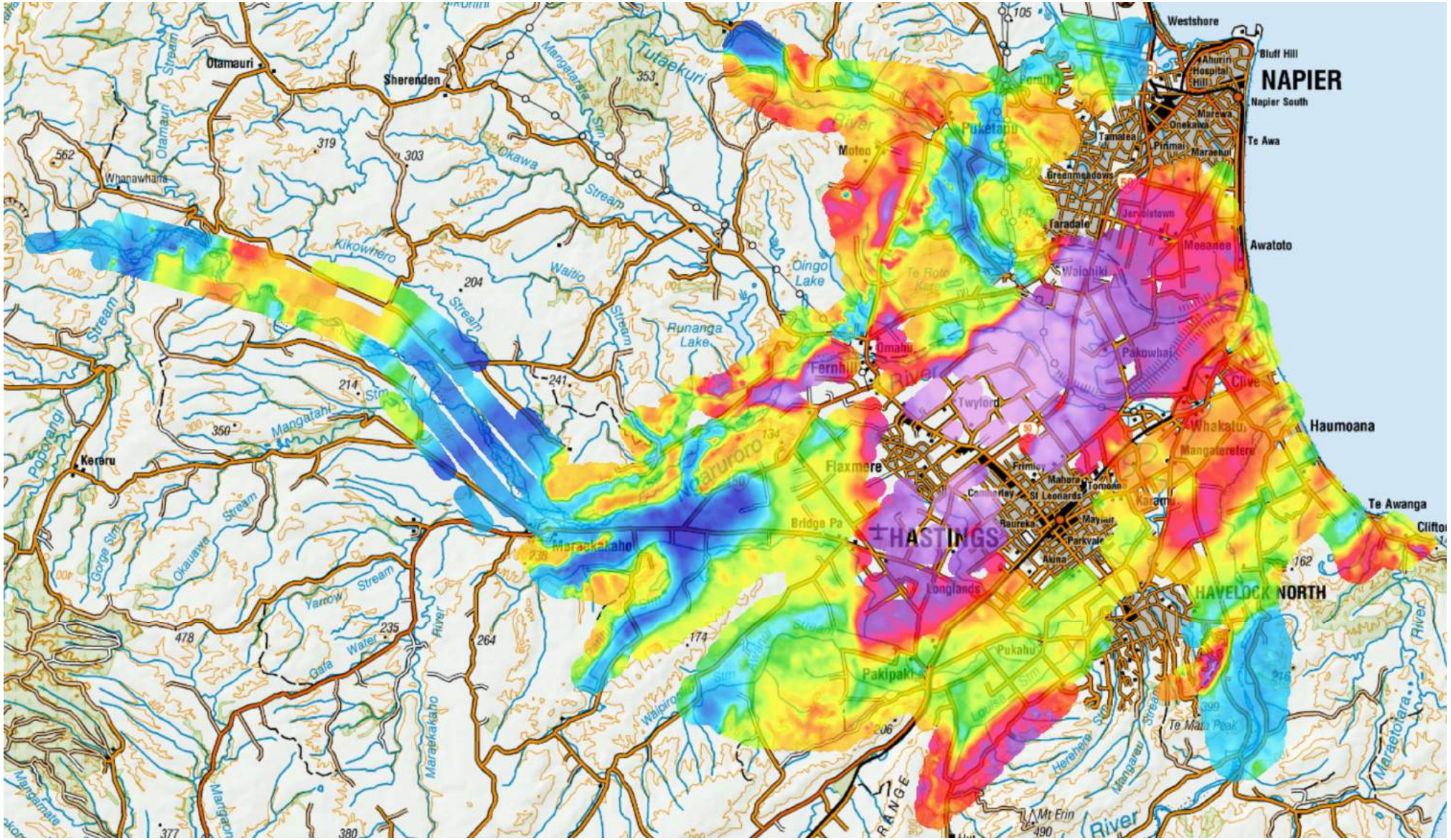

Confidential 2021

GNS SCIENCE TE PŪ AO

GNS Science Consultancy Report 2021/93

SkyTEM Survey Heretaunga 2020

Mean Resistivity, Depth 100-110 m (ohm-m)

SCI Smooth Model - Kriging, Search Radius 400 m

NZTM2000

15 km

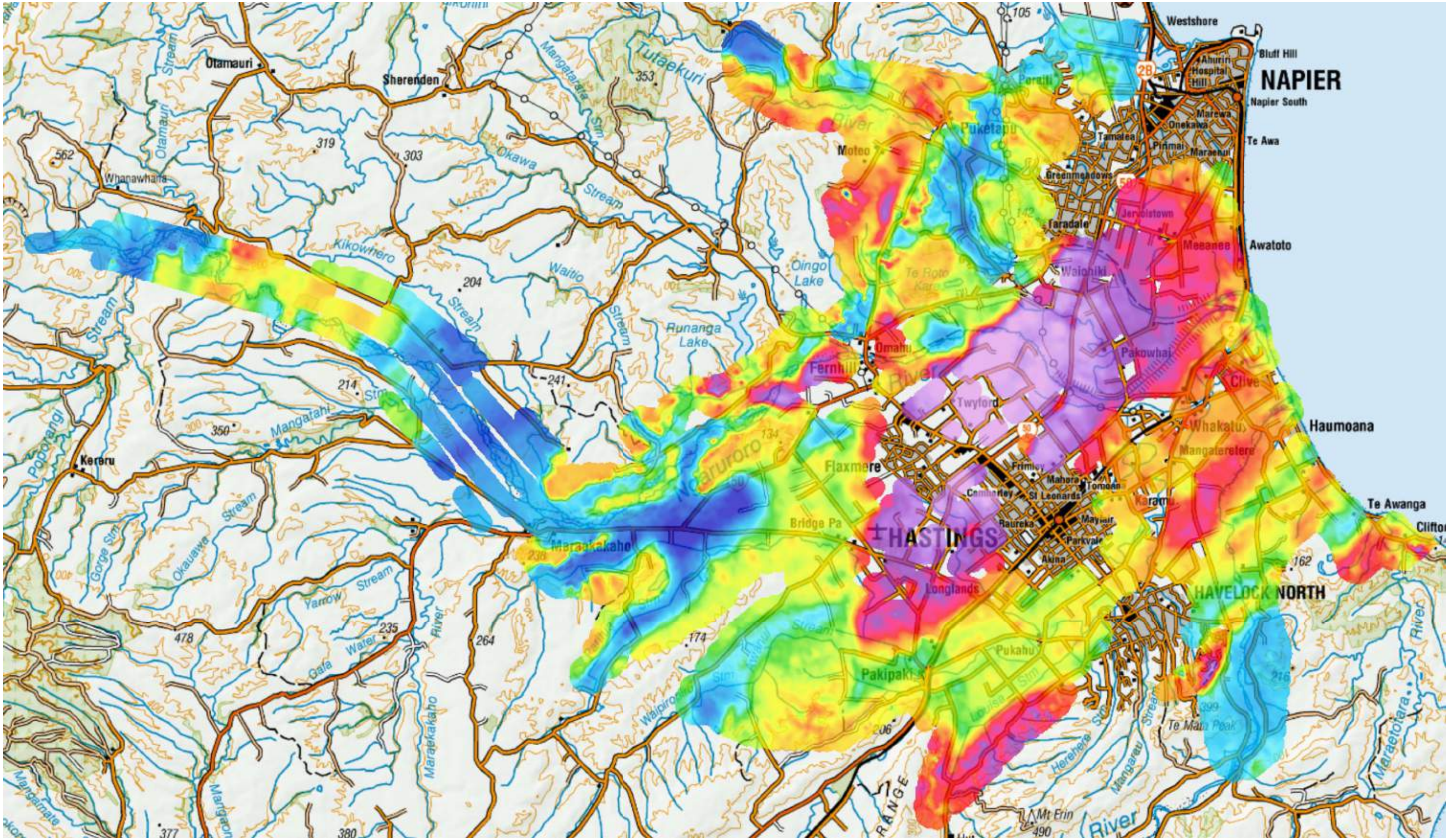

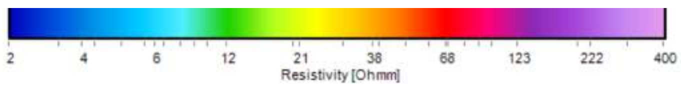

Confidential 2021

GNS SCIENCE TE PŪ AO

GNS Science Consultancy Report 2021/93

SkyTEM Survey Heretaunga 2020

Mean Resistivity, Depth 110-120 m (ohm-m)

SCI Smooth Model - Kriging, Search Radius 400 m

NZTM2000

15 km

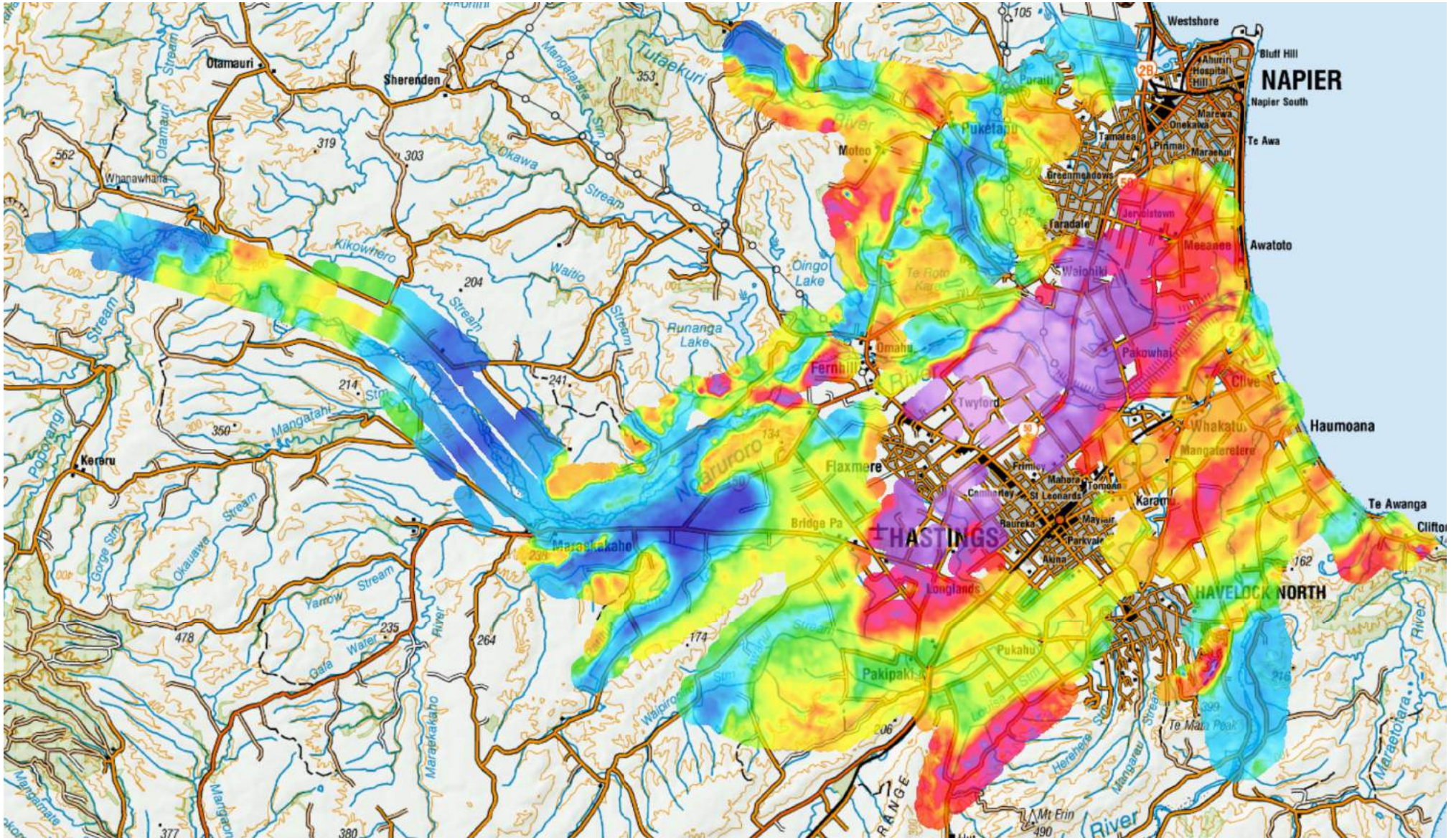

Confidential 2021

GNS SCIENCE TE PŪ AO

GNS Science Consultancy Report 2021/93

SkyTEM Survey Heretaunga 2020

Mean Resistivity, Depth 120-130 m (ohm-m)

SCI Smooth Model - Kriging, Search Radius 400 m

NZTM2000

15 km

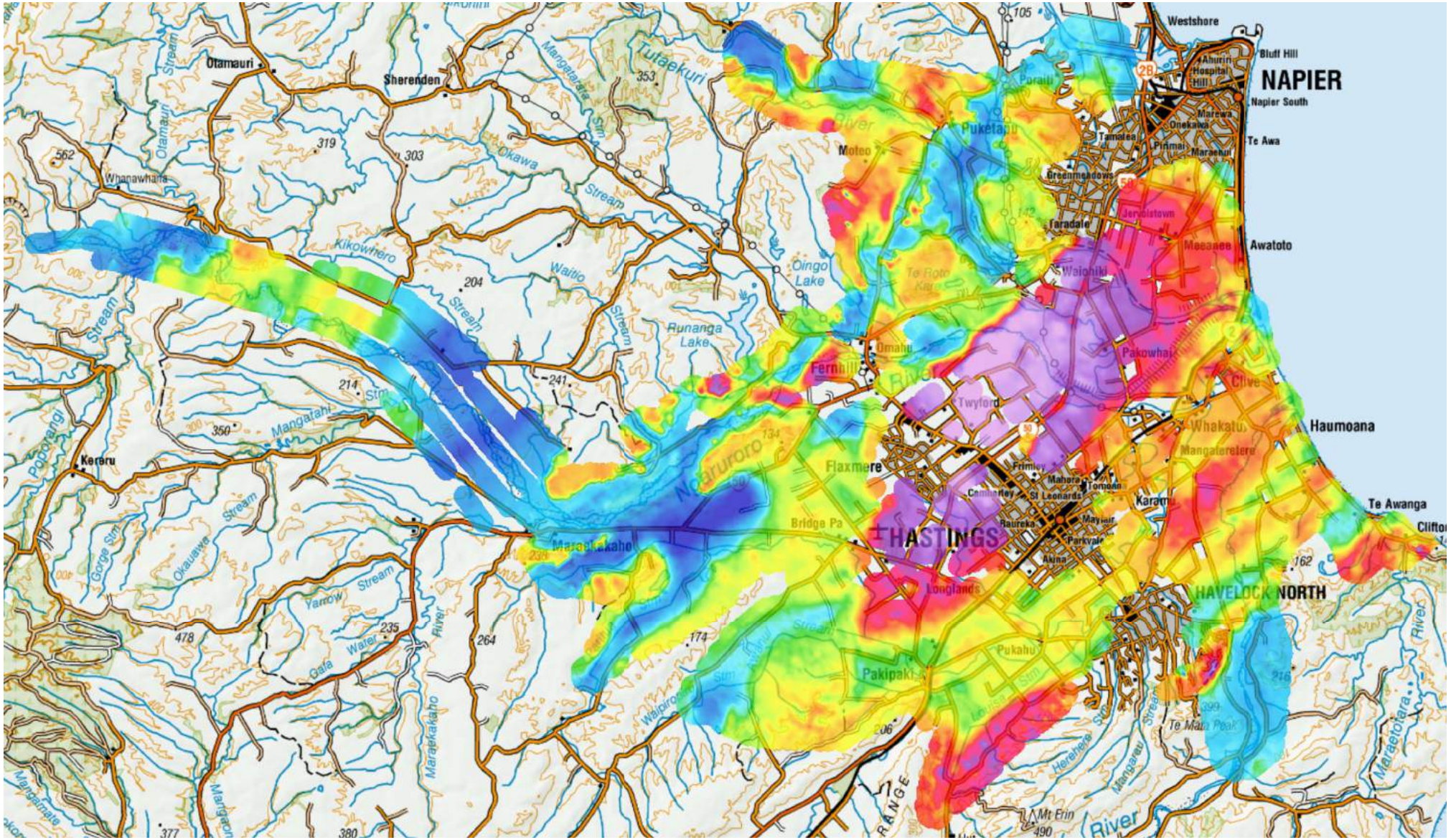

Confidential 2021

GNS SCIENCE TE PŪ AO

GNS Science Consultancy Report 2021/93

SkyTEM Survey Heretaunga 2020

2 4 6 12 21 38 68 123 222 400

Resistivity [Ohmm]

Mean Resistivity, Depth 130-140 m (ohm-m)

SCI Smooth Model - Kriging, Search Radius 400 m

NZTM2000

15 km

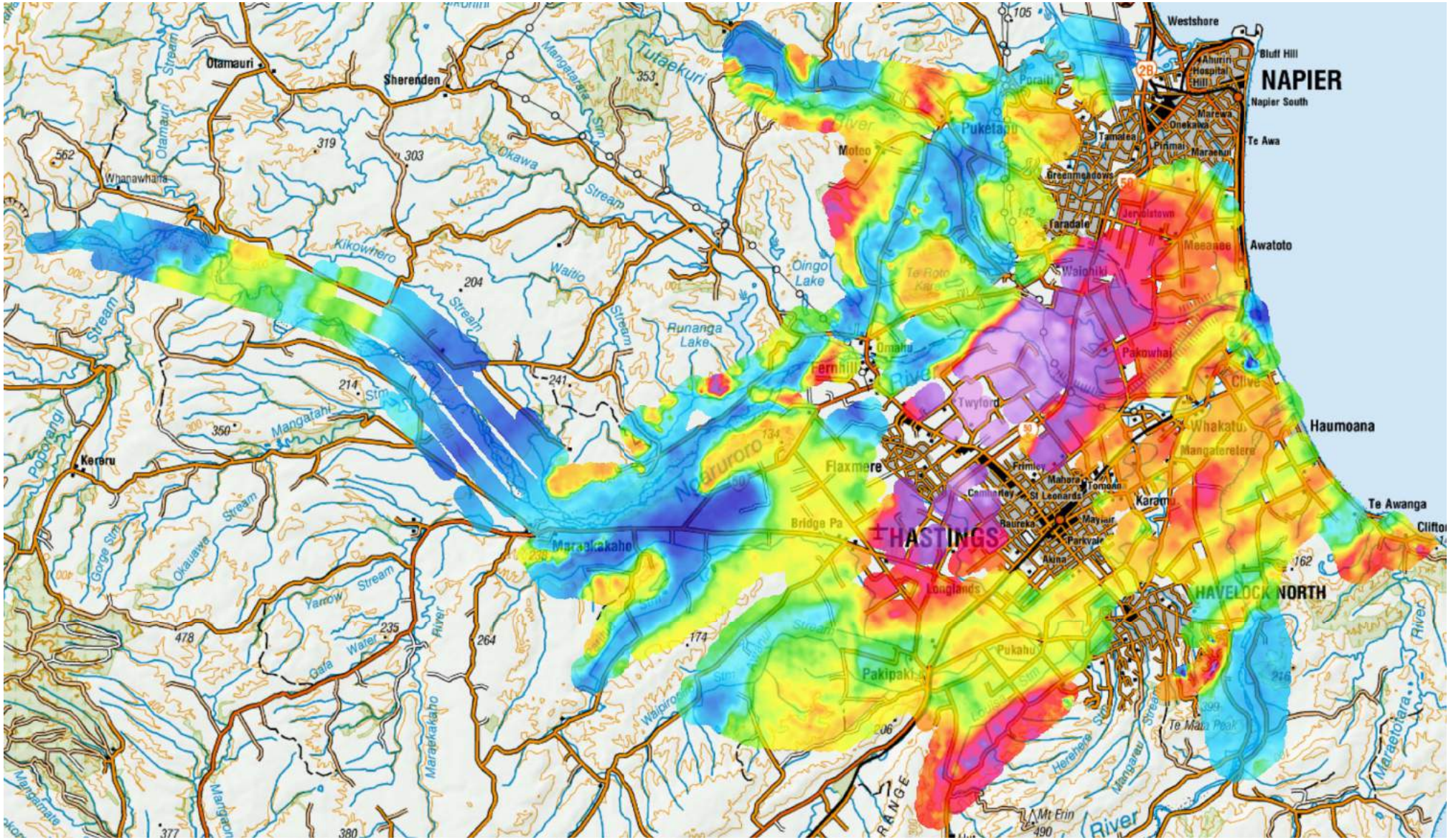

Confidential 2021

GNS SCIENCE TE PŪ AO

GNS Science Consultancy Report 2021/93

SkyTEM Survey Heretaunga 2020

2 4 6 12 21 38 68 123 222 400

Resistivity [Ohmm]

Mean Resistivity, Depth 140-150 m (ohm-m)

SCI Smooth Model - Kriging, Search Radius 400 m

NZTM2000

15 km

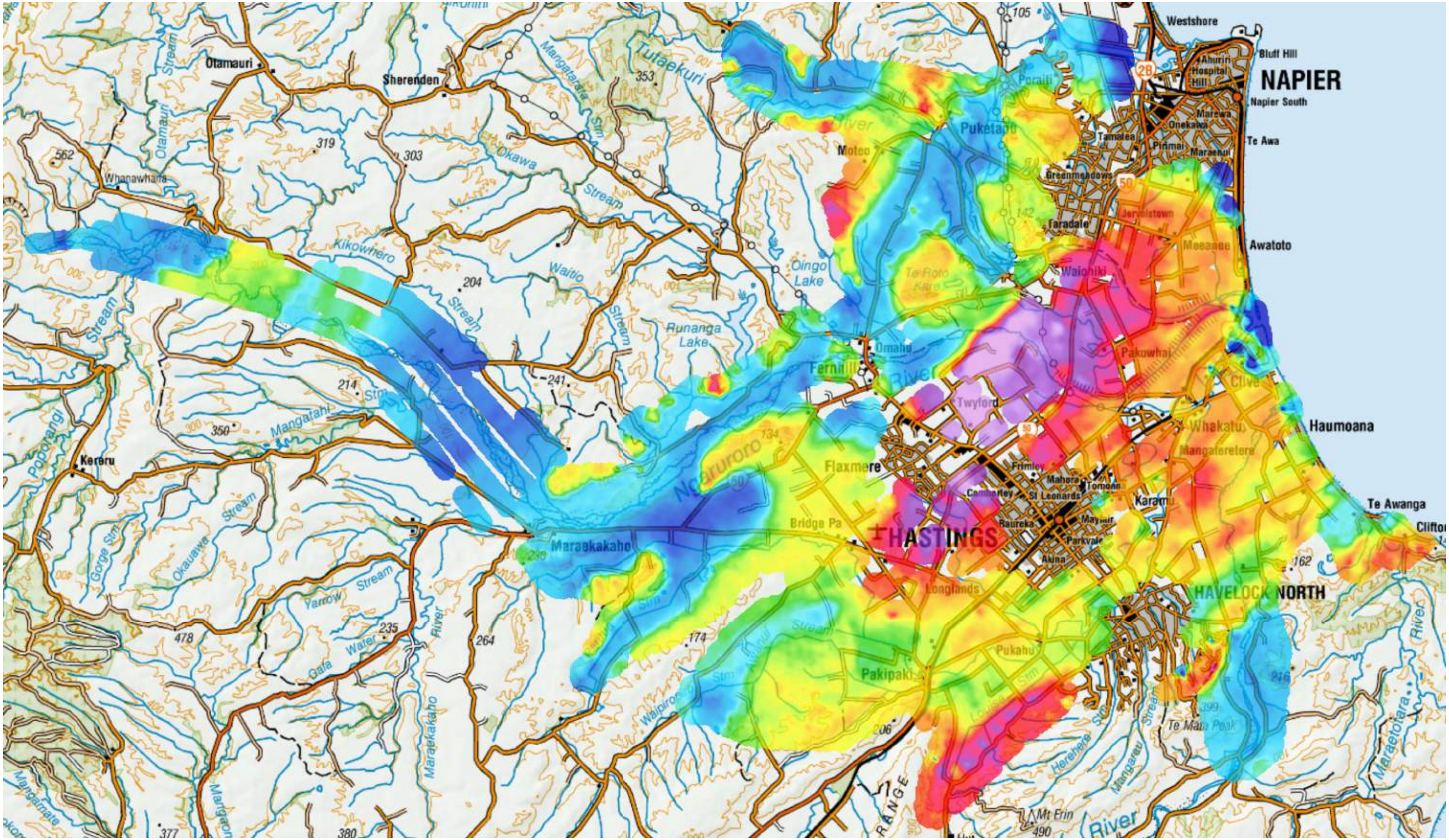

GNS SCIENCE TE PŪ AO

GNS Science Consultancy Report 2021/93

SkyTEM Survey Heretaunga 2020

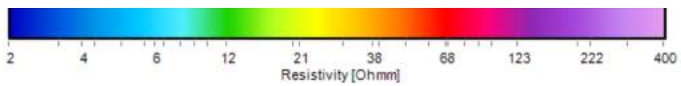

Mean Resistivity, Depth 150-200 m (ohm-m)

SCI Smooth Model - Kriging, Search Radius 400 m

NZTM2000

15 km

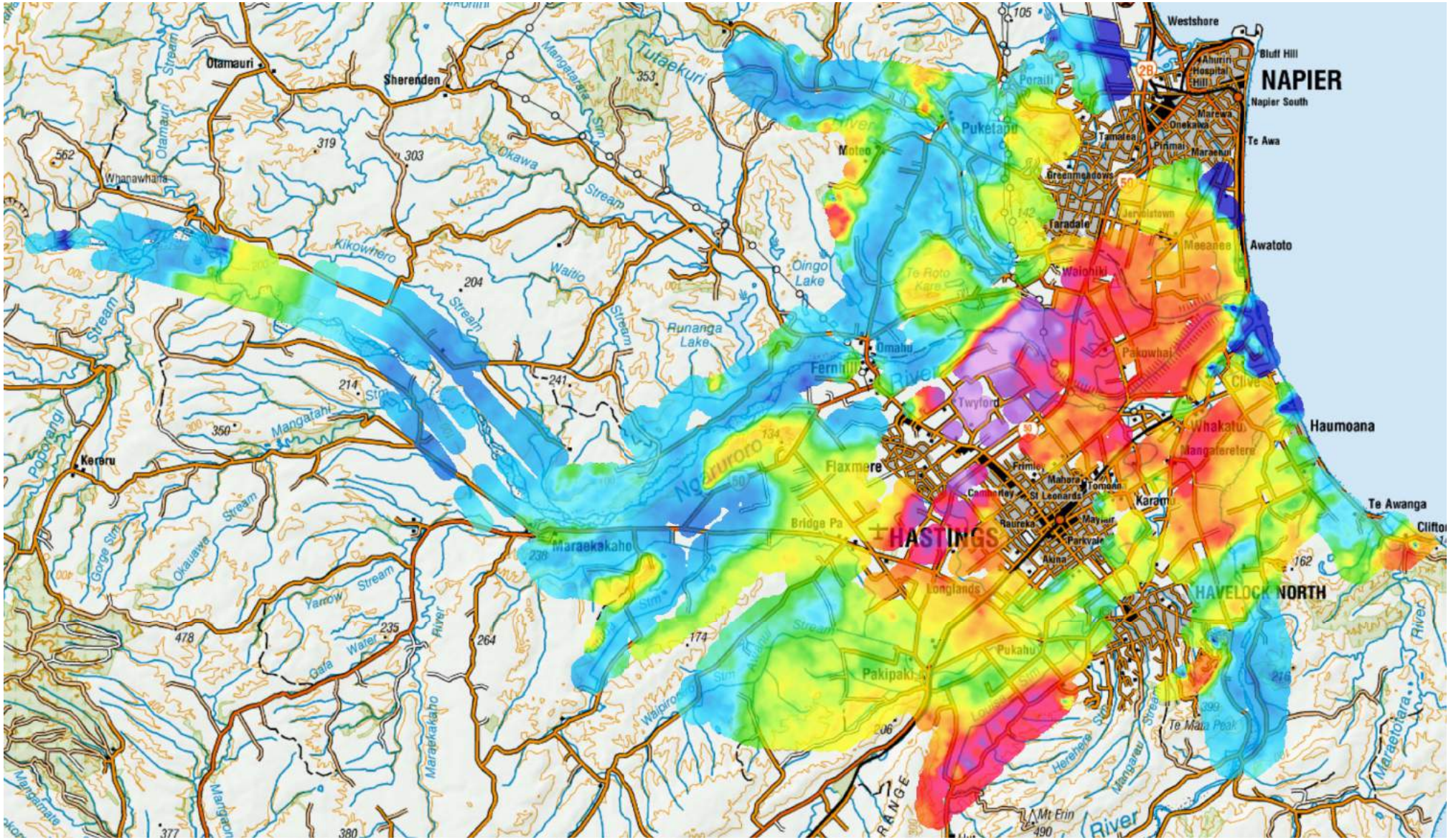

Confidential 2021

GNS SCIENCE TE PŪ AO

GNS Science Consultancy Report 2021/93

SkyTEM Survey Heretaunga 2020

2 4 6 12 21 38 68 123 222 400

Resistivity [Ohmm]

Mean Resistivity, Depth 200-250 m (ohm-m)

SCI Smooth Model - Kriging, Search Radius 400 m

NZTM2000

15 km

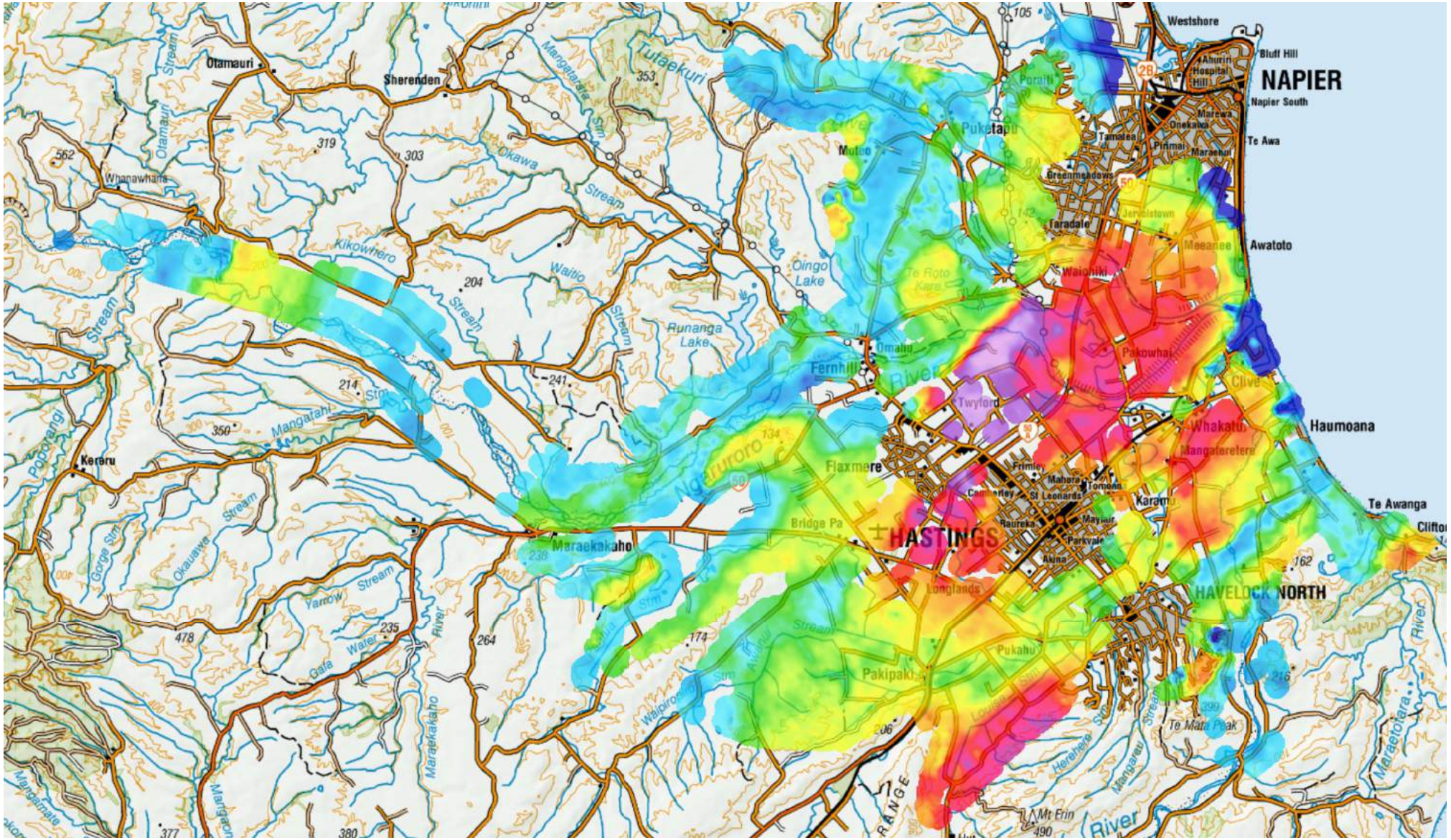

Confidential 2021

GNS SCIENCE TE PŪ AO

GNS Science Consultancy Report 2021/93

SkyTEM Survey Heretaunga 2020

Mean Resistivity, Depth 250-300 m (ohm-m)

SCI Smooth Model - Kriging, Search Radius 400 m

NZTM2000

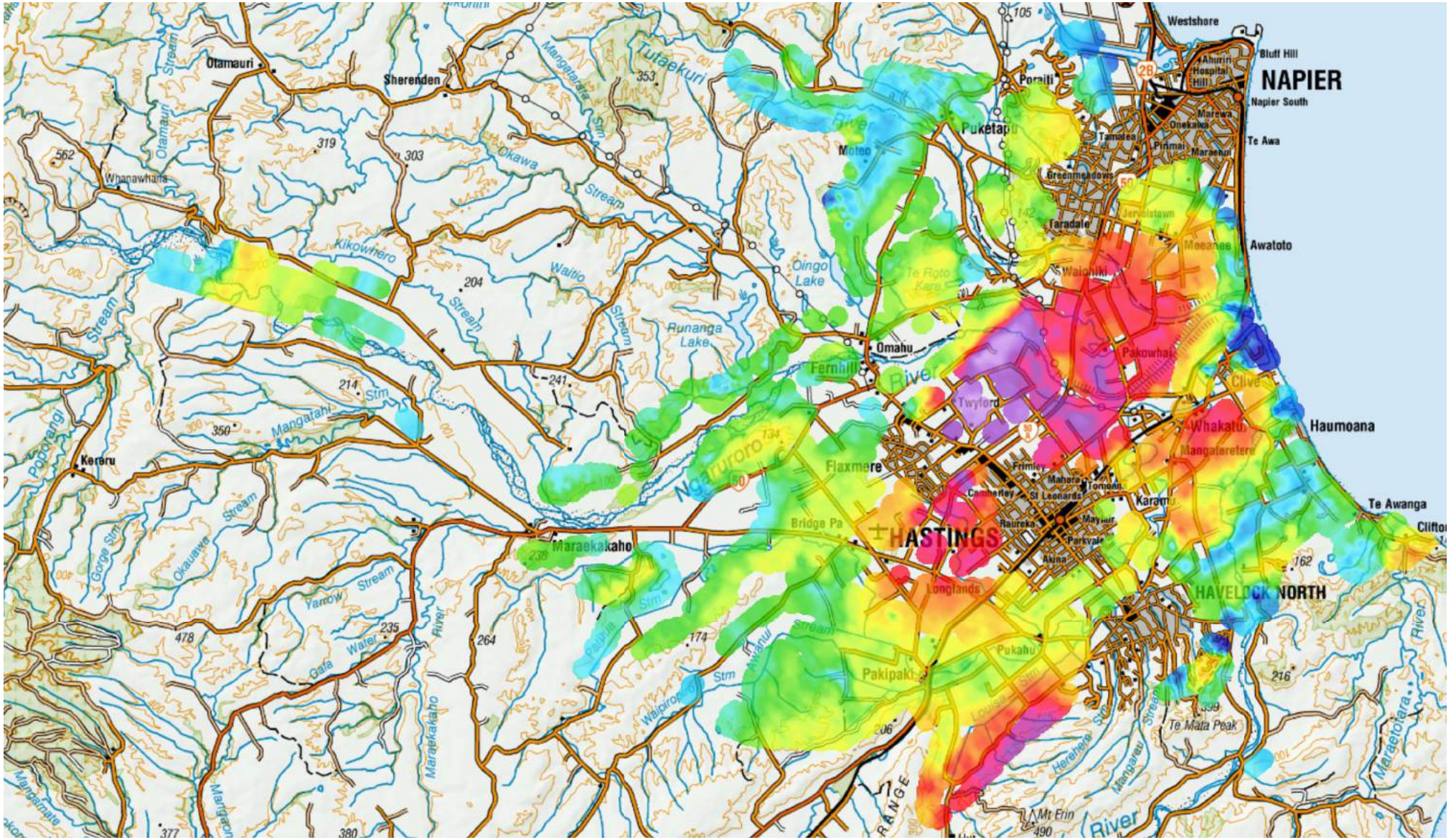

Confidential 2021

GNS SCIENCE TE PŪ AO

GNS Science Consultancy Report 2021/93

SkyTEM Survey Heretaunga 2020

2 4 6 12 21 38 68 123 222 400

Resistivity [Ohmm]

Mean Resistivity, Depth 300-350 m (ohm-m)

SCI Smooth Model - Kriging, Search Radius 400 m

NZTM2000

15 km

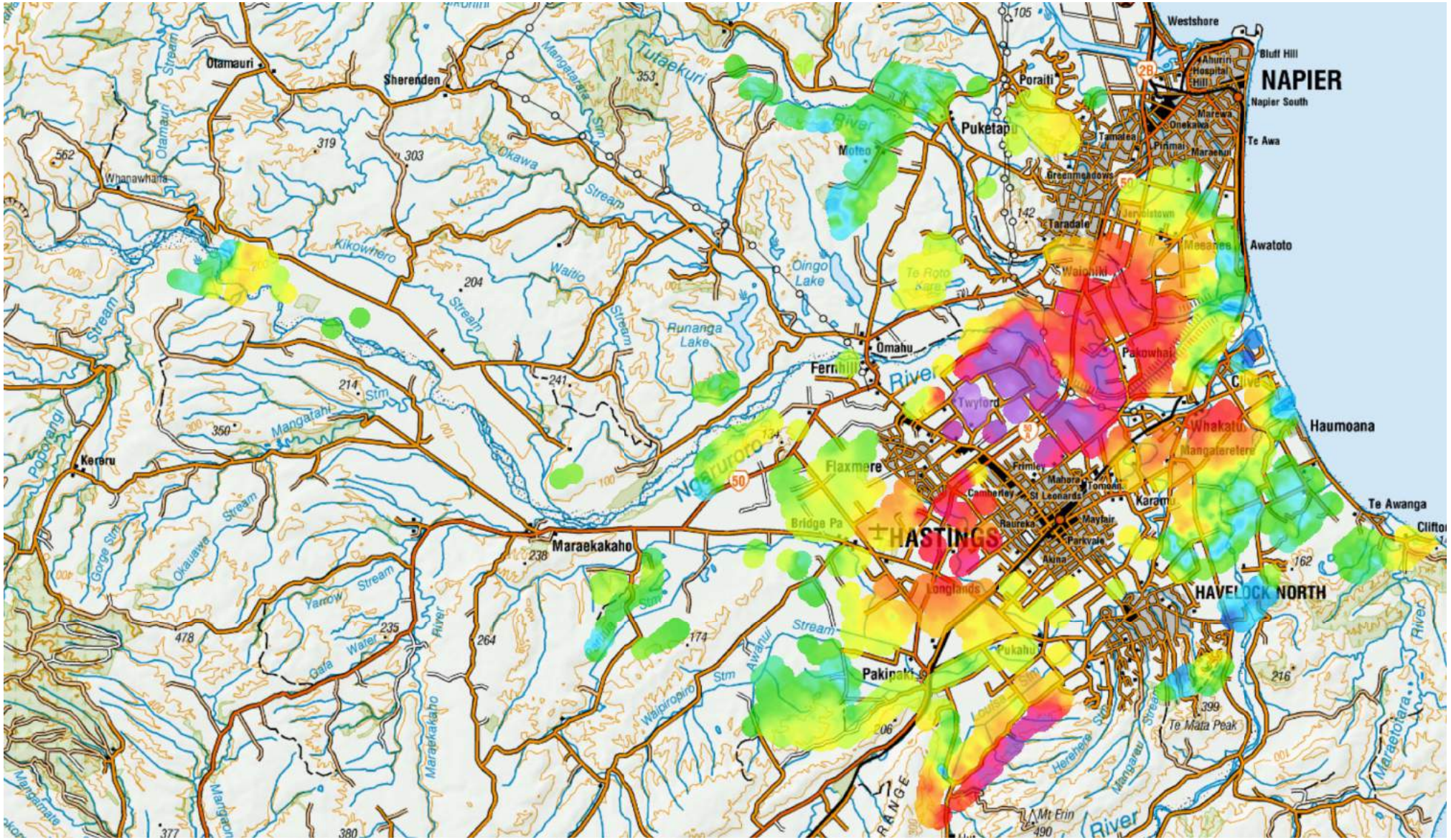

Confidential 2021

GNS SCIENCE TE PŪ AO

GNS Science Consultancy Report 2021/93

SkyTEM Survey Heretaunga 2020

2 4 6 12 21 38 68 123 222 400

Resistivity [Ohmm]

Mean Resistivity, Depth 350-400 m (ohm-m)

SCI Smooth Model - Kriging, Search Radius 400 m

NZTM2000

15 km

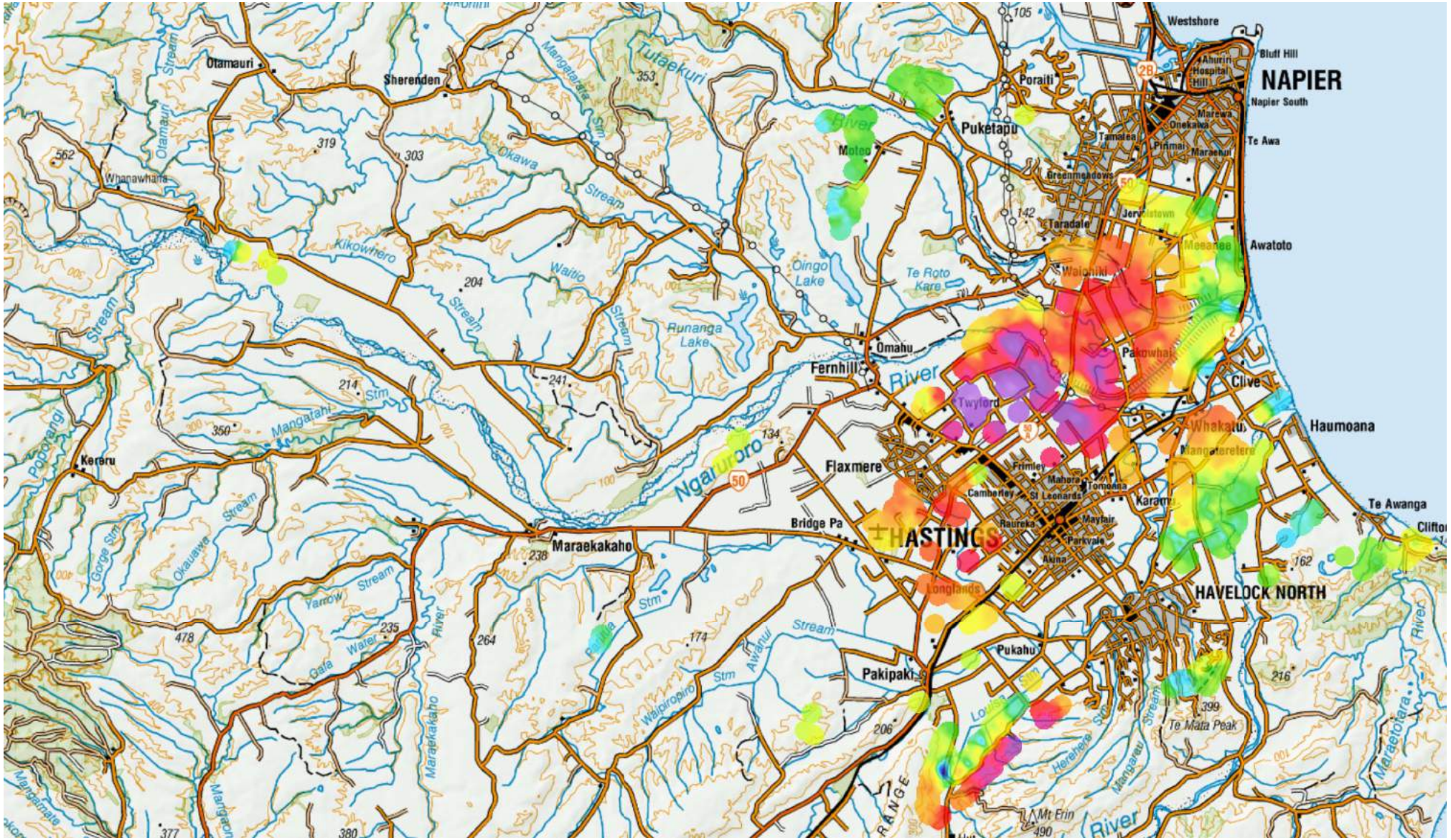

Confidential 2021

GNS SCIENCE TE PŪ AO

GNS Science Consultancy Report 2021/93

SkyTEM Survey Heretaunga 2020

2 4 6 12 21 38 68 123 222 400

Resistivity [Ohmm]

Mean Resistivity, Depth 400-450 m (ohm-m)

SCI Smooth Model - Kriging, Search Radius 400 m

NZTM2000

15 km

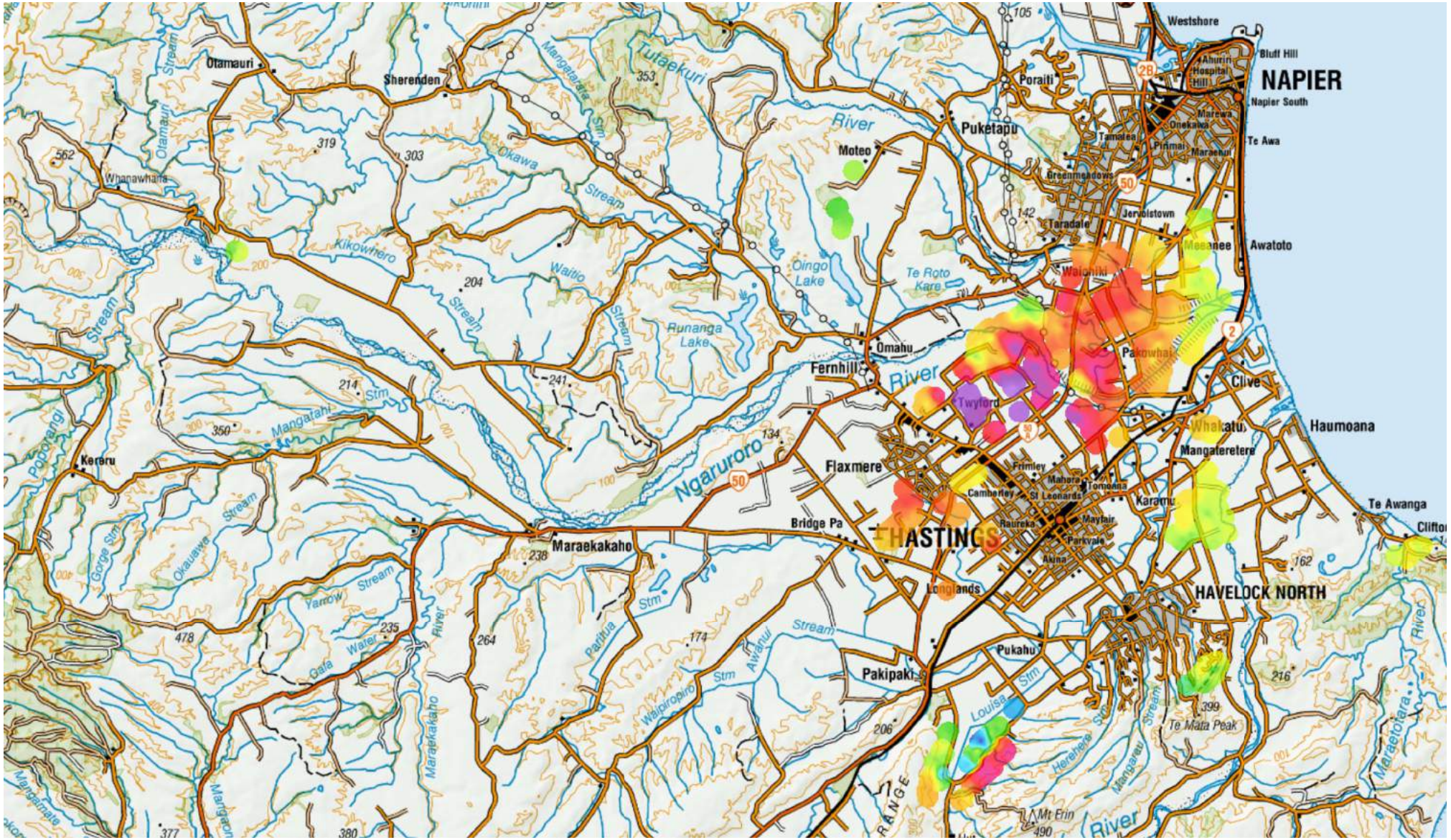

Confidential 2021

GNS SCIENCE TE PŪ AO

GNS Science Consultancy Report 2021/93

SkyTEM Survey Heretaunga 2020

2 4 6 12 21 38 68 123 222 400

Resistivity [Ohmm]

Mean Resistivity, Depth 450-500 m (ohm-m)

SCI Smooth Model - Kriging, Search Radius 400 m

NZTM2000

15 km

APPENDIX 4 DELIVERABLE FILE DESCRIPTIONS

In all cases, STD refers to Standard Deviation and UTC refers to Coordinated Universal Time.

Elevations in Tables A4.1–A4.6 utilise a DEM for calculations. The DEM utilised was a 10 m resolution DEM in NZVD2016, which was derived from a 5 m resolution DEM that was created by HBRC using a combination of LiDAR and SRTM V2 data (Farrier 2020; see Section 3.5).

Table A4.1 Format of the resistivity model xyz-ascii files for both the sharp and smooth models, for example: *\xyz_ascii\Heretaunga_smooth_resistivitymodel_V1_2021_inv.xyz*

Attribute	Description
LINE_NO	Line number
UTMX	Easting NZTM
UTMY	Northing NZTM
TIMESTAMP	Time (days) using epoch starting 30 December 1899, in UTC
FID	Fiducial
RECORD	Record
ELEVATION	Topography (m; from imported DEM)
ALT	Input altitude (metres above ground level)
INVALT	Inverted altitude (metres above ground level)
INVALTSTD	STD on inverted altitude
DELTAALT	Difference between input and inverted altitude (m; inverted – input altitude)
TILT	NA (not utilised by SkyTEM Z-component inversion)
INVTILT	NA (not utilised by SkyTEM Z-component inversion)
INVTILTSTD	NA (not utilised by SkyTEM Z-component inversion)
SHIFT	NA (not utilised by SkyTEM Z-component inversion)
INVSHIFT	NA (not utilised by SkyTEM Z-component inversion)
INVSHIFTSTD	NA (not utilised by SkyTEM Z-component inversion)
NUMDATA	Number of gates inverted (number of data points)
SEGMENTS	Moment ID (low moment = 1, high moment = 2, both = 12 or 21)
RESDATA	Data mis-fit (Equation A4.1 for each 1D inversion)
RESTOTAL	Total mis-fit (Equation A4.2 for the entire inversion)
RHO_I_1	Resistivity (Ohm.m) for layer_1
RHO_I_2	Resistivity (Ohm.m) for layer_2
…	…
RHO_I_N	Resistivity (Ohm.m) for layer N
RHO_I_STD_1	STD on resistivity for layer_1
RHO_I_STD_2	STD on resistivity for layer_2
…	…
RHO_I_STD_N	STD on resistivity for layer_N
SIGMA_I_1	Conductivity (mS/m) for layer_1

Attribute	Description
SIGMA_I_2	Conductivity (mS/m) for layer_2
…	…
SIGMA_I_N	Conductivity (mS/m) for layer_N
DEP_TOP_1	Depth (m) to top of layer_1
DEP_TOP_2	Depth (m) to top of layer_2
…	…
DEP_TOP_N	Depth (m) to top of layer_N
DEP_BOT_1	Depth (m) to botttom of layer_1
DEP_BOT_2	Depth (m) to botttom of layer_2
…	…
DEP_BOT_N-1	Depth (m) to botttom of layer_N-1
THK_1	Thickness (m) of layer_1
THK_2	Thickness (m) of layer_2
…	…
THK_N-1	Thickness (m) of layer_N-1
THK_STD_1	STD on thickness of layer_1
THK_STD_2	STD on thickness of layer_2
…	…
THK_STD_N-1	STD on thickness of layer_N-1
DEP_BOT_STD_1	STD on depth bottom of layer_1
DEP_BOT_STD_2	STD on depth bottom of layer_2
…	…
DEP_BOT_STD_N-1	STD on depth bottom of layer_N-1
DOI_CONSERVATIVE	DOI Conservative for resistivity (m)
DOI_STANDARD	DOI Standard for resistivity (m)

$$\left(\frac{1}{N}\sum_{i=1}^{N}\frac{\left(d_{obs,i}-d_{forward,i}\right)^2}{C_{obs,i}}\right)^{\frac{1}{2}}$$

Equation A4.1 Calculation of RESDATA. Observed data (d_{obs}), forward model calculation of data from inversion model ($d_{forward}$), standard deviation of the measured data (C_{obs}).

$$\left(\frac{1}{N}\sum_{i=1}^{N}\frac{\left(d_{obs,i}-d_{forward,i}\right)^2}{C_{obs,i}}\right)^{\frac{1}{2}}+\left(\frac{1}{M}\sum_{i=1}^{M}\frac{\left(m_i-m_{prior,i}\right)^2}{C_{P,i}}\right)^{\frac{1}{2}}+\left(\frac{1}{N_{con}}\sum_{i=1}^{N_{con}}\frac{\left(m_{par1,i}-m_{par2,i}\right)^2}{C_{R,i}}\right)^{\frac{1}{2}}$$

Data **A priori** **Constraints**

Equation A4.2 Calculation of RESTOTAL. Data related calculation: observed data (d_{obs}), forward model calculation of data from inversion model ($d_{forward}$), standard deviation of the measured data (C_{obs}). *A-priori*-related calculation: model parameter (m_i), *a priori* model parameter (m_{prior}), standard deviation of *a priori* model parameter (C_P). Inversion constraint (regularisation) -related calculation (laterally or vertically): model parameter (m_{par1}), model parameter (m_{par2}), standard deviation given to the regularisation constraints (C_R).

Table A4.2 Resistivity models in *.xyz* files (e.g. for importing into Leapfrog Software) for both the sharp and smooth models, for example: *\xyz\Heretaunga_smooth_resistivitymodel_V1_2021.xyz*

Attribute	Description
ID	Model ID
Line_No	Line number
Layer_No	Layer number
UTMX	Easting NZTM
UTMY	Northing NZTM
Elevation_Cell	Elevation of the middle of the layer (m)
Resistivity	Resistivity (Ohm.m)
Resistivity STD	STD on resistivity
Conductivity	Conductivity (mS/m)
Depth_top	Depth (m) to top of layer
Depth_bottom	Depth (m) to bottom of layer
Thickness	Thickness (m) of layer
Thickness_STD	STD on thickness of layer

Table A4.3 Format of the xyz-ascii files for both the sharp and smooth models: **_dat.xyz* (data as it was used in the inversion) and **_syn.xyz* (synthetic forward calculation of the final model), for example: *\xyz_ascii\Heretaunga_smooth_resistivitymodel_V1_2021_dat.xyz*. This does not include DataSTD, which only appears in *_dat.xyz*

Attribute	Description
LINE_NO	Line number
UTMX	Easting NZTM
UTMY	Northing NZTM
TIMESTAMP	Time (days) using epoch starting 30 December 1899, in UTC
FID	Fiducial
RECORD	Record
ELEVATION	Topography (m; from imported DEM)
ALT	Input altitude (metres above ground level)
INVALT	Inverted altitude (metres above ground level)
INVALTSTD	STD on inverted altitude
DELTAALT	Difference between input and inverted altitude (m; inverted – input altitude)
TILT	NA (not utilised by SkyTEM Z-component inversion)
INVTILT	NA (not utilised by SkyTEM Z-component inversion)
INVTILTSTD	NA (not utilised by SkyTEM Z-component inversion)
NUMDATA	Number of gates inverted (number of data points)
SEGMENT	Moment ID (low moment = 1, high moment = 2)
RESDATA	Data mis-fit (Equation A4.1 for each 1D inversion)
RESTOTAL	Total mis-fit (Equation A4.2 for the entire inversion)

Attribute	Description
DATA_1	Voltage (V/Am^4) for gate_1
DATA_2	Voltage (V/Am^4) for gate_2
…	…
DATA_N	Voltage (V/Am^4) for gate_N
DATASTD_1	STD on voltage for gate_1
DATASTD_2	STD on voltage for gate_2
…	…
DATASTD_N	STD on voltage for gate_N

Table A4.4 Format of the mean resistivity files, for example: *\MRESD_smooth\XXXm_YYYm.shp*

Attribute	Description
XUTM	Easting NZTM
YUTM	Northing NZTM
ELEVATION	Topography (m; from imported DEM)
ISDATASET	Internal Aarhus Workbench reference
ID	Internal Aarhus Workbench reference
IDTYPE	Internal Aarhus Workbench reference
NAME	Internal Aarhus Workbench reference
POSITION1	Internal Aarhus Workbench reference
POSITION2	Internal Aarhus Workbench reference
POSITION3	Internal Aarhus Workbench reference
POSITION4	Internal Aarhus Workbench reference
DATASET	Internal Aarhus Workbench reference
DATYPE	Internal Aarhus Workbench reference
DAPOSITION	Internal Aarhus Workbench reference
DAPOSITI01	Internal Aarhus Workbench reference
ENABLED	Internal Aarhus Workbench reference
VALUE	Resistivity (Ohm.m)

Table A4.5 Format of the layer resistivity files, for example: *\layers\smooth_ResInv_LayerX.shp*

Attribute	Description
XUTM	Easting NZTM
YUTM	Northing NZTM
ELEVATION	Topography (m; from imported DEM)
DEP_TOP_N	Depth (m) to top of layer_N
DEP_BOT_N	Depth (m) to bottom of layer_N (except for N = 35, which is an infinite half-space)
RHO_I_N	Resistivity (Ohm m) for layer_N
RHO_I_STDN	STD on resistivity for layer N
layer	Layer number (N)
ELEV_TOP	Elevation (m) of top of layer (ELEVATION – DEP_TOP_N)
ELEV_BOT	Elevation (m) of bottom of layer (ELEVATION – DEP_BOT_N) (except for N = 35, which is an infinite half-space)

Table A4.6 Quality control datasets. All have the format: XUTM (Easting NZTM), YUTM (Northing NZTM), VALUE (described below). Matching datasets are provided for *\QC_maps\Heretaunga_offshore**

Attribute	Description
\QC_maps\Heretaunga_AltInp.shp	Input altitude (m; Section 5.1.3)
\QC_maps\Heretaunga_ChaNum.shp	Moment ID: low moment = 1, high moment = 2, both = 12 or 21 (Section 5.1.2)
\QC_maps\Heretaunga_NoData_ChAll.shp	Number of gates inverted (number of data points; Section 5.1.5)
\QC_maps\Heretaunga_sharp_DOICon.shp	Conservative DOI, depth (m; Section 5.1.6)
\QC_maps\Heretaunga_sharp_DOIConE.shp	Conservative DOI, elevation (m; Section 5.1.6)
\QC_maps\Heretaunga_sharp_DOISta.shp	Standard DOI, depth (m; Section 5.1.6)
\QC_maps\Heretaunga_sharp_DOIStaE.shp	Standard DOI, elevation (m; Section 5.1.6)
\QC_maps\Heretaunga_sharp_DataRes_ChAll.shp	Data mis-fit (Section 5.1.4)
\QC_maps\Heretaunga_smooth_DOICon.shp	Conservative DOI, depth (m; Section 5.1.6)
\QC_maps\Heretaunga_ smooth_DOIConE.shp	Conservative DOI, elevation (m; Section 5.1.6)
\QC_maps\Heretaunga_ smooth_DOISta.shp	Standard DOI, depth (m; Section 5.1.6)
\QC_maps\Heretaunga_ smooth_DOIStaE.shp	Standard DOI, elevation (m; Section 5.1.6)
\QC_maps\Heretaunga_ smooth_ResData_ChAll.shp	Data mis-fit (Section 5.1.4)

www.gns.cri.nz

Principal Location

1 Fairway Drive, Avalon
Lower Hutt 5010
PO Box 30368
Lower Hutt 5040
New Zealand
T +64-4-570 1444
F +64-4-570 4600

Other Locations

Dunedin Research Centre
764 Cumberland Street
Private Bag 1930
Dunedin 9054
New Zealand
T +64-3-477 4050
F +64-3-477 5232

Wairakei Research Centre
114 Karetoto Road
Private Bag 2000
Taupo 3352
New Zealand
T +64-7-374 8211
F +64-7-374 8199

National Isotope Centre
30 Gracefield Road
PO Box 30368
Lower Hutt 5040
New Zealand
T +64-4-570 1444
F +64-4-570 4657